UNIVERSITY OF OSLO
Department of Chemistry
Faculty of Mathematics and Natural Sciences

Preparations for a Reduction and Liquid-Liquid Separation Experiment for Element 106, Seaborgium

Master Thesis in Chemistry

Hans Vigeland Lerum

May 28, 2014

ABSTRACT

The purpose of this thesis was to check if it was possible to prepare a mechanical and chemical system that can reduce Seaborgium, element 106, and separate between the reduced and the oxidized state. To do this the liquid-liquid extraction system SISAK has been coupled to a flow electrolytic column, which is able to reduce single atoms. To overcome the high difference in flow rate between these two systems a membrane degasser has been utilized which managed to severely reduce the amount of fluid needed.

Several extraction schemes have been tested. These had the goal that they should manage to strongly extract only one of the oxidation states. As a model for Sg experiments Mo and W have been used. During the work of this thesis it has been shown that it is possible to reduce and separate between two oxidation states of Mo. Furthermore, slight separation has been achieved for W in some systems. This have been done to model Sg in such a way that it is realistic to believe that Sg will behave in the same way.

In addition a proof of concept has been achieved were the newly developed membrane degasser, the flow electrolytic column and the SISAK centrifuge have been coupled together. This managed to reduce enough Mo and separate between the reduced and oxidized Mo species at a flow rate of 0.2 mL/s and with the aquatic solution 0.1 M HCl + 0.9 M LiCl and an organic solution of 0.01 M hinokitiol in Toluene. Some kinetic studies have been performed at 0.2 mL/s flow rate with HDEHP as an extractant in toluene and an aquatic solution of 0.1 m H_2SO_4. Additionally retention on the carbon electrode is discussed.

The work presented in this thesis have been performed as a part of a large collaboration between the nuclear chemistry group at the university of Oslo, Norway and between the superheavy element group in Tokai, Japan. An importan part of this work has therefore been to set up a working SISAK set-up in Tokai and a working flow electrolytic column in Oslo.

Acknowledgements

The work for this thesis started in the fall of 2012. I started as a part of Jon Petter Omtvedt's group which study the chemistry of the "deep end" of the periodic table. The work performed in this thesis has been rather novel for this group as we try to incorporate redox chemistry in to a group which have mostly worked with liquid extraction.

So I would like to thank Jon Petter Omtvedt for great suggestions in both the practical and theoretical work done for the duration of this thesis. I would also like to thank Atsushi Toyoshima for teaching me about the FEC. Thanks to Kazuhiro Ooe for advancing the work with the MDG. Thanks to Kazuaki Tsukada for showing me and my family around in Tokai. I would also like to thank all the Postdocs, PhDs, master students, bachelor students, and secretaries in Tokai which made my stay in Japan fun and welcoming. Thanks to Tor Bjørnstad who bothered to read trough this thesis at a early stage. Thanks to Mohammed Abdo who read trough this thesis at an even earlier stage and who tolerated my occasional illogical behaviour in the lab. Thanks to Matthias Schädel and Jens Volker Kratz for a lot of good suggestion on what to test.

I must thank the cyclotron operators in Norway for a stable beam. My thanks also goes to the tandem accelerator operators in Tokai which made this huge machine work even dough the earthquake some years ago proved a problem. Special thanks to Miki Tsuruta for general excellency in fixing everything Japanese. I must thank my fellow students in Oslo both those who are in the Nuclear Chemistry group and those who were not. You made it possible to talk about something other than distribution ratios, you know who you are.

I must thank my family for being supportive and actually bothering to read trough parts of the thesis and commenting.

ABBREVIATIONS

AKUFE = Anordning för Kontinuerlig Undersökning av Fördelingjamvikter vid Vätske Extraktion. This translates to: device for continuously research of equilibrium with liquid liquid extraction
CDG = Centrifuge Degasser
DC = Direct Catch, a term used when filtering aerosols particles carried in the gas-jet system.
D-ratio = Distribution Ratio
FEC = Flow Electrolytic Column/Cell
GSI = Gesellschaft für Schwerionenforschung mbH
HDEHP = Diethylhexylphosphoric acid
HPGe = high purity germanium detector
HSE = Healt, Enviroment and Safety
MDG = Membrane Degasser
LBNL = Lawrence Berkeley National Laboratory
LLE = Liquid Liquid Extraction
LS = Liquid Scintillation
PEEK = Poly Ether Ether Ketone
PI = principal investigator
RIKEN = Rikagaku Kenkyusho
RPM = Rounds Per Minute
SISAK = Short lived Isotopes Studied by the AKUFE-technique.
StHe = Standar Hydrogen Electrode
SHE = Super Heavy Element
TOA = Trioctylamine
ZZ = Zic Zac mixer

CONTENTS

1. INTRODUCTION

1.1 Studies of Superheavy Elements

The elements are the essential chemical building-blocks. One of the most fundamental chemical investigations that can be undertaken is to study a new element. However, all commonly available elements (e.g. that are found in nature) have been extensively investigated. From the systematics of the Periodic Table, some elements like technetium (Tc, Z=43) and promethium (Pm, Z=61) are missing in nature, but have been produced in nuclear reactions and are today well known [1–3]. Even elements heavier than uranium, the heaviest element found in nature with Z=92, are available in macroscopic quantities: Up to around element 98 (californium) these transuranium elements are routinely produced in nuclear reactors [4–11]. As one moves far away from the stable or at least long-lived elements, it gets harder and harder to synthesize even heavier elements, both due to very low cross sections (expressing the probability for a successful nuclear reaction) and shorter and shorter half-lives. Nevertheless, elements all the way up to element 118 have been produced [12], but for the heaviest only single atoms that mostly disintegrate in less than a second. This provides a substantial challenge for any chemist who contemplates to study their chemical properties. At present the heaviest element witch have been studied chemically is element 114 [13, 14].

Superheavy elements will here be defined as elements containing 104 or more protons. The term Superheavy Elements (SHEs) are used differently by different people and should be used with caution. Formally the elements with Z=104 and above are termed transactinide elements. In this work Superheavy elements and transactinides are used synonymously. The SHEs are the ”last frontier” for the chemists with respect to access. The new elements are intriguing to study due to the fact that their chemical behaviour is largely unknown. Their chemical behaviour can deviate from the expected trends of their homologues. The reason for this is the so called relativistic effect. Due to the highly charged and heavy core in these elements the innermost electrons are accelerated to such an extant that their mass changes band they orbit closer to the nucleus. The relativistic effect roughly increases as a function of Z^2 . This changes he outermost shell structure of the atoms which determine their chemical properties and binding [15].

1.2 Purpose and Motivation

There were two central goals for the work presented here. The first is substantial, to improve the understanding of the atomic structure of element 106, seaborgium (Sg). The second was procedural, exploring the capability of available instrumentation to achieve this goal.

Sg has never been reduced chemically, which is a major chemical challenge. This thesis is part of a larger project aiming to develop a system capable of separating two oxidation states of this element. Seaborgium is not available for development work, therefore lighter elements that are assumed to have similar chemical properties are used as models. The homologues molybdenum (Mo) and tungsten (W) were used as models for Sg in this work.

Due to the low production cross-section and short half-life of Sg, the reduction, separation and detection system must be capable of ”single atom chemistry”. Single atom chemistry represents considerable challenges as the mass action law cannot be applied in the regular way [16]. Finding the single atom is a great challenge and it is only done upon decay.

The thesis explored the use of the instrument Flow Electrolytic Column (FEC) to change the oxidation state of single atoms. Further, the Liquid-liquid Extraction (LLE) system SISAK[1] was utilized to investigate the difference in behaviour between the two oxidation states.

The purpose of this thesis was to investigate the possibility to use these two systems, the FEC and SISAK, together and develop a chemical system which can separate between two oxidation states. A significant challenge for this is that the normal flow rate for the phases in SISAK is 0.4-0.5 mL/s while The FEC utilizes flow rates around 0.1 mL/min. I. e. the flow rates used for normal SISAK operations are over 200 times higher. Work is in progress to reduce the flow rate of the SISAK system. In particular the developed Membrane DeGasser is able to reduce the flow rate of the SISAK system to about 50% of what have been used earlier [17–19]. The other purpose have been to develop a chemical system where the two oxidation states behave so differently that it is possible to separate them by using LLE.

1.3 Collaborators

The experiments in this thesis have been performed in collaboration between the superheavy chemistry groups in Tokai and Oslo. Seminars, discussions, planning and experiments have been performed jointly at both sites. Furthermore, personnel from

[1] SISAK: Short lived Isotopes Studied by the AKUFVE-technique. Where AKUFE is a Swedish acronym which stands for: Anordning för Kontinuerlig Undersökning av Fördelingjamvikter vid Vätske Extraktion

both groups have been participating both in Tokai and Oslo. E.g. as part of this thesis work, three months were spent in Japan to participate in an intense experimental campaign. Even when personnel from the other group was not present, extensive joint effort were put into planning and analysing experiments, using video meetings, e-mail and a common wiki-system [20]. This collaboration was formed to take advantage of both groups previous experiences. The Oslo group's usage of the SISAK systems and previous LLE experiments, and the Tokai group's experience with single atom reduction. In addition, the difference in experimental facilities provided a wider set of experimental tools. In addition to the two experiment sites (Oslo and Tokai), substantial theoretical support was obtained from Dr. Valeria Pershina (GSI[2]) and Prof. Jens V. Kratz (Univ. Mainz). The current thesis does not undertake to present all the work performed within the Oslo-Japan project, but focus on experiments and results in which the author have been significantly involved, either as principal investigator (PI) or at least major participant. In cases where results in which the author played a more peripheral role is mentioned or presented, this will be clearly stated.

1.4 Thesis Outline

This thesis starts with an outline of the background of the methods used. In Chapter 2, Background. Here an outline of relevant work and the most important equipment is discussed.

Following this, in Chapter 3, Theory, the most essential theory for this thesis is discussed. Then in chapter 4, Instrumentation, There is a close description of the equipment used. This then leads to Chapter 5, Experimental Procedures this describes how the chemicals and the chemical equipments was used. In the process of this work several different types of experiments have been performed: In Chapter 6, Experiments and Results these experiments are ordered in the following way: The instrumental experiments, how they function as a unity will be presented first. This is followed by the batch experiments where the experiments that the author has directly participated in are presented first. Then results from Japan are presented.

In the last Chapter 7 Discussion and Conclusions, the results from the different experiments are discussed and conclusions are drawn.

[2] Gesellschaft für Schwerionenforschung mbH

2. BACKGROUND

2.1 Superheavy Elements

Rutherfordium is the lightest Superheavy element (SHE) with 104 protons. Superheavy elements are not found in nature but are formed in nuclear reactions induced by high intensity heavy ion-particle accelerators.

This thesis focuses on the chemistry of element 106, seaborgium (Sg). It has been placed in group six of the transitional elements together with its homologues; tungsten, molybdenum, and chromium. The first time it was created was in 1974 at the Lawrence Livermore Laboratory [21].

In this review recent article by Türler and Pershina [12] the gas-phase experiments with Sg and other superheavy elements are discussed. However the focus of this thesis is on aqueous phase experiments to allow determination of redox potentials. Previously only two experiments have been performed in the aqueous phase [12, 22, 23]. These experiments concluded that Sg behave similar to it homologues but has a stronger tendency to hydrolyse. Thus, there is not much empirical knowledge of Sg in the aqueous phase. Therefore, theoretical calculations coupled with trends in the homologues are used as guidlines.

2.2 The SISAK System

The SISAK system performs liquid-liquid extractions in a continuous way using small-volume separator centrifuges [24]. Since its development in the 1970's the system has gone through several major changes, particularly important was it that the volume of the centrifuge chamber was reduced from 100 mL to 0.3 mL [25, 26]. In addition, the construction material was changed from titanium passivated palladium to a composite material PEEK (Poly Ether Ether Ketone). The change in material made the system more resistant against aggressive acids and the reduction in size improved the transport time at maximum flow rate from 2.4 s to 0.05 s [25, 27]. A sketch of the SISAK centrifuge can be seen in Fig 2.1. The separation chamber rests as a cup on top of he engine. The engine then spins the cup this forces the liquid with the highest density against the outer wall, and the less dense liquid towards the inner wall. A more thorough description of the parts used can be found in chapter 4.4, Set-up for Liguid-Liquid Extraction

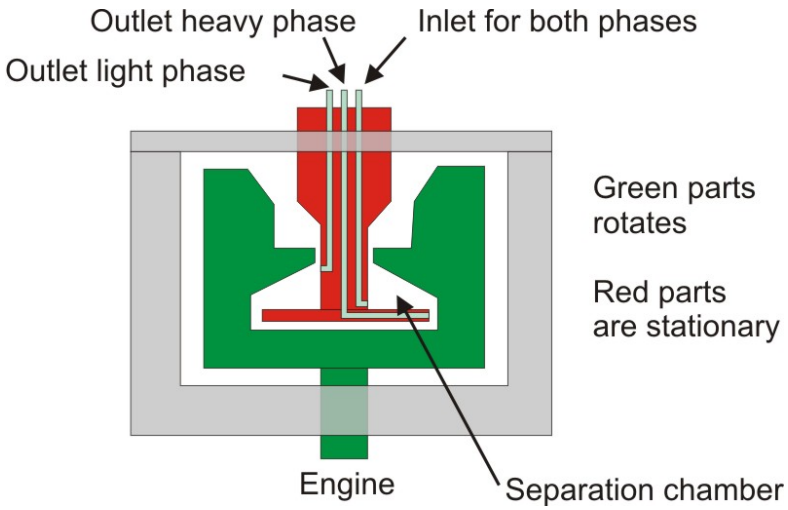

Fig. 2.1: A simplified schematic drawing of the SISAK centrifuge. The green parts spin, thereby forcing the denser liquid out to the edges. The red part is stationary with two inlets for the denser and the less dense fluid.

on Sg

2.3 Flow Electrolytic Column

The Flow Electrolytic Column (FEC) was developed to study reduction potentials of short-lived heavy nuclei [28]. It can operate in a continuous way as long as the potential is in the correct range. It has been used to empirically define the reduction potential of No and Md [29, 30]. In these experiments the working electrode was coated in a resin which retained the reduced element. The reduced species were washed out with acid.

The FEC was developed from an early version which was used to test for trace amount of uranium in solutions [31], in particular the amount of uranium in seawater [32]. For a schematic sketch of the FEC see Fig 2.2. The solution enters trough the inlet and metal ions are reduced at the working electrode. The reduced metal ions stay in the solution and exits at the outlet with the continuously flowing solution. The Pt mesh functions as a counter electrode and Ag|AgCl assembly functions as a reference electrode.

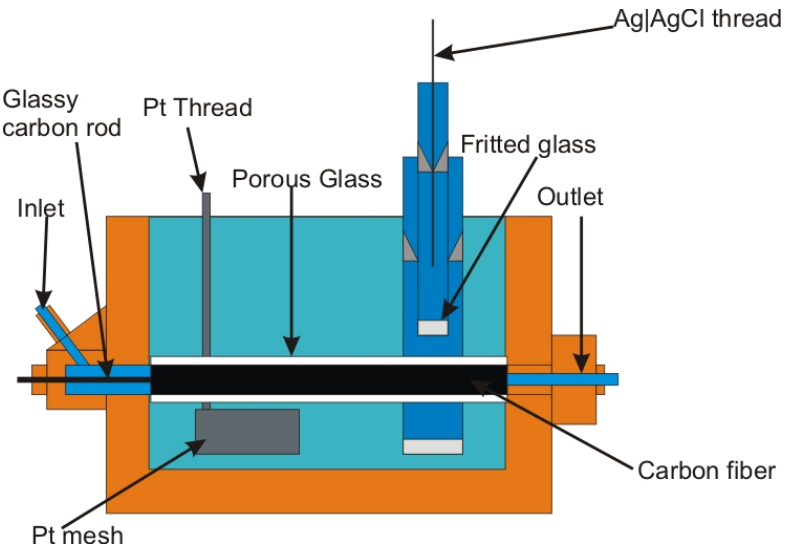

Fig. 2.2: A schematic sketch of the FEC set-up. This sketch shows the working electrode marked as carbon fibre. In addition the counter electrode and the reference electrode is shown here as platinum and Ag|AgCl respectively.

3. THEORY

3.1 Liquid-liquid Extraction

Liquid-liquid Extraction (LLE) refers to the distribution of a solute (the minor component of a solution which is regarded as having been dissolved by the solvent) between two immiscible liquid phases. The two phases are forced into contact thus enabling the solute to travel across the phase boundary. The distribution between the two phases is usually expressed as the distribution ratio, from here on referred to as the D-ratio. The definition of the D-ratio is:

$$D = \frac{[A]_{org}}{[A]_{aq}} \tag{3.1}$$

Were $[A]_{org}$ is the total analytical concentration of solute A in the organic solution while $[A]_{aq}$ is the total analytical concentration of solute A in the aqueous solution [33].

In many cases it is useful to express the D-ratio as the fraction extracted, this is defined as [34]:

$$R = \frac{D}{D+1} \tag{3.2}$$

Were R is the fraction of solute extracted. This formula is valid for one extraction step and for equal liquid volumes i.e. $V_{org} = V_{aq}$.

The D-ratio of a compound can be controlled by using different adduct formers in the aqueous solutions and different extractants in the organic solution. For LLE there are several terms commonly used. Those that are relevant are defined below:

An adduct is a new chemical species AB, of which each molecular entity is formed by direct combination of two separate molecular entities A and B. This occur in such a way that there is a change in connectivity, but no loss of atoms within the moieties A and B. Stoichiometries other than 1:1 are also possible. An intra-molecular adduct can be formed when A and B are groups contained within the same molecular entity. This is a general term which, whenever appropriate, is preferred to the less explicit term complex [35].

A complex is a molecular where entity formed by a loose association involving two or more component molecular entities (ionic or uncharged). The bonding between the components is normally weaker than in a covalent bond [35].

A ligand is an inorganic or organic coordination entity, the atoms or molecular groups are bound to the central atom [35].

A Coordination entity is an assembly consisting of a central atom (usually metallic) to which there is attached a surrounding array of other groups of atoms (ligands) [35].

Chelation is the formation or presence of bonds (or other attractive interactions) between two or more separate binding sites within the same ligand and a single central atom. A molecular entity in which there is chelation (and the corresponding chemical species) is called a 'chelate'. The terms bidentate (or didentate), ... multidentate are used to indicate the number of potential binding sites of the ligand, at least two of which must be used by the ligand in forming a 'chelate' [35]. (The use of the term is often restricted to metallic central atoms.)

3.1.1 Extracting Agents

In the following the different extracting agents are described and a suggested extraction mechanism is given. In this thesis a line over the compound designates that the compound is in the organic phase. The organic phase for all experiments performed in this work has been some amount of extractant dissolved in toluene. Toluene was used because it is very important that the organic solvent is compatible with Liquid Scintillation (LS). Toluene has been proven to useful when mixed with the scintillation solution without any severe quenching. For a more thorough description of the LS system read Stavsetra thesis [36]. For the extractant to be applicable in a Sg experiment the D-ratios for Mo and W have to be similar.

Hinokitiol (HT, 2-Hydroxy-6-propan-2-cylohepta-2,4,6-trien-1-one) chelates with cations making them more lipofilic [37]. In Fig 3.1 hinoktiol is drawn. It protolysis and a chelate is formed between the two oxygen atoms on the seven ring for each positive charge on the metal ion, see M. C. Barret et al [38] for further details. The suggested extraction mechanism is:

$$\overline{nHT} + M^{n+} \rightleftharpoons \overline{MT_n} + nH^{+} \tag{3.3}$$

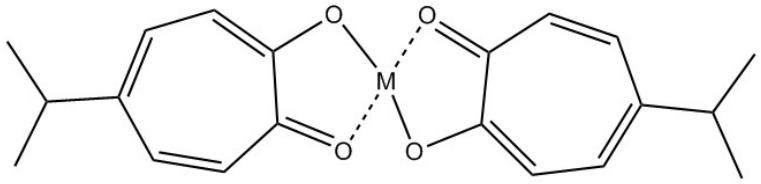

Fig. 3.1: Suggested drawing of the Hinokitiol chelation with metal that has a positive charge n=1.

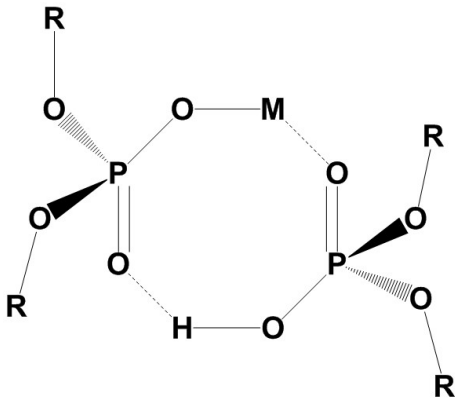

Fig. 3.2: Suggested complex between HDEHP and a n charged metal ion [39]. The M symbolises a singly charged metal, while the R symbolise the 2-ethylhexyl groups on the HDEHP molecule.

Diethylhexylphosphoric acid (HDEHP) forms a dimer in non-polar solution. The dimerization will be lost in a polar media. The suggested form of the complex is drawn in Fig 3.2. After the metal has been transported to the organic phase it forms a 8-membered ring [39–41]. So that the complete formula for extracio is suggested as:

$$\overline{n(HDEHP)_2} + M^{n+} \rightleftharpoons \overline{M(DEHP)_n \cdot (HDEHP)_n} + nH^+ \tag{3.4}$$

Where $DEHP$ symbolize a solvolised HDEHP molecule, M^{n+} symbolise a metal ion with a charge of n, and n is a number.

Trioctylamine (TOA) binds with anions making them more lipophilic and therefore more extractable in toluene. The general reaction of extraction by TOA can be written as:
Protonation:

$$\overline{(R_3N)} + H^+ + A^- \rightleftharpoons \overline{(R_3NH^+A^-)} \tag{3.5}$$

Exchange:

$$\overline{(R_3NH^+A^-)} + B^- \rightleftharpoons \overline{(R_3NH^+B^-)} + A^- \tag{3.6}$$

The extraction of the metal ions is not only controlled by the extractants in the organic phase but also from the adducts formed in the aquatic phase. Strong acids are common ligands to use for this, in addition several weak acid can be used they will not

be discussed here. A rule of thumb for the binding strength of aqueous ligands are [42]: $ClO_4^- < NO_3^- < Cl^- < HSO_4^- < F^-$.
Here fluoride is the strongest ligand and perchlorate is the weakest ligand.

3.2 Redox Chemistry

In thesis valence state have solely been used to describe the oxidation state. Hexavalent is oxidation state VI. Tetravalent is oxidation state IV. In general a redox reaction is written as half reactions, one for the material being reduced and one for the material being oxidized:

$$M + e^- \rightarrow M^- \text{ reduction} \tag{3.7}$$

$$M \rightarrow M^+ + e^- \text{ oxidation} \tag{3.8}$$

Here M represents an atom and e^- is an electron. The atom and the electron react and the oxidation state is changed. The reaction can go either way: When there is an electron added to the atom it is called reduction; when there is an electron taken away from the atom it is called oxidation. The deviation from the standard potential related to the Standard Hydrogen Electrode (StHE) is given by the Nernst equation:

$$E_{rev} = E^o + \frac{RT}{nF} ln \left(\frac{\gamma_{Ox}}{\gamma_{Red}} \right) \tag{3.9}$$

Here E^o is the standard potential compared to StHE, and E_{rev} is the reversible potential. R is the gas constant, T is the absolute temperature ,and F is the Faraday constant. n is the number of electrons transferred. γ_{Ox} is the activity of the oxidized species, γ_{Red} is the activity of the reduced species [43]. E^o is related to ΔG^o the Gibbs free energy as:

$$\Delta G^o = -nFE^o \tag{3.10}$$

Therefore a negative potential will symbolise a reaction driven towards an oxidation while a positive potential symbolise a reaction driven towards reduction [44].

The basic idea behind the project is to measure the reduction potential of seaborgium. Since this is impossible to do directly in the ”normal way”, the idea is to observe the difference in extraction behaviour between reduced and non-reduced species. ”Normal way” would be behaviour visible in macro amounts, e.g observed color change or current change in Cyclic Voltammetry (CV). Thus, LLE is used to determine the oxidation state. In order for this to work an aqueous mixture that yield Sg-complexes of such a type that they can be distinguished in the subsequent extraction, i.e. one species extracts and the other do not, must be found. An example of an ideal case is presented in Fig 3.3, this show what the extraction would look like if complete separation between two

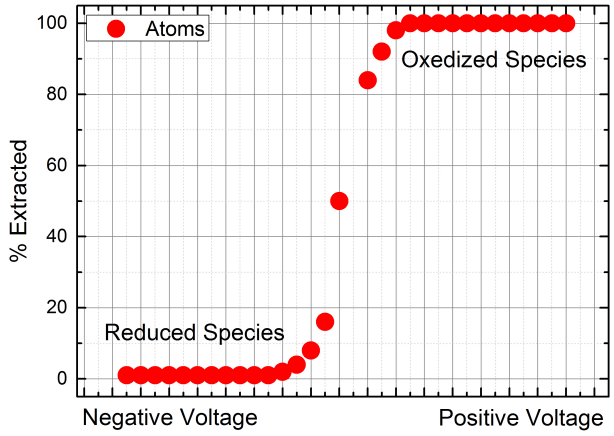

Fig. 3.3: Simulating an extraction as a function of potential. In this model the oxidized specie is completely extracted while nothing of the reduced specie is extracted.

oxidation states were achieved. With this ideal case finding the point where half of the atoms are reduced the Nernst equation is then simplified to:

$$E_{rev} = E^o \tag{3.11}$$

Thus, it would then be possible to derive the standard potential. However, overpotential shouls also be taken into account. This is defined as:

$$\eta = E - E_{rev} \tag{3.12}$$

Where η is the overpotential and E is the potential applied. There are several different aspects which can affect the overpotential. In the scope of this thesis there have not been enough time to discuss this thoroughly. More about overpotential can be read here [45].

The standard reduction potential is given in relation to the standard hydrogen electrode StHE [46]. This half-cell is defined as a platinum electrode in contact with H_2 gas and an aqueous solution at standard state condition.

3.2.1 Cyclic Voltammetry

In cyclic voltammetry the potential is changed back and forth between a lower and upper voltage limit. The resulting current is followed as a function of time. When the voltage is swept from the negative to the positive potential it is called an anodic sweep. When it goes from positive to negative potential it is called a cathodic sweep. In an anodic sweep oxidation of the solute occurs, provided the potential is sufficient to perform the oxidation. The oxidation will be observed as a sudden positive increase of current passing through the electrodes. In a cathodic sweep the reduction occurs, and this will be observed as a sudden negative current [47].

3.3 Tracer Scale Chemistry

Normally chemistry is carried out in what will be called macro-scale, in this thesis macro scale will be defined as the solvent containing more than 100 ppm of the solute. When working with superheavy elements it is impossible to work in macro-scale. This is due to the difficulty in creating these elements and their short half-lives. The longest-living known isotope for Sg is ^{271}Sg with 2.4 min half-life. Due to its low cross section it is unlikely that more than one atom will be formed per day [1]. Therefore there will only be one atom in the solution at any given point [48]. Chemistry on this level of dilution is often called single-atom-chemistry.

This level of dilution raises several challenges. In LLE the distribution of one atom is impossible to measure. A single atom can only be in one phase at the time. Therefore the probability of an atom being in one state as opposed to another is used instead of concentration [16, 49]. Additional challenges are that the atom can be adsorbed to walls or particles in the solution, significantly changing the behaviour. There is even the possibility that the single atom might be oxidized by trace amount of an oxidizing agent in this solution [48]. Generally trace impurities that have no effect can significantly change the behaviour in micro scale.

In single atom chemistry the experiments are developed in such a way that the atom changes phase or state thousands of times i.e. until they reach equilibrium. Thereby, repeating the experiment results in a statistical distribution between the two phases. Therefore LLE is a suitable technique to perform experiments on SHEs as the atoms travels across the phase boundary quickly and continuously [50, 51].

3.4 Nuclear Reactions and Production of Superheavy Elements

The nuclear reactions discussed in this thesis will be described with the commonly used notation:

$$ {}^{a}_{z}A(x,y)^{a'}_{z'}B \tag{3.13} $$

Here a is the atomic mass number, z is the number of protons in the nucleus, x is the incident particle reacting with the nucleus A, y is the escaping particle and B is the particle formed where a' and z' is the new mass number and proton number respectively.

3.4.1 Accelerators

There are several types of particle accelerators appropriate for this study. In this thesis a cyclotron and a tandem accelerator was used.

If a charged particle is placed in a uniform magnetic field it will experience a force that acts perpendicular to the field [52]. Utilizing this, a cyclotron can accelerate charged

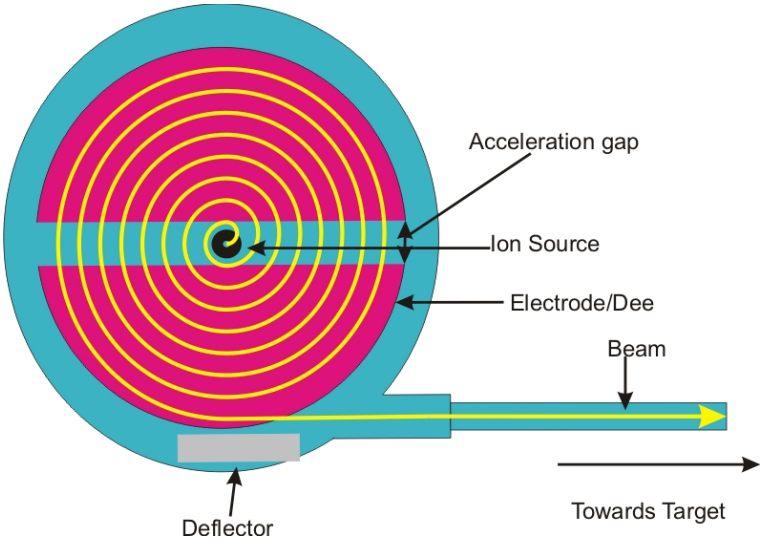

Fig. 3.4: Principle sketch of a cyclotron with the particles trajectory shown. The electrodes are shown D-shaped. The magnet is not shown.

particles by trapping them between two magnets and accelerate them between two electrodes. The first cyclotrons used two D-shaped hollow electrodes; they were sandwiched in between electro-magnet. The magnet forced the particles to travel in a spiral pattern while the gap between the electrodes forced the particles to accelerate, see Fig 3.4 [53].

A tandem accelerator is in general terms a type of electrostatic accelerator. Tandem accelerators utilize a two-step acceleration of ionic particles. Anions are produced in the negative ion source. They arrive at a high voltage terminal. Here the electrons are stripped from the ions either by a carbon foil or by N_2 gas. The cations are then accelerated away from the electrode towards a negative electrode [54]. See Fig 3.5 for a simple sketch of a tandem accelerator.

3.4.2 Activity Transport

In this thesis the activity was transported from the production chamber to the laboratory with a gas-jet. This is a technique where the radionuclei adheres to aerosols suspended in a gas stream. When the nuclei recoils out of the target it is in a highly charged state. This makes them adhere to the aerosols by Van der Waals forces [55].

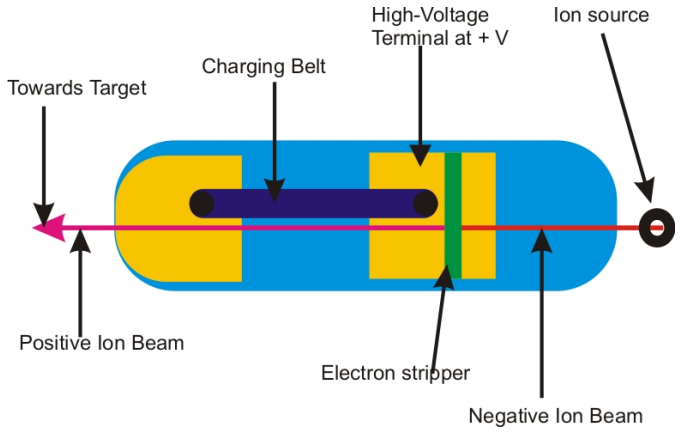

Fig. 3.5: A principle sketch of a tandem accelerator. Anions are expelled from the ion source accelerating towards the positively charged electrode.

3.5 Separation of Reduced and Oxidized Species

The basic idea behind this project is to reduce Sg, and then use LLE to separate between the reduced and the oxidized species. It was suggested that the best way to do this was to ensure that the species had an opposite charge. To model the reduced tetravalent species the speciation of group four was used. The assumption is that under conditions where group four is anions the reduced species of group six will also be anions.

3.5.1 The Oxidized Specie is a Cation

One strategy is to keep the oxidized specie as a cation. Fig 3.6 shows the speciation of the heavier group six atoms as a function of acid concentration. This suggests that the acid concentration should be kept above 0.1 M. However, the acid concentration cannot be raised indefinitely as this will result in trouble separating the oxidized and reduced species. To form negative tetravalent species the free F^- ion concentration should be kept around 10^{-4} M, this should form MF_6^{2-} [56, 57]. However, if the H^+ concentration is increased too high it will be very difficult to get a reasonable amount of free F^-. This is because it is a weak acid and in a highly acidic media it will not disassociate [58]. The following reaction schemes then apply:
Reduction:

$$SgO(OH)_3^+ + 6F^- + 2e^- + 5H^+ \rightleftharpoons SgF_6^{2-} + H_2O \tag{3.14}$$

Extraction of the negative specie:

$$2\overline{L} + SgF_6^{2-} \rightleftharpoons \overline{L_2SgF_6} \tag{3.15}$$

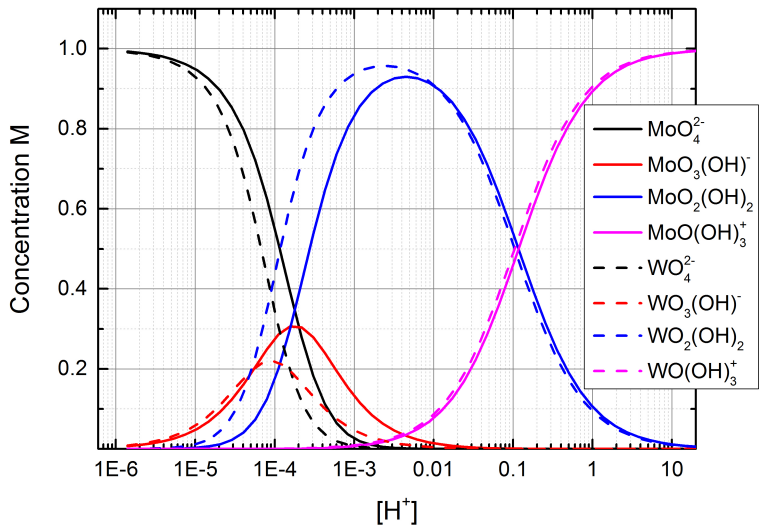

Fig. 3.6: The most relevant complexes of the group 6 elements and how they behave as a function of acid concentration [59].

Where $\overline{L}$ represent the anion extractant in the organic phase. Then the hexavalent specie can be extracted with a cation extractant:

$$\overline{C} + SgO(OH)_3^+ \rightleftharpoons \overline{CSgO(OH)_3} \tag{3.16}$$

Here $\overline{C}$ represents a cation extractant in the organic phase. Formula 3.15 and 3.16 have an unbalanced charge as it is not yet clear which extractants will be used.

3.5.2 The Oxidized Specie is an Anion

Here the tetravalent will be cationic and the hexavalent species will be anionic. The chemical system needed for this is a low acid concentration coupled with an extremely low free fluoride concentration. The suggested acid concentration is 10^{-3} M. The hexavalent species should form MO_4^{2-} [60]. The hydrofluoric concentration should then be 10^{-4} M. In these condition, the reduced species should form the coordination entity MF^{3+} [50]. If the concentration is increased more and more fluoride will bind to the metal and the cationic charge will decrease and become neutral and then negative. The reaction scheme for this path will then be nearly the same as the previous mentioned one:
Reduction:

$$SgO_4^{2-} + F^- + 4H^+ + 2e^- \rightleftharpoons SgF^{3+} + 4OH^- \tag{3.17}$$

Extraction of the negatively charged species:

$$2\overline{L} + SgO_4^{2-} \rightleftharpoons \overline{L_2SgO_4} \tag{3.18}$$

Extraction of the positively charged species:

$$3\overline{C} + SgF^{3+} \rightleftharpoons \overline{C_3SgF} \tag{3.19}$$

Formula 3.18 and 3.16 have unbalanced charges as it is not yet clear which extractants are to be used.

3.6 Summary of Chemistry of Relevant Groups

There is limited knowledge of the reduced species of tungsten (W) and molybdenum (Mo) and no relevant information was found for tracer scale conditions. To have some data to plan the experiments, it was assumed that the group four elements behave in a similar way to the reduced group six elements. Therefore the tracer scale behaviour of Zr, Hf and Rf has been scrutinized, as well as the chemistry of Mo, W and Sg, in relevant concentrations.

3.6.1 The Chemistry of Chromium, Molybdenum, Tungsten, and Seaborgium

The sixth group in the periodic table consists of chromium (Cr), molybdenum (Mo), tungsten (W) and seaborgium (Sg).

In macro scale group six will form polyoxoanions in aqueous form. Large structures composing of several metal ions bound together with oxygen. They will form large structures and they will do this in several strong acids e.g. H_2SO_4, HCl, and HNO_3 [61]. Therefore experiments performed in macro scale cannot be compared to experiments performed in tracer scale.

The most important oxidation state in aquatic chemistry for Cr is the trivalent state, while for Mo and W it is the hexavalent [62]. The later is also expected to be the case for Sg. Theoretical calculations suggests that the oxidation states III, IV, and V will be more unstable for Sg than comparable states of the homologues [63]. Stable, soluble compounds for the pentavalent states are known for the lighter homologues but the structure is not known for tungsten [63, 64].

From the hexavalent state they cannot be oxidized further. Thus, the redox experiment with Sg will have to be a reduction experiment. Therefore it is important to find which state is the most stable below the hexavalent. In addition it must be possible to reach this state in an aqueous environment without reducing the solvent (water). In Fig 3.7 the different redox potentials for the different homologues are shown. Theoretically estimated reduction potentials are read from left to right.

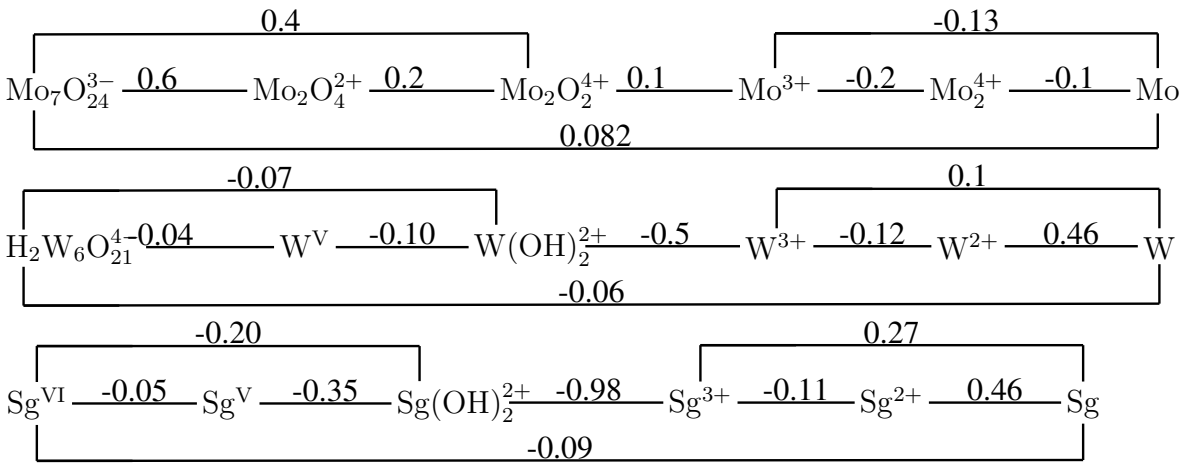

Fig. 3.7: Standard theoretical reduction potentials for Mo, W and Sg aqueous compounds in acidic solution [63]. Oxidation states with unknown structures are marked with a Roman numeral.

Sg is expected to be more difficult to hydrolyse. This has also been verified by chemical experiments [23, 59].

Sg is expected to behave somewhat different from its homologues when reacting with different concentrations of HF acid. When the concentration is low, below 10^{-5}M, it will not form negative complexes as strongly as W. Within an intermediate concentration, 10^{-5} M to 0.1 M, it will have stronger complex formation that W but weaker than Mo. In concentrations above 0.1 M HF Sg will have the strongest complex formation. These complexes are expected to be negative [60].

3.6.2 The Chemistry of Titanium, Zirconium, Hafnium, and Rutherfordium

The fourth group in the periodic table is represented by titanium (Ti), zirconium (Zr), hafnium (Hf) and rutherfordium (Rf). The most common oxidation state for these elements is the IV state. For titanium also II and III are important. The lower lying states are less and less dominant as the metals become heavier [65].

In solutions with HF concentration of 0.2 M. Hf will sorb to anionic resins [66].

Rf will adsorb to cation exchangers with concentrations of at least 0.1 M HCl and HF concentrations lower than 10^{-3} M. Within these concentrations Mo and W are poorly adsorbed to the resin. These should be hexavalent under these conditions, so the behaviour is expected to be different from the tetravalent species [67].

In 6 M nitric acid Rf forms positive nitrate complexes. The suggested species are $Rf(NO_3)_2^{2+}$ or $RfO(NO_3)^{+}$. These species can then be extracted with dibutyl-phosphoric acid (HDBP) in toluene. The suggested type of complex extracted is some kind of nitrate-dibutyl-phosphate complex [51].

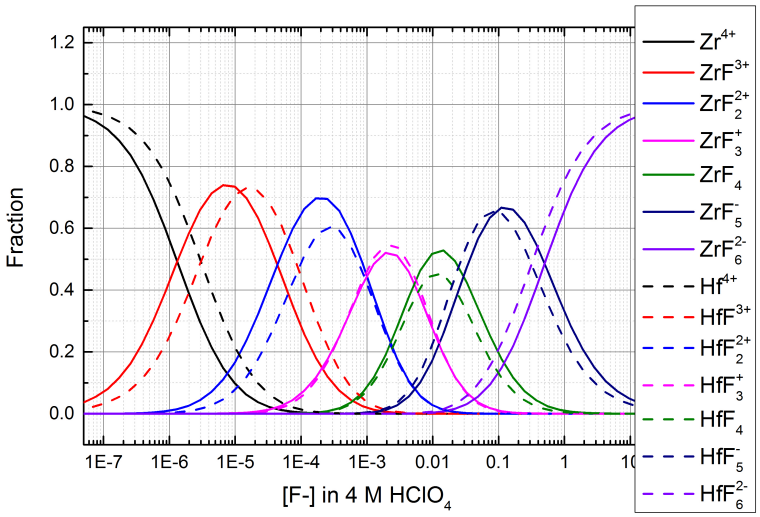

Fig. 3.8: Formation of different complexes of the heavier group 4 elements as a function of free fluoride in 4 M $HClO_4$, stability constants from [69].

In the concentration $5 \cdot 10^{-4}$M<[HF]<0.013 M with 0.010 M>[NO_3^-]<0.015 Rf forms negative anions. Concentration of the compound is here symbolised with brackets. The most dominant form is most likely $(RfF_6)^{2-}$ [56].

With free F^- concentration up to 10^{-3} M, Rf will sorb to a cation exchanger resin [50, 56, 67].

Hf will strongly bind to oxalic acid forming a negatively charged complex. Thereby making it easily extracted by TOA [68]. If Mo or W behave in a different way this could be used to separate them.

In Fig 3.8 the speciation of the heavier group 4 elements are given in bulk scale. Since polyspecies is not predominant as for group VI, the data also serve as a guide for tracer scale experiments [69]. These suggest that if the group four elements are to be kept negative the F^- concentration should be kept above 0.01 M in e.g. 4 M $HClO_4$.

4. INSTRUMENTATION

4.1 The OCL Cyclotron

The OCL cyclotron is a scanditronic M35 cyclotron. It can utilize several different beams as specified in Table 4.1.

4.1.1 OCL Target Chamber

For a schematic drawing of the target chamber at the OCL lab see Fig 4.1. The ion beam enters the target assembly from the left side of the figure. Here it passes a collimator which removes stray beam which otherwise would hit the target mounting the beam. After the collimator there is a scintillation screen which is viewed with a camera, it is pneumatically opperated to enable it to be removed in and out of the beam path. This gives the option to see how the beam strikes the target in real time. The beam then passes through the window, strikes the target, passes through the exit window and is deposited on the beam dump which also serves as a faraday cup.

All experiments in Norway, used a beam of 30 MeV $^{4}He^{2+}$ with an intensity from 300 to 400 nA. Several different targets were used in this set-up. The most frequently used target was a 0.025 cm thick natural Zr target the reaction ^{90}Zr(α,n)^{93m}Mo half-life of 6.9 h [1].

To create ^{89}Zr and ^{93m}Mo at the same time, a mixed target was used. This consisted of three metal foils. One large sheet of Zr with 0.025 cm thickness on this there was

Tab. 4.1: Available beams for the MC-35 Scanditronix cyclotron at OCl .

Particle Type	Energy (MeV)[a]	Beam Intensity (μA)
Proton	2-35	100
Deuterium	4-18	100
^{3}He[b]	6-47	50
^{4}He	8-35	50

[a] This energies are the specification from the producer.
[b] For economic reasons, this beam is currently not available.

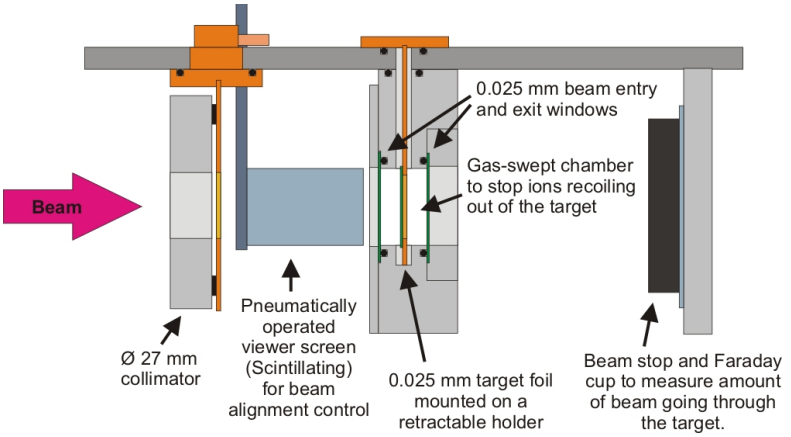

Fig. 4.1: Schematic of the target chamber at OCl.

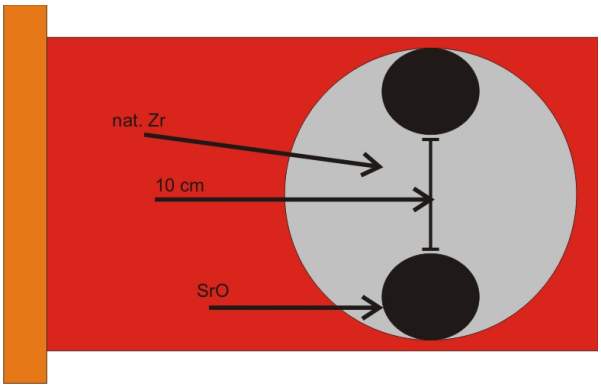

Fig. 4.2: The Sr in the SrO had a natural isotopic distribution.

glued two plates made of SrO deposited on Be backing. The diameter of the two sheets of SrO was 8 mm and the distance between their centres is 18 mm, as seen in Fig 4.2. The reason for this somewhat unorthodox target assembly was that the 8 mm SrO targets was available from an old experiment.

The gas transport system in Fig 4.3. In this setup the valves used were controlled by the computer. When the He gas comes to the valves it can be sent to the bypass which deposits the KCl in a filter and the He gas is sent outh trough the fume hood. From this valve it can be sent to Direct Catch (DC). Here the aerosols are deposited on a filter which is possible to remove. The final tube sends the He gas into the chemical set-up.

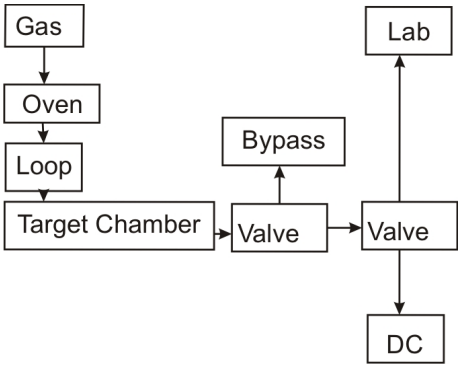

Fig. 4.3: A schematic drawing of a gas-jet system. This shows the gas path from the flask bank and trough all stations until it is sent to bypass laboratory or to DC.

4.2 The Tokai Tandem Accelerator

The Tokai tandem accelerator can accelerate ions from hydrogen to uranium. In this thesis a $^{7}Li^{+3}$ beam was used. The intensity of the beam at the initial targets was 1 μA and the energy was 62 MeV. A sketch of a tandem accelerator can be seen in Fig 3.5.

4.2.1 Tokai Target Chamber

During the work in this thesis several different targets were used. The same targets were used for all the experiments they were hold in an assembly, see fig 4.2.1 and fig 4.4 (see Table 4.3 where the target and beam strength are listed). In table 4.2 the different products from Tokai can be seen.

Tab. 4.2: The nuclei formed form the targets in the Tokai target set-up.

target	product	half-life
^{89}Y	^{93m}Mo	6.9 h
^{89}Y	^{91m}Mo	64.6 sec
^{89}Y	^{89m}Y	15.7 sec
^{89}Y	^{89m}Zr	4.2 min
^{175}Lu	^{93m}Mo	2.5 h

The beam from the tandem accelerator passes trough a mylar foil which is cooled by a He flow. Subsequently it strikes a Lu target, after this it passes trough 2 metallic Y targets, then it is degraded by a sheet of aluminium whereupon it strikes three new Y targets until it is finally deposited in the beam stop. The beam stop is cooled water.

Tab. 4.3: Configuration of the Tokai target ladder for experiments in Japan during spring 2013. The yttrium targets are metallic while the Lu target is electroplated on a beryllium backing. Energy degradation was calculated by M. Asai.

Material	Thickness (mg/cm^2)	Gap between targets (mm)	Particle energy at target (MeV)
Havar Foil [70]	2.11	5	62.0
Be	1.86	0	61.4
Lu	0.495	15	60.7
Y	11.2	20	60.4
Y	11.2	18	57.4
Al	37.8	0	54.2
Y	11.2	15	38.4
Y	11.2	10	34.1
Y	11.2	N/A	29.4

For a drawing of the target see Fig 4.4. A picture of the interior of the target chamber is shown in Fig 4.5. The specific beam energies and the distance between the targets can be seen in Table 4.3

The gas-jet setup in Tokai is similar to the set-up in Oslo. The difference is that the valves in Tokai are very quickly changed by hand. Additionally because when the gas-jet is changed to bypass, a helium gas flow will take its place and give the same flow rate and pressure on the chemical equipment. This means that the set-up is similar to the set-up that can be seen in Fig 4.3 with the only addition that there is an extra path going into the lab and keeping the pressure here constant.

4.3 Tokai Cf Fission Source

To enable experiments on tracer scale a spontaneously fissioning (SF) ^{252}Cf source was used. This nuclide has a half-life of 2.645 y and the SF branch is 3.092% [71]. The activity of the source used was 1.85 MBq on 1st Jan 2013. The fission products were transported by a gas-jet. This enabled us to test out the MDG and the SISAK system with a directly fission fragments. The nuclide used in these experiments was ^{104}Mo, with a half-life of 1 min.

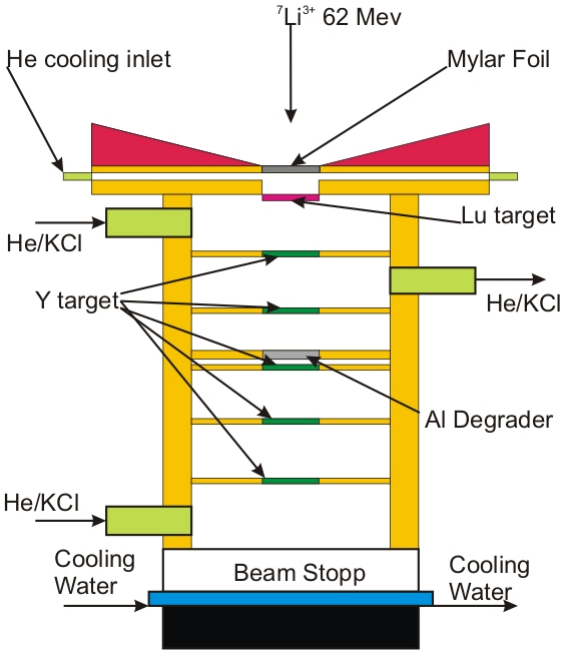

Fig. 4.4: Sketch of the Tokai target chamber which have the possibility to use several different materials as targets at the same time.

4.4 Set-up for Liguid-Liquid Extraction on Sg

4.4.1 SISAK Centrifuges

Essential to the SISAK system is the centrifuges which separate the two phases. The two liquid phases are mixed and then pumped into the centrifuge. Here the difference in density forces the heavier fluid outwards and the lighter fluid, inwards. The fluids comes out from two outlets at the top of the SISAK centrifuge. The outlets on the head have a throttles. When needed this throttle is used to tune the phase to enable an acceptable phase separation. In Fig 4.6 the SISAK system used in for Rf experiments [51].

The purity of the phases is detected by phase-purity monitors. They function by utilising a small LED-diode and a photo transistor. These function by utilising the refraction index of the fluids in the tubes. A small bubble of an entrainment will make the refraction index change. This is readily measurable and is continuously monitored.

4.4.2 Mixers

The mixers in the SISAK system are used to ensure that the phases are thoroughly mixed before they enter the centrifuge. There are several types of mixers used in the SISAK system. Only the ones that have been used during this thesis will be presented here.

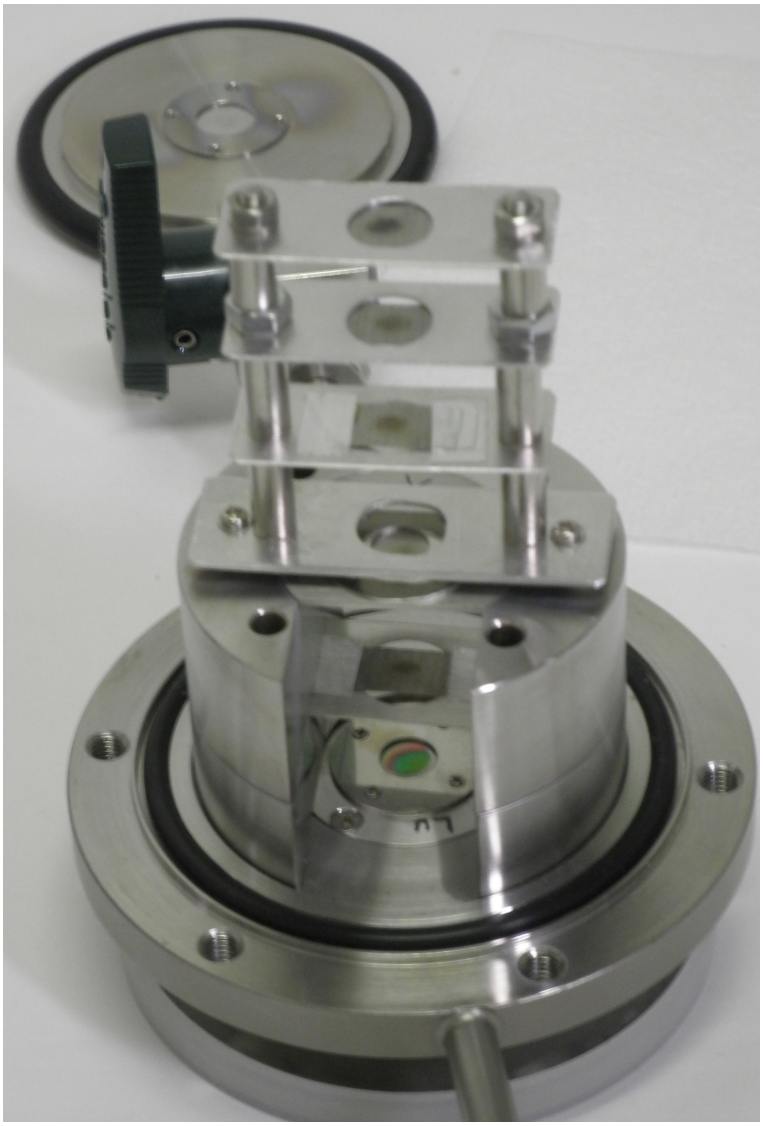

Fig. 4.5: Picture of the interior of the target chamber used in the Tokai tandem accelerator. Picture taken by Y. Kitayawa.

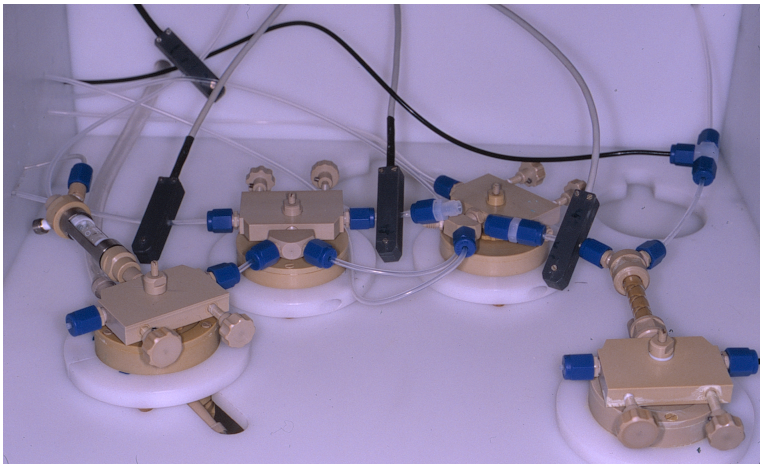

Fig. 4.6: Several SISAK centrifuges coupled in series with different types of mixers used as well as several phase-purity monitors. Picture taken by J. P. Omtvedt.

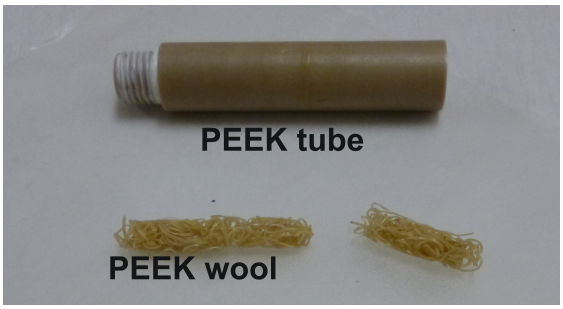

Fig. 4.7: A picture of the tube used for the PEEK-wool mixer. The amount of wool used is shown on the outside of the tube.

The most used type of mixer is a tube filled with PEEK shavings. This mixer type will be refereed to as PEEK-wool mixer. They consist of a hollow PEEK tube filled with PEEK shavings. This device gives a very efficient random mixing inside the tube. The amount of PEEK wool is weighed for each mixer, and the wool is packed into the mixer in a similar way each time. This is done so that the packing inside the mixer is uniform and fairly equal each time a mixer is prepared. It is important that there is not too much PEEK wool packed into the mixer as this can lead to a high back pressure. For a picture of the PEEK-wool mixer see Fig 4.7.

Another mixer used is called a ”zic-zac mixer”. In this mixer two inter-crossing milled tracks, giving a zic-zac pattern, were used to mix the two fluids. The tracks are connect to two different inlets and would ensure good mixing of the two phases. However the volume of this mixer is rather high compared to the PEEK mixer. A picture

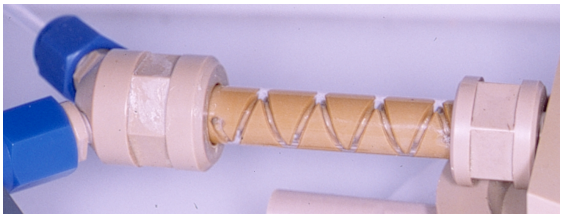

Fig. 4.8: A picture of the zic-zac mixer.

of the zic-zac mixer is shown in Fig 4.8.

4.4.3 Membrane Degasser

The Membrane DeGasser (MDG) was developed as preparation for a Sg-experiment. The main motivation behind this development was to reduce the amount of liquid needed to extract the radionuclides from the gas-jet. The MDG is a significant simplification to the previous method using a centrifuge degasser (CDG). The MDG consists of only static parts and the membrane inside is changeable if there is some structural damage on it. The optimum flow rate for the MDG is a factor ten lower than the optimum flow rate for the CDG. For a sketch of the MDG see Fig 4.9.

The MDG is made up of four parts: The top part, the middle, the membrane and the bottom part. The top part is coupled to a vacuum pump, this lowers pressure on the top side of the membrane so that the helium gas will be sucked out. The middle part is perforated with several holes and acts as a physical support for the membrane. The membrane separates the aquatic phase and the gas phase and rest upon the support grid of the middle part. The bottom part has an inlet where the aqueous phase and the gas phase is lead into the separation chamber. The aquatic phase carrying the aerosols and the radionuclides then leaves trough the outlet of the bottom part.

For the MDG to work there needs to be a certain pressure difference across the membrane. However, if the suction at the gas outlet is too high, or if there is to high liquid flow, the aqueous phase will go through the membrane.

Fluoropore membranes from Millipore with pore sizes of 0.2 μm, 0.45 μm, and 1.0 μm were tested during of this during. The smallest pore sizes were used as this was found to have the smallest chance of leaking.

The membrane will fail if there is any organic solution coming into contact with the membrane. This will clog up the pores in the membrane and force the He to pass through the aquatic outlet.

If the conditions are stable the MDG can run for many hours. Before the membrane must be changed.

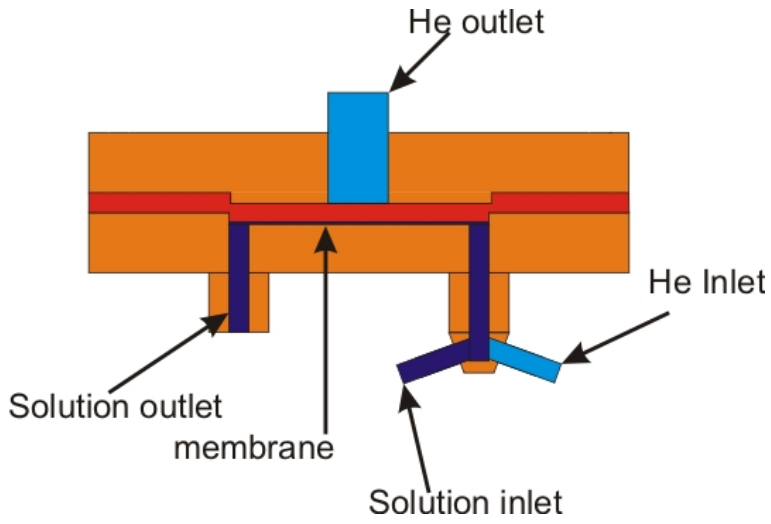

Fig. 4.9: A sketch of the MDG showing the path of the gas phase and the aqueous phase.

4.4.4 Flow Electrolytic Column

The working electrode is made of a bundle of glass-carbon fibre of 11 μm average diameter (GC-20, Tokai Carbon co. ltd.) that is packed in a porous Vycor glass tube (4.8 mm i.d., 7 mm o.d., 30 mm long, Corning co., ltd.). The porous glass tube is connected to the outlet and the inlet and kept tight with Teflon rings and O-rings on both sides. The porous glass tube is in a bath of the desired electrolyte. In this bath there is also lowered a Ag or Pt net bent around the porous glass tube. This net works as a counter electrode keeping the potential of the solution stable. As reference electrode an Ag|AgCl reference electrode from Metrohnom was used. The contact between the working electrode and the potentiostat is a rod made of glassy carbon.

Glassy carbon can also be referred to as ”vitreous carbon”. This type of carbon is hard and solid and it has a black, glassy appearance and fracture in a similar way to glass. Glassy carbon has low permeability of gas. This is because it contains significant amount of closed voids giving it a low density but it does not allow for continuous gas permeability. The structure of glassy carbon consists of long microfibrils that twist, bend and interlock and forms strong interfibrillar bonds [72]. Glassy carbon is desirable in electro-chemistry because it is highly resistant to chemical attack, electrically conductive, available in high purity, and it has a high potential window [73]. The glassy carbon rods used were cut to appropriate length and had a diameter of 1.5 mm.

The liquid is pumped into the FEC. Once entering the FEC it comes into contact with the carbon fibre and efficiently reduce the metal ions.

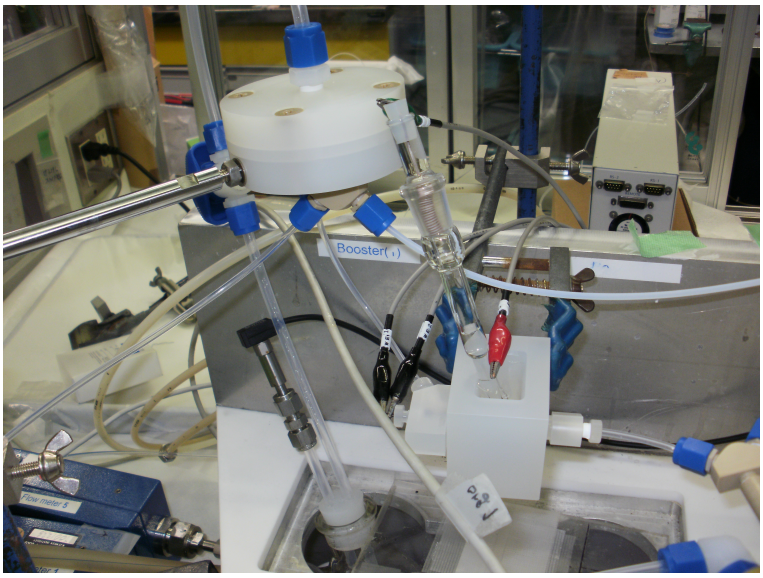

Fig. 4.10: A picture of the FEC coupled together with the MDG. In the lower right part of the picture it is possible to see the tube connecting the FEC to the SISAK mixer and centrifuge.

5. EXPERIMENTAL PROCEDURES

5.1 MDG Performance

To test the yield of the MDG the gas-jet was directly deposited on a filter. This filter was then dissolved in the desired amount of liquid. The dissolved filter was measured with an HPGe (High Purity Germanium Detector) detector. The filter was assumed to give the maximum yield. Therefore, subsequent samples from the MDG were compared to this value. With regular intervals a filter was measured to ensure that there was no change in the yield from the target chamber.

5.2 Test of FEC With Different Flow Rates and Different Amounts of Packing

The FEC was tested with different amounts of carbon fibre packed inside the porous glass tube. The carbon fibre was winded around a 6 cm wide cardboard sheet. After a sufficient amount of carbon fibre was measured out it was packed inside the porous glass tube. This was done by shaping a paper clip as a hook and using this hook to drag the carbon fibre into the tube. The parts of the carbon fibre sticking out of the tube were the cut off and the FEC was assembled. A double plunger HPLC pump was used to pump the fluid into the FEC. The back pressure was read of the pump and it was measured at different pump speeds and with different amount of carbon fibre inside the tube.

5.3 Cyclic Voltammetry on W and Mo in Different Aqueous Solutions

The solutions were made by weighing out K_2MoO_4 and K_2WO_4. These solutions where then injected into the FEC using a six-port Rheodyne valve and a two piston HPLC pump. With each solution change a blank measurement was performed. The blank measurements were performed using the same solutions but lacking the metal that was to be reduced. The potentiostat used was a Hokuto Denko potentiometer HSE-100. 4-5 scan cycles were used on the samples and the cycles went from 0.0 V to 1 V to -1 V vs a Ag |AgCl electrode in 1 M LiCl solution. The scan rate was 20 mV/s.

5.4 Aerosol Generation

To carry the activity from the target area, aerosols suspended in a helium gas stream was used. All aerosols were created by sublimating KCl in a tube oven at 640 ^{o}C. The aerosols were carried in a helium gas stream, which subsequently to leaving the oven passed through a coil to remove the largest aerosols.

5.5 Batch Experiments

Several different methods were used to perform batch experiments. For the different results which method used will be indicated.

5.5.1 Experimental Procedure used in Tokai

The activity was deposited on a teflon filter (Naflon), with an area approximately 1.5 cm^2 it was acquired for 3 min. The gas-jet flow was 1.5 L/min. The filter was then washed with 100 μL of the aqueous solution. The solution was then added to 600 μL aquatic solution in a plastic vial. Subsequently, 700 μL organic solution was added. After shaking with a Vortex mixer for 3 sec to 300 sec, the mixed sample was centrifuged for 30 sec. From both phases, 500 μL were separated into 2 vials. The samples were then measured by γ-spectroscopy with HPGe detector.

In this procedure the HPGe detectors were calibrated by measuring two different active filters dissolved in equal amount of fluid as used in the experiment.This then gave rise to a efficiency ratio between the two detectors ϵ:

$$\epsilon = \frac{C_{sol1}}{C_{sol2}} \tag{5.1}$$

Where C_{sol1} and C_{sol2} is the number of counts for the dissolved sample. Because of this formula 3.1 is changed to:

$$D = \frac{A_{org}}{A_{aq}\epsilon} \tag{5.2}$$

Here A_{aq2} and A_{org1} are the count rates in each phase.

5.5.2 Experimental Procedure used in Oslo

The activity was deposited on glass fibre filter (a Whatman grade GF/C 5.0 cm lot, no 1822-056). The activity was gently washed off the filter. Then 4 mL of the aqueous solution was mixed with 4 mL of the organic solution, thoroughly mixed by shaking for 5 min and centrifuged at 2000 RPM for 2 min. After this the organic and the aqueous

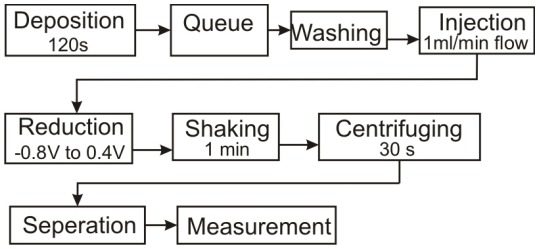

Fig. 5.1: Flow chart of the procedure for batch experiments performed with the FEC.

phase were sampled with an automatic pipette. 3 mL of the least dense phase was first extracted then the last mL was discarded, together with the pipette used. Subsequently 1 mL of the top layer was withdrawn and discarded, together with the pipette used. Then the remaining 3 mL aqueous phase was extracted.

In this procedure only one detector was used therefore no efficiency calibration was needed.

5.5.3 Reduction and Subsequent Extraction Using FEC in Tokai

This was performed in the same way as the procedure described in chapter 5.5.1 Experimental Procedure used in Tokai. The only difference was that before the aqueous phase was mixed with the organic phase, for extraction, it was passed through the FEC. The potential of the FEC was changed when needed. For a flow chart of this procedure see Fig 5.1.

5.5.4 Reduction and Extraction Using FEC in OCL

The activity was deposited on glass fibre filter (a Whatman grade GF/C 5.0 cm lot, no 1822-056) . This glass filter was then inserted into a reagent tube where it was gently washed so that as little as possible of the glass fibre would be dissolved in the solution. This solution was then diluted and fed into the FEC using a cogwheel pump (Micropump). The solution in this experiment was pumped in a circuit: The outlet of the FEC was feed back into the flask holding the solution to be pumped into the FEC. 4 mL samples were collected from the outlet of the FEC and mixed with 4 mL organic solution. This was then shaken for 5 min by a vortex shaker and then subsequently centrifuged at 3 kRPM for 2 minutes. The LLE was performed as described in chapter 5.5.2, Experimental Procedure used in Oslo. For a diagram of the experiment see Fig 5.2

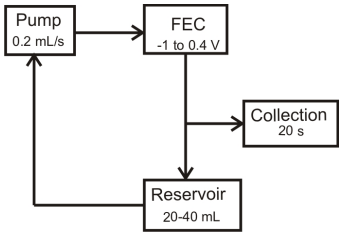

Fig. 5.2: Schematic drawing of reduction experiments done in OCL. The inlet to the pump was placed in the bottom of the reservoir, collection of samples were always done at the outlet of the FEC.

5.6 On-Line Experiments with SISAK

The gas-jet was connected to the MDG with a flow varying from 1.3 to 1.6 L/min in Japan and 1.8 L/min in Norway. The aqueous phase was pumped into the MDG with speeds varying from 0.1 mL/s to 0.4 mL/s. The organic and aqueous phase was then connected by a Y-connector before they either were sent into a mixer or connected directly to the SISAK-centrifuge. Two phase purity meters were connected to the outlets.

To test reduction and extraction together the set up was the same as a normal extraction experiment with SISAK, except that the FEC was connected after the MDG and before the SISAK centrifuge.

5.6.1 D-ratios for Online Experiments

Deciding the D-ratios of the SISAK experiments were done in two different ways. In data from experiments performed in Tokai the calculations were done as described in chapter 5.5.1, Experimental Procedure used in Tokai.

However in Oslo the process was slightly different. In Oslo two different detectors but these have different amount of shielding and geometry. These detectors will be called detector 1 and detector 2. The efficiency difference between these two detectors were not measured. Instead, a sample was collected and the aqueous phase was counted by detector 1 and the organic phase was counted by detector 2. When the next sample was collected the organic phase was counted by detector 1 while the organic phase was counted by detector 2. Therefore the following can be derived [74]:

$$C = \epsilon I_\gamma A \tag{5.3}$$

Here C is the count rate, ϵ is the efficiency of the detector, I_γ is the intensity of the incident γ-ray and A is the activity of the sample. Formula 3.1 shows how we calculate

the D-ratio. Using formula 5.3 to calculate the D-ratio the result is:

$$D = \frac{\epsilon_1 I_\gamma A_{Org1}}{\epsilon_2 I_\gamma A_{Aq2}} \tag{5.4}$$

Here ϵ_1 is the efficiency of detector 1 and ϵ_2 is the efficiency of detector 2. A_{org1} is the activity of the organic phase while A_{Aq2} is the activity of the aquatic phase. The intensity of the γ particles cancels each other. Combining this with formula 5.4 where the organic solution has been measured in detector 2 and aqueous has been detected in detector 1 we get:

$$D^2 = \frac{\epsilon_1 A_{Org1} \epsilon_2 A_{Org2}}{\epsilon_1 A_{Aq1} \epsilon_2 A_{Aq2}} \tag{5.5}$$

From formula 5.5 ϵ cancel out and the D-ratios can be presented as:

$$D = \sqrt{\frac{A_{org1} A_{org2}}{A_{Aq1} A_{Aq2}}} \tag{5.6}$$

This procedure for calculating the D-ratios is often used in Oslo it has been described in several Masters thesis's from Oslo e.g. [74]

5.6.2 Estimation of Transfer Time in SISAK mixers

The transfer time Δt in SISAK wool mixer and in the zic zac mixer was estimated by the formula:

$$\Delta t = \frac{V}{F} \tag{5.7}$$

Where V is the volume of the mixer and F is the flow rate in mL/s.

5.7 Titration of Solutions

TOA is an anion extractant. To examine if it would extract the equivalent base of the acids used, extraction experiments with subsequent titrations were performed. The extractions where performed as described in chapter 5.5.2, Experimental Procedure used in Oslo but without any activity. The extracted solutions were then titrated with a Metrohm 877-titrion plus. The base used was 0.1 M NaOH. The change in acid concentration will be expressed as:

$$\frac{E}{A} \cdot 100 = L \tag{5.8}$$

Where E is the titration endpoint after mixing with TOA and A is the titration endpoint before mixing with TOA, L then represent the % acid left in the solution.

6. EXPERIMENTS AND RESULTS

6.1 Results from MDG Experiments

A certain pressure difference across the membrane is needed to achieve gas/liquid separation. This became relevant when a mixer was put in front of the MDG: This led to a pressure drop and separation between gas and aqueous phase became impossible. In addition the liquid flow quickly started fluctuating making it impossible to separate the organic and the aqueous phase. Thus, these experiments were performed without mixer in front of the MDG. However the yield of the MDG still exceeded 70% without mixers. The MDG seemed to work best when the flow rate was around 0.2 mL/s. For lower flow rates it was difficult to achieve phase separation with the SISAK mixer. A more thorough analysis is given in [19].

6.2 Results from Tests of FEC With Different Flow Rates and Different Amounts of Packing

There is a limit to how much pressure difference the target chamber can handle. The pressure in the target chamber in Tokai should not exceed 1.5 bars. Therefore the back pressure from the FEC was measured using several different measurements of carbon fibre. The surface area and numbers of carbon fibre was calculated from [28]. The amount of carbon fibre previously used in reduction experiments with this cell was $1.4{\cdot}10^5$. This generated a too high back pressure and a suitable amount of fibre was found to be $0.9{\cdot}10^5$ carbon fibres. In Table 6.1 how the back pressure is affected by carbon fibre amount and flow rate is shown.

6.3 Results from Cyclic-Voltammetry on W and Mo in Different Aqueous Solutions

In total six different solutions were made with a volume of 50 mL. The solutions were:

1. 0.01 M Mo in a solution of 10^{-3} HCl, 10^{-4} M HF, and 1 M LiCl (Fig 6.1a.).
2. 0.01 M Mo in a solution of 0.1 M HCl, $10^{-}4$ M HF, and 0.1 M LiCl (Fig 6.1b.).

Tab. 6.1: Testing FEC back pressure under different conditions.

Surface (cm^2)	sum of carbon fibre	Flow	Pressure (MPa)
1500	$1.4 \cdot 10^5$	0.4	0.7
1500	$1.4 \cdot 10^5$	0.3	0.4
1500	$1.4 \cdot 10^5$	0.2	0.2
1333	$1.2 \cdot 10^5$	0.4	0.1
1333	$1.2 \cdot 10^5$	0.2	0.1
1167	$1.1 \cdot 10^5$	0.4	0.0
750	$0.7 \cdot 10^5$	0.4	0.0
500	$0.5 \cdot 10^5$	0.4	0.0

3. 0.01 M Mo in a solution of 0.1 M HCl and 0.9 M LiCl (Fig 6.1c.).
4. 0.01 M W in a solution of 10^{-3} HCl, 10^{-4} M HF, and 1 M LiCl (Fig 6.2a.).
5. 0.01 M W in a solution of 0.1 M HCl, 10^{-4} M HF, and 0.1 M LiCl (Fig 6.2b.).
6. 0.01 M W in a solution of 0.1 M HCl and 0.9 M LiCl (Fig 6.2c.).

Before reduction with trace amounts was started, cyclic voltammetery measurements with macro amounts. This was done to check if there was an observable reduction taking place. For all experiments performed with 0.1 M HCl there is clearly a reactions occurring. On the cathodic sweep there are several peaks showing change in the current as can be seen in Figs 6.1c, 6.1b, 6.2b and 6.2c. However with the low acid concentration there does not seem to be a reaction, neither for tungsten nor molybdenum, as can be seen in Figs 6.1a and Fig 6.2c.

6.4 On-Line Experiments with SISAK

These experiments was performed as described in 5.6. The SISAK system is essential to future experiments with Sg, thus it is very important that the FEC and SISAK can be used together.

For these tests a 0.1 M HCl + 0.9 M LiCl solution was tested together with HT to see if it was possible to achieve separation of Mo(VI) and W(VI) with Mo(IV) and W(IV). In Fig 6.3 D-ratio as a function of the potential is shown. This shows that the is it possible to use the SISAK and FEC together and achieve a different D ratio as a function of the voltage.

The kinetics of HT was tested with PEEK wool mixer at different length. The results can be seen in Table 6.2. Due to the limitations on back pressure in the Tokai target chamber it was not possible to use more PEEK wool or longer mixers.

Back pressure with the SISAK system together with the MDG was tested with different amount of PEEK wool in the mixers. These tests were performed using the ^{252}Cf

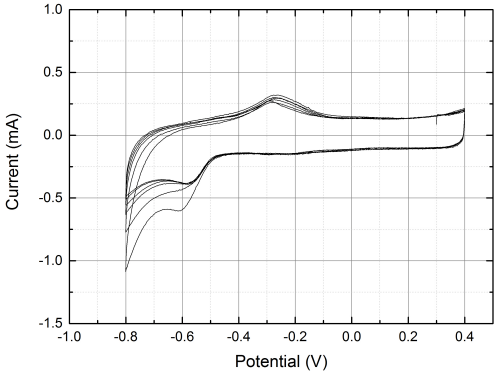

(a) Aquatic solution 0.01 M Mo in 10^{-3} M HCl + 1 M LiCL + 10^{-4} M HF

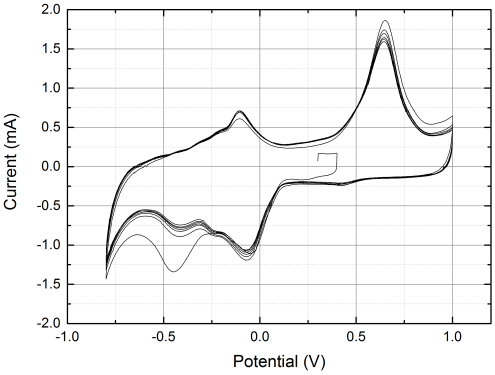

(b) Aquatic solution 0.01 M Mo in 0.1 M HCl + 0.9 M LiCl 10^{-4} M HF.

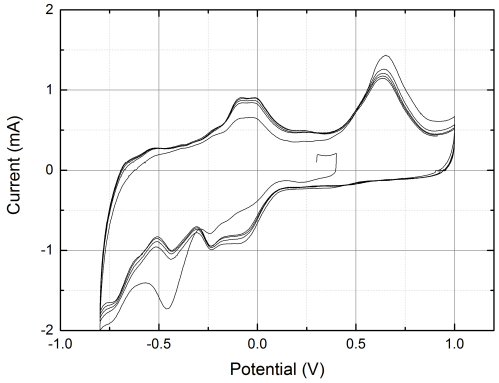

(c) 0.01 M Mo in a solution of 0.1 M HCl and 0.9 M LiCl.

Fig. 6.1: Cyclic voltammetry on Molybdenum in different aqueous solutions

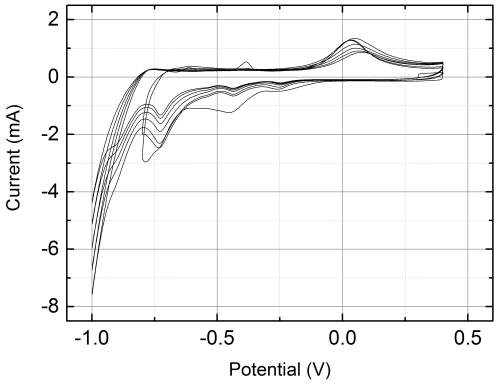

(a) Aquatic solution 0.01 M W in 0.1 M HCl + 0.9 M LiCl 10^{-4} M HF.

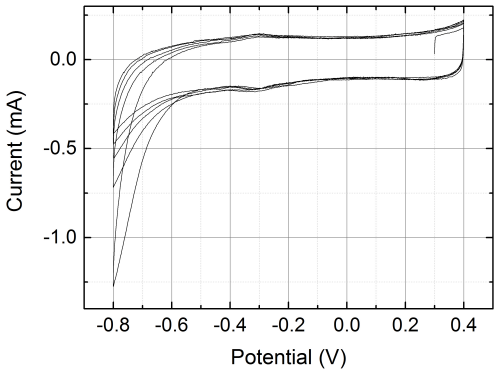

(b) Aquatic solution 0.01 M W in 10^{-3} M HCl + 1 M LiCL + 10^{-4} M HF .

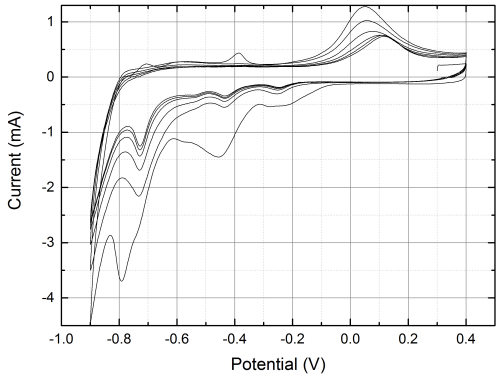

(c) 0.01 M W in a solution of 0.1 M HCl and 0.9 M LiCl.

Fig. 6.2: Cyclic voltammetry on Wolfram in different aqueous solutions

Tab. 6.2: Different lengths of mixer filled with different amount of PEEK wool. The D-ratio presented and the aqueous solution used was 0.1 M HCl with 0.9 M LiCl. The concentration of the extractant was 10^{-3} M HT in toluene. A simple "plug flow" was assumed for the Δt calculations.

Length Wool Weight (cm/mg)	D-ratio ^{104}Mo	Back Pressure (bar)	Δt (0.2 mL/s)
2/152	0.5±0.1	1.36	0.3
4/113	0.64±0.07	1.34	1
4/190	0.7±0.1	1.35	0.8
4/288	0.7±0.2	1.56	0.6
4/0	0.63±0.03	1.3	1.3
2/0	0.3±0.1	1.3	0.6
5.2/325	1.2±0.1	1.4	0.3
Zic Zac mixer	0.8±0.1	1.3	1.3

fission source. Results from this can be seen in Table 6.2. This shows the D-ratio, back pressure and an estimated residence time for the different mixers.

6.5 Batch Experiments Results

The following experiments were performed with the methods described in chapter 5.5, Batch Experiments. All lines in graphs are to guide the eye.

6.5.1 Extraction and Reduction Using Hinokitiol (HT)

For these experiments the method described in chapter 5.5.3 Reduction and Subsequent Extraction Using FEC in Tokai was used. The following experiments were performed with the hypothesis put forth in chapter 3.5.1 The Oxidized Specie is a Cation.

The D-ratio of Mo and W was tested as a function of voltage. These experiments showed that HT does manage to separate between the reduced and the oxidized species. However, there is a large difference in the D-ratio between W and Mo. In addition the difference in the D-ratio for W is so small that any difference between negative potential and high potential could be due to uncertainty (see Fig 6.4). The aqueous solution in this experiment was 0.1 M HCl + 0.9 LiCl.

In Fig 6.5 a minute amount of HF was added to the solution to see if this helped the separation factor. The aqueous solution used in the graph on the right was 0.1 M HCl + 0.01 M HF + 0.9 M LiCl. The aqueous solution used for the graph on the left was 0.1 M HCl + 10^{-3} M HF + 0.9 M LiCl There seems to be a slightly larger difference between the negative and the positive potential for W.

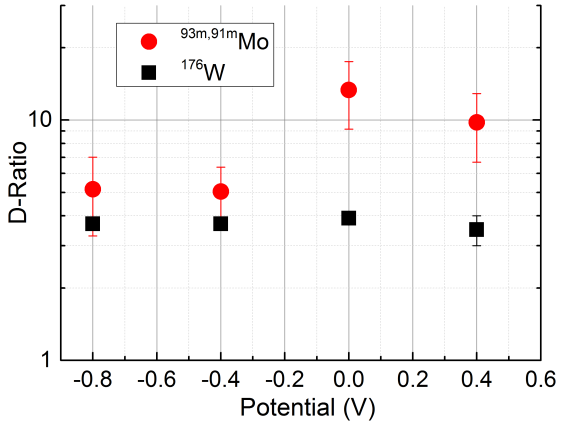

Fig. 6.3: Reduction of tracer amount of Mo. This experiment was done on-line using SISAK. The flow rates of both phases were 0.2 mL/s. The mixer used was 4 cm long filled with 190 mg of PEEK wool. The concentration of HT was 0.01 M in toluene.

In an effort to purify the solution before reduction, an additional FEC set to a constant voltage of -0.8 V was used to pre-treat. The acid solution before dissolved the gas-jet carried activity. The intention was to remove oxygen and any other impurities in the solution. Results can be seen in the right graph in Fig 6.4. Comparing this to the left graph in Fig 6.4 or Fig 6.5 there is an intriguing dip at a -0.2 V that does not occur in the other experiments. However there are too few experimental points to say anything conclusive.

The data presented in Fig 6.6 were obtained under conditions were the oxidized species should be a anion and the reduced species should be a cation. Using 10^{-4} M HCl + 1 M LiCl a small difference in D-ratio was obtained. However this was in opposition to the hypothesis put forth in 3.5.2. This can be explained by the high chloride content in the solution. Which will form more easily form negative complexes.

6.5.2 Extraction of Zr and Mo Using HDEHP and TOA

The experiments in Fig 6.7, 6.9 and 6.8 was performed by the method described in chapter 5.5.2, Experimental Procedure used in Oslo. Using an aerosols gas-jet with a flow rate of 1.8 L/min.

Using the aqueous solution 0.1 M H_2SO_4 + 0.01 M HF gives a high separation factor with the extractant TOA, however there is still more than 50% of Zr extracted as can be seen in the left graph of Fig 6.7. The right graph of Fig 6.7 shows how Zr and Mo is extracted by HDEHP. The two elements seem to have a similar D-ratio. There is a change when the concentration of HDEHP in toluene is 0.5 M where the D-ratio of Mo increases while Zr D-ratio drop.

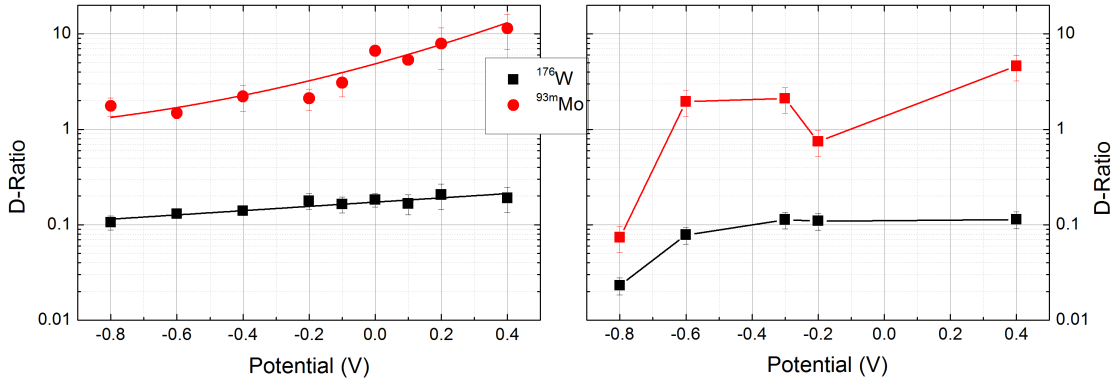

Fig. 6.4: Reduction of Mo and W in aqueous solution of 0.1 M HCl + 0.9 M LiCl, extracted using 10^{-4} M hiokitiol in toluene. Graph to the left only uses the FEC to reduce, while to the right uses an additional FEC to purify the solution prior to reduction.

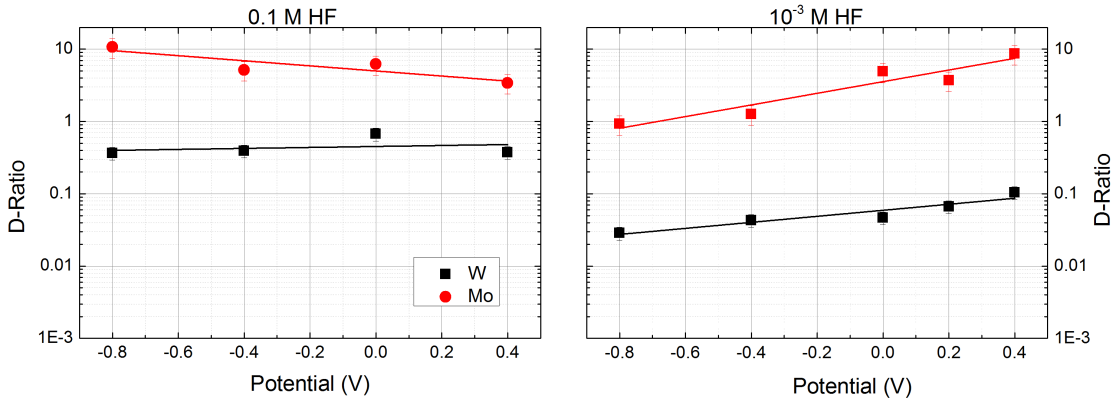

Fig. 6.5: Reduction with different concentrations of HF solution. To the right an aqueous solution of 0.1 M HCl + 0.9 M LiCl + 10^{-3} M HF, extracted with 10^{-4} M HT in toluene. To the left 0.1 M HCl + 0.9 M LiCl + 0.01 M HF, extracted with 0.01 M HT in toluene.

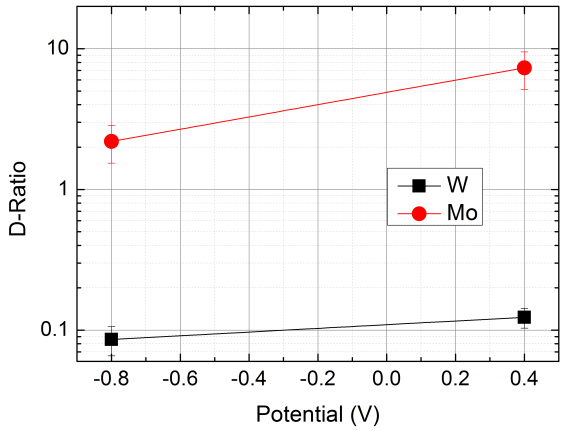

Fig. 6.6: Reduction in an aqueous solution of 10^{-4} M HCl + 1 M LiCl, extracted with 10^{-4} M HT in toluene.

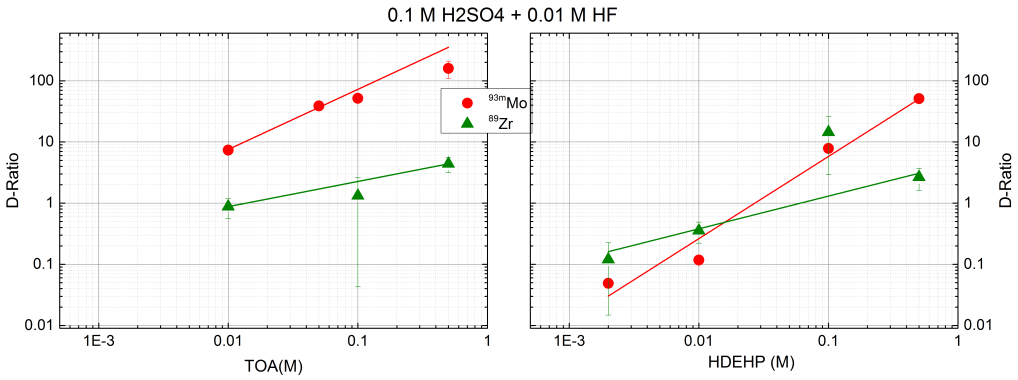

Fig. 6.7: Extraction of Zr and Mo in 0.1 M H_2SO_4 + 0.01 M HF. In the left graph different concentrations of TOA was used as an extractant. In the right graph different concentrations of HDEHP was used as an extractant.

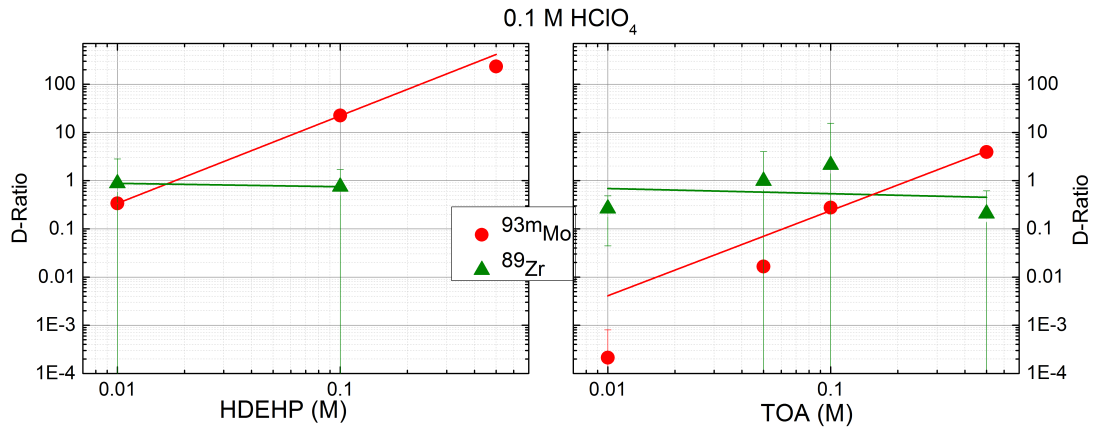

Fig. 6.8: Left graph show extraction of Zr and Mo from 0.1 M $HClO_4$ with different concentration of HDEHP in toluene. Right graph shows extractions of Zr and Mo from 0.1 M $HClO_4$ with different concentrations of TOA.

To check how a weaker adduct forming acid would make the Zr and Mo react some tests were run with this acid as well see Fig 6.8 for extractions in 0.1 M $HClO_4$ with different concentrations of HDEHP and TOA in toluene.

How 0.01 M HF concentrations would affect the extractions of Zr and Mo was also tested in 0.1 M $HClO_4$.

HDEHP was tested as an extractant for the reduced form of Mo. This experiment was performed as described in chapter 5.5.4, Reduction and Extraction Using FEC in OCL. Fig 6.10 show the results. The aquatic solution was 0.1 M H_2SO_4 + 0.01 M HF. The organic was 0.1 M HDEHP in toluene. From this it becomes clear that HDEHP manages to separate between two oxidation states. However, the distribution of the D-ratio at the negative potential is rather wide. Therefore, the solution was sent several times through the FEC, at a potential of -0.8 V, and after each pass a small amount was sampled. This was done to see if the D-ratio was affected by the contact time with the working electrode. The results from these extractions can be seen in the left graph of Fig 6.11. The stability of the reduced species was tested by leaving a sample alone on the laboratory bench for up to 4 hours. The solution was sampled at increasing intervals to see if there was a change in the D-ratio. The results from these experiments can be found in the right graph of Fig 6.11.

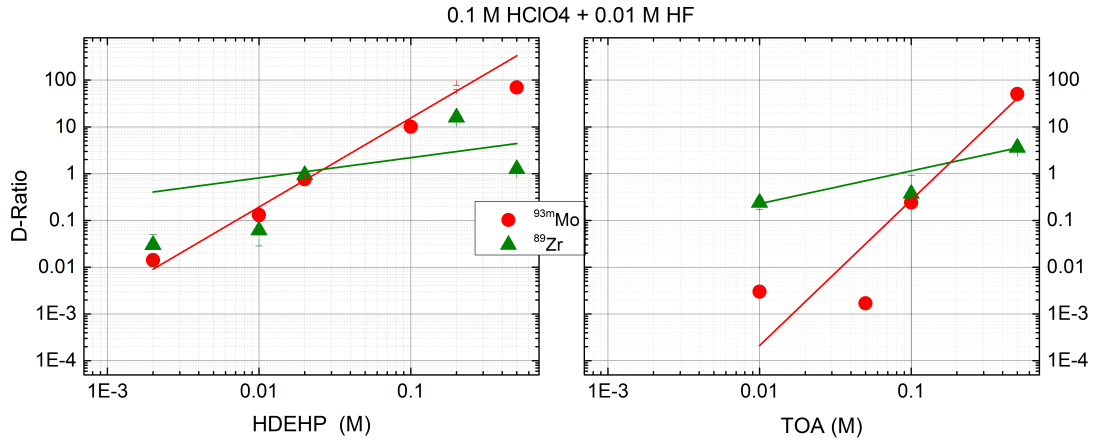

Fig. 6.9: Left graph show extraction of Zr and Mo from 0.1 M $HClO_4$ + 0.01 M HF with different concentration of HDEHP in toluene. Right graph shows extractions of Zr and Mo from 0.1 M $HClO_4$ +0.01 M HF with different concentrations of TOA.

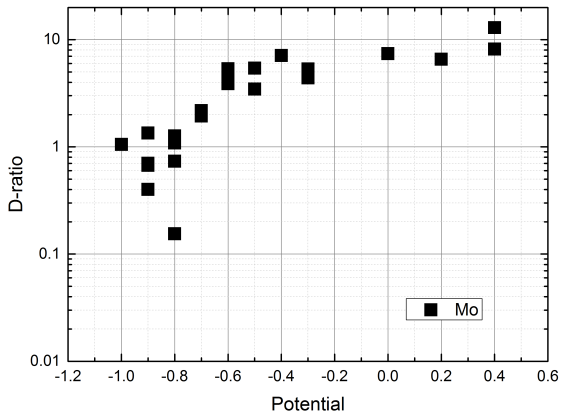

Fig. 6.10: Reduction of Mo when the solution is pumped in a loop.

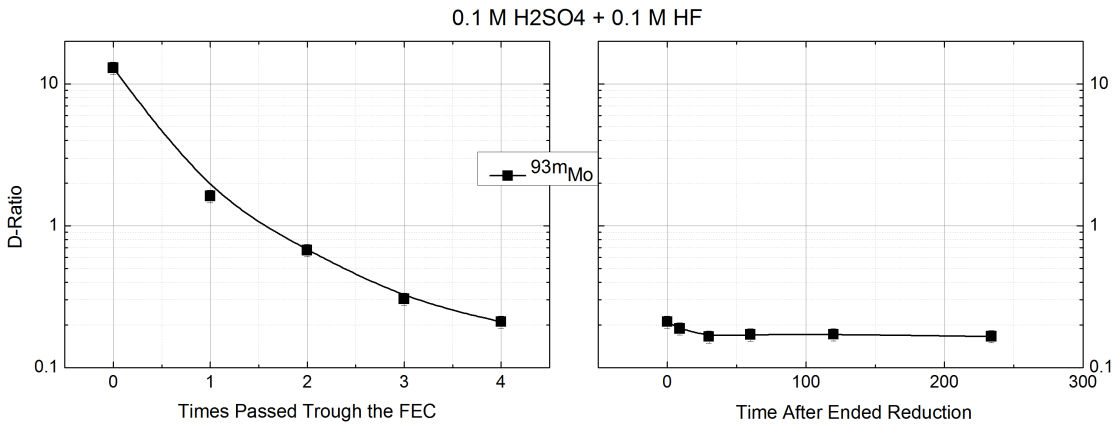

Fig. 6.11: The left graph shows reduction of Mo at room temperature with 0.2 mL/s flow, and an aqueous solution of 0.1 M H_2SO_4 + 0.01 M HF. The reduction is shown as a function of number of times the solution was passed trough the FEC. The first point for the graph on the right is the last point for the graph on the left. The right graph shows how the D-ratio changes as a function of time, when the solution is in contact with air.

6.6 Data Received from Collaborators in Japan

Several experiments where performed in Japan were Oslo participated in planning the experiments. The results from these experiments will be presented here. These experiments were performed as described in chapter 5.5.1 Experimental Procedure used in Tokai. Uncertainty in the data was estimated as outlined in chapter 7.2 Uncertainty Estimations.

The aqueous solution 0.1 M H_2SO_4 + 0.1 M HF extracted by varying HDEHP concentrations in Fig 6.13.

In systems dominated by sulphuric acid the D-ratio of W seems to change in opposition to the D-ratio of Mo as a function of voltage, see Fig 6.12

Extraction and reduction of Mo and W in 0.1 M $HClO_4$ and the concentration of extraction agent TOA was 0.5 M (see Fig 6.15).

Several experiments were performed to check if there was a difference in reduction as a function of H_2SO_4 concentration. In Fig 6.16 and Fig 6.17 the $HClO_4$ concentration was kept constant while H_2SO_4 was tested with different concentrations.

Reducing W and Mo in 0.1 M H_2SO_4 + 0.1 M $HClO_4$ and extracting with 0.2 M TOA in toluene seems to have a high difference in the D-ratio for Mo but not for W, as can be seen in Fig 6.17. Due to the high separation managed with the 0.1 M H_2SO_4 + 0.1 M $HClO_4$ solution it was tested if the separation would increase at higher TOA concentrations. In Fig 6.18 the results from this shown.

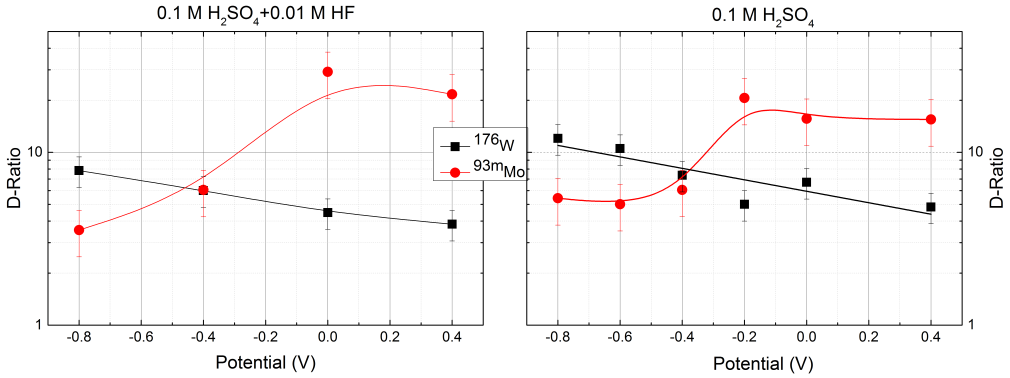

Fig. 6.12: Reduction of W and Mo in H_2SO_4 solutions extracted with 0.1 M TOA in toluene. Left graph has an aqueous solution of 0.1 M H_2SO_4 +0.01 M HF while the right graph has an aqueous solution of 0.1 M H_2SO_4. 1 mL/min flow rate was used.

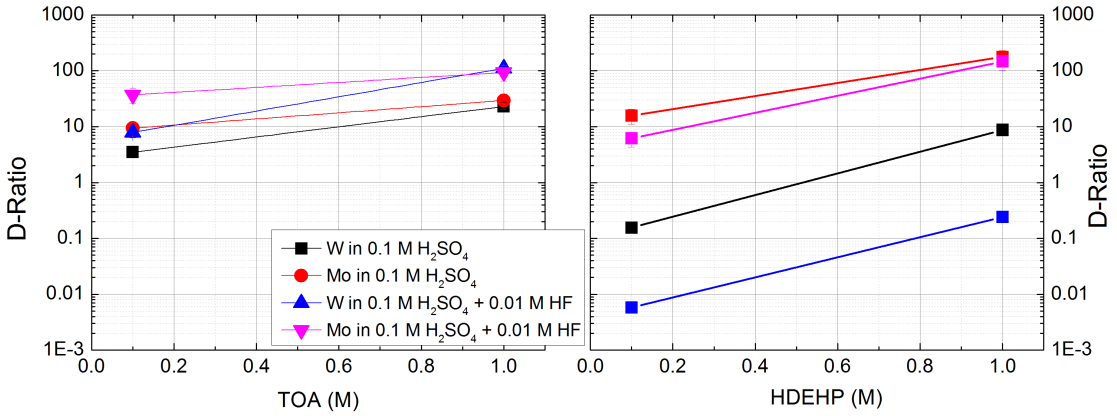

Fig. 6.13: Extraction of Mo and W isotopes from different H_2SO_4 solutions. With varying concentration of HDEHP in the right graph and varying concentrations of TOA in the left graph.

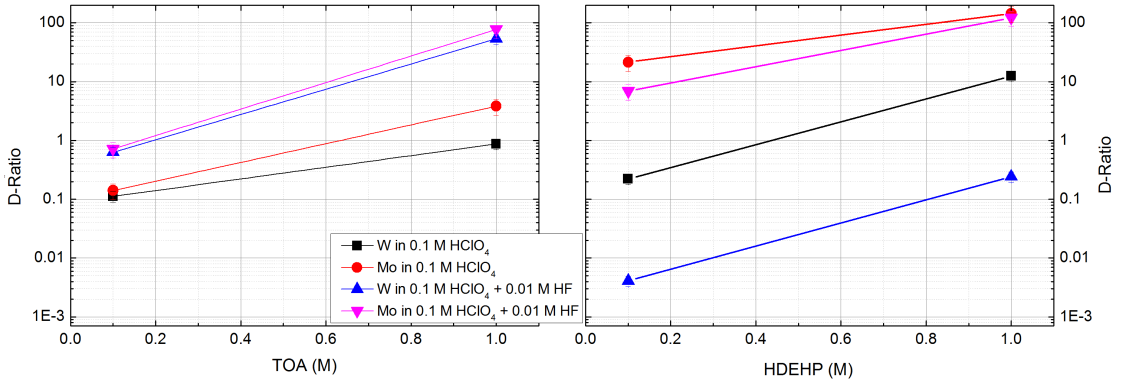

Fig. 6.14: extraction of Mo and W in different $HClO_4$ solutions extracted with different HDEHP concentrations on the graph to the right and to the left different concentrations of TOA.

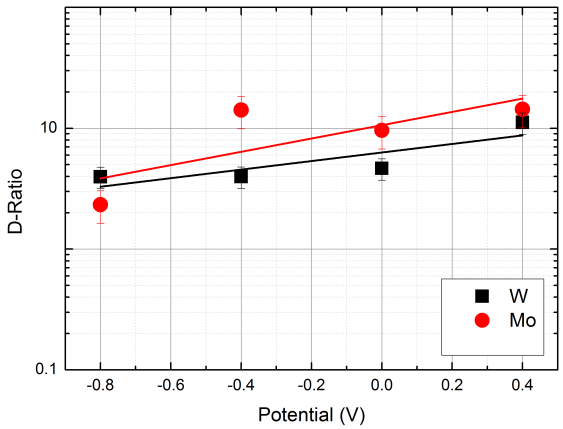

Fig. 6.15: Reduction of Mo and W in 0.1 M $HClO_4$. Extractant used 0.5 M TOA.

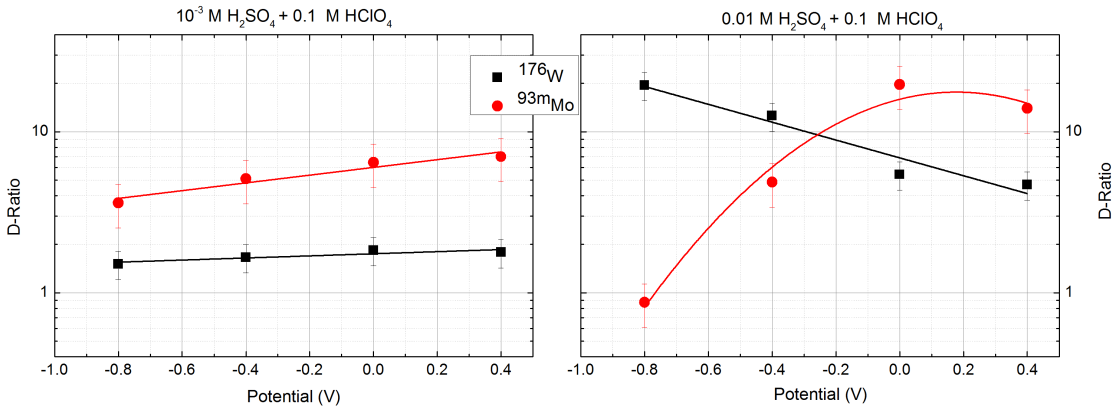

Fig. 6.16: Reduction and extraction of ^{176,177}W and ^{93m}Mo. The left graph shows in 10^{-3} M H_2SO_4 and 0.1 M $HClO_4$ while the right graph shows in 0.01 M H_2SO_4 and 0.1 M $HClO_4$ solution . Extractant used was 0.2 M TOA in toluene.

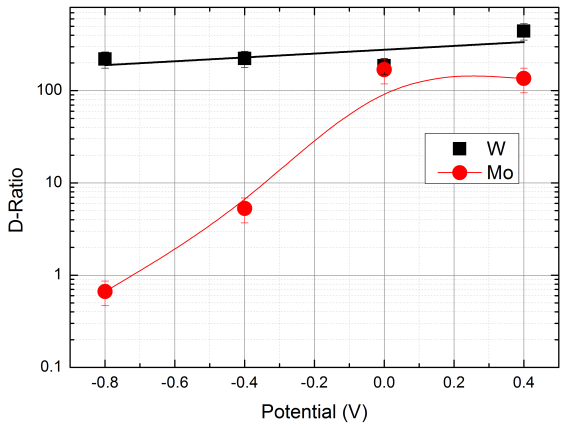

Fig. 6.17: Reduction of W and Mo in 0.1 M H_2SO_4 + 0.1 M $HClO_4$ extracted with 0.2 M TOA.

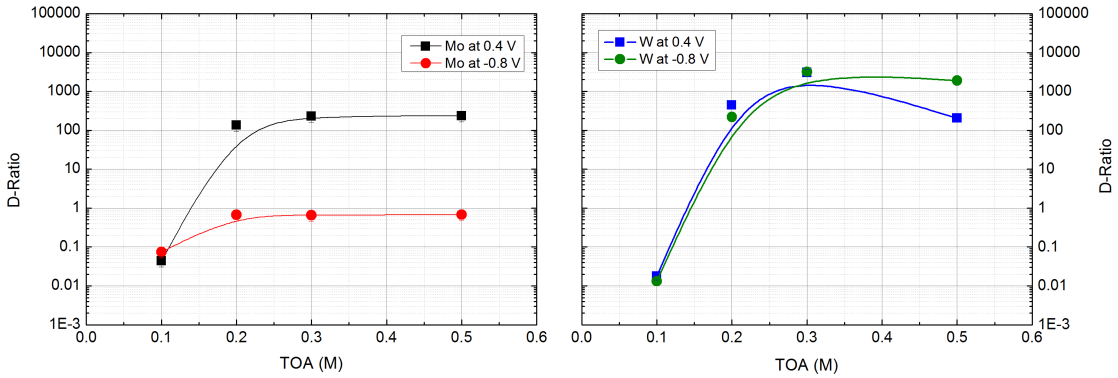

Fig. 6.18: D-ratio of of Mo to the left and W to the right at different potential shown as a function of TOA concentration. The aqueous solution used was 0.1 M H_2SO_4 + 0.1 M $HClO_4$.

6.7 Results from Titration of Solutions

0.1 M concentraions of $HClO_4$ and H_2SO_4 was extracted with 0.1 M TOA. The organic and the aquatic phase was seperated and the aquatic phase was measured with 0.1 M NaOH solution. Using formula 5.8 the remaining quantity of H_2SO_4 was measured to be 0.46 M $\pm$ 0.04. of the starting concentration the remaining quantity of the $HClO_4$ was measured to be 0.01 M $\pm$ 0.03.

7. DISCUSSION AND CONCLUSIONS

The work presented in this thesis is part of a large and ambitious project to measure reduction potentials for element 106, seaborgium. The project is a collaboration between the Super-Heavy Element research groups in Oslo and Tokai (headed by Prof. Omtvedt and Dr. Schädel, respectively). The thesis work and the overall project started simultaneously, which have provided the opportunity to be 100% involved right from the start and participate in all discussions and developments. However, it also implies that the foundation for this thesis work was rather thin. As a result, many experiments were performed which provided fundamental and important insight into equipment and chemistry limitations. However it did not necessarily yield directly applicable results for the construct of the final apparatus and chemical system reduction studies on seaborgium. On the contrary, as the work progressed it has become clear how challenging the task really is.

An example of this is that quite recent experiments in Tokai (March 2014) pointed out that there is a problem with retention of reduced Mo (and possibly W, but no direct experimental evidence on this is currently available) inside the FEC. After lengthy discussions and considerations, Prof. Kratz (Mains Univ.) suggested that retention was due to the underpotential effect. This is an effect where the metal is reduced to the elemental state at a more positive potential than calculated: This is because the binding energy between the elemental metal and the working electrode is high enough to overcome the barrier for reduction to the elemental state [75]. As a consequence, this put in question the interpretations of some of the results obtained in this thesis work. Further experiments is needed to clarify the correct interpretation, but with the limited time-scope of a MSc thesis (and availability of beam-time), it is not possible to perform these experiments before the thesis is handed in. This is just one illustration of the complexity of the undertaken project. In fact, in a recent meeting in Tokai (26th - 27th March 2014), the project leaders decided to redefine the project from the original 3-5 year project (ending with conclusive seaborgium experiments in 2014/2015) to a be an initial study of the applicability of reduction-extraction method (FEC coupled with SISAK) to studies of super-heavy elements. After 1-2 years further work the status will again be reviewed and a decision made whether or not to proceed with a Sg experiment.

7.1 Discussion

All experiments performed have been performed at room temperature. This is because the final extraction scheme has yet to be decided. Therefore the focus have been to find a suitable extraction scheme. Heating the solution would force equilibrium to be reached faster and recent results from the reduction experiments shows that this is needed.

7.2 Uncertainty Estimations

Due to the exploratory nature of this thesis there was not enough time to do enough measurements. Therefore estimates were made for extractions of Mo and W in Tokai and for extractions of Mo in Norway. The counting uncertainty for experiments performed in Norway was so high that they probably exceed the variance of repeated experiments.

For experiments where several parallels were performed the standard deviation was calculated as:

$$s = \sqrt{\frac{\sum_i (x_i - \overline{x})^2}{n-1}} \tag{7.1}$$

Here s is the standard deviation, x_i is an individual measurement, $\overline{x}$ is the mean value of the measurement, n is the number of individual measurements performed [76]. However, the experiments performed in this thesis have been of an exploratory nature and there were restrictions in available beam. Therefore, experiments following the method described in chapter 5.5.1, Experimental Procedure used in Tokai an approximate deviation, from a ”true” value, were estimated. This approximation was done by performing a secondary polynomial fit on the measurement points from the graph on the right in Fig 6.4. This line was then set as a true value. From this the percent deviation from this line was calculated:

$$\frac{x_i - x_{line}}{x_{line}} \cdot 100 = \%deviation \tag{7.2}$$

Here x_i is a measurement point and x_{line} is the corresponding point on the line. The spread in the data was then determined using a gaussian fit. In Fig 7.1 for the Mo points from the graph on the left in Fig 6.4. The ”standard deviation” deduced by this method was then used as deviation for other experiments performed with the same procedure and equipment. The same was done for the W measurements except this time he ”true” values were estimated by a linear fit. The sigma value of 27% was rounded up to 30 due to its large uncertainty. This method is not perfect but it should suffice to give an indication off the distribution of the measurements.

For experiments using the procedure explained in chapter 5.5.2 Experimental Procedure used in Oslo and 5.5.3 Reduction and Subsequent Extraction Using FEC in Tokai

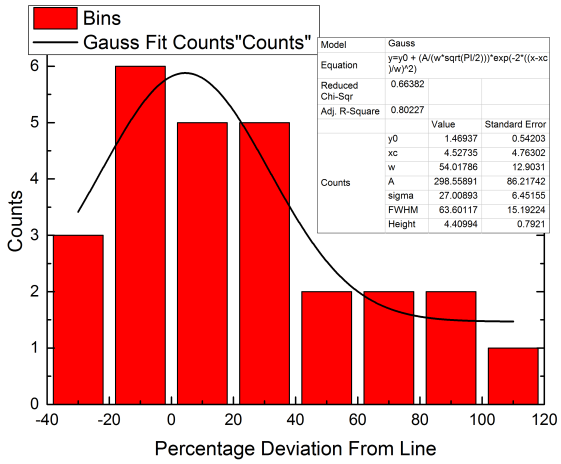

Fig. 7.1: Histogram of percentage deviation from the ”true” curve. Data collected from the left graph in Fig 6.11.

uncertainty was estimated using measurement points from the graph on the right in Fig 6.11. This gave a relative uncertainty of 10%. For Zr the counting uncertainty was so high that this alone dominated the measurement uncertainty.

7.2.1 Separation Schemes

A future Sg experiment must manage to separate between the two oxidation states. This imply that the D-ratios must be such that separation is achieved. Say that the system have a D-ratio of the oxidized specie in excess of 10 and a D-ratio for the reduced species less than 0.01. Using formula 3.2 this means that the oxidized species have more than 90% chance of being detected in the organic solution and the reduced species has more than 90% chance of staying in the aqueous phase. However if one of the species have a D-ratio of around 1 there is a 50% chance for it to be in the ”wrong” phase. This problem can be seen in the HT experiments (Fig 6.4, 6.5, 6.6.): The D-ratios are different enough to enable measurable separation between reduced and the oxidized species for Mo available in a large number of atoms, but since the D-ratio for the reduced species is around 1 this chemistry will never work out for a Sg experiment with only 10-20 atoms detected. In addition they show a too large difference between the extraction of W and Mo which indicates that Sg might extract differently than either. This makes it hard to predict the suitability of such a system for an Sg-experiment.

The reduction experiment with HDEHP manages a higher degree of separation, as seen Fig 6.10. However, as can be seen from the right graph in Fig 6.7, this extraction scheme is not suitable as it has a large difference between the D-ratio of Mo and W. There is a large difference in D-ratio between reduced Mo and experiments where Zr

has been used as an model for reduced Mo (Fig 6.8 and Fig 6.9.). This indicates that Zr is not suitable as a model for reduced Mo. However the count rate for Zr was low and the uncertainty in these measurements are large. There are some explanations for this: It is possible that species in tracer scale are not reduced to the tetravalent state, meaning that the group four elements are not a good model. The group four elements do not work as a model for the reduced species of Mo. Or the counting statistics for Zr produced is too low.

However when there is a change as a function of voltage this does not mean that the reduced species behave in any way similar. In solutions dominated by H_2SO_4 Mo and W seems to exhibit opposite behaviour. Here less Mo gets extracted as a function of potential while more W gets extracted as a function of potential. This behaviour can be seen inn Fig 6.12.

Mo and W seems to behave more similar when 0.1 M $HClO_4$ is used see Fig 6.15. Here both elements have a similar D-ratio in oxidized and reduced state. This holds true when the extracting agent is TOA however when HDEHP is used the difference increases above one order of magnitude (see Fig 6.13.). This is also the only experiment where W's D-ratio drops as a function of potential. However, the change in the D-ratio is too small to be used, it is also unclear why W behave as it does at the high potential. However, using a mixture of 0.1 M $HClO_4$ and H_2SO_4 gave the biggest difference in D-ratio for oxidized and reduced Mo (Fig 6.17), but this does not mean that the fraction extracted changes enough, as seen in Fig 6.17. When similar types of experiments are tried with HDEHPs, W does not get extracted. A likely explanation for this is that TOA extracts the acid as well as the metal ions (see chapter 6.7 Results from Titration of Solutions and other sources [77, 78].). This significantly lower the acid concentration and hence the extraction conditions. This do not happen with HDEHP. In addition with sulphuric acid it can form several species where $(TOA)H_2SO_4$ and $(TOA)_2H_2SO_4$ are the most dominant [79, 80]. This could explain why the change in acid concentration is much less for H_2SO_4 than for $HClO_4$. Since two TOA molecules are needed to extract one H_2SO_4. However, the formation between TOA and $HClO_4$ was not found.

7.2.2 Equipment

That the MDG can provide the same yield with significantly lower aqueous flow-rate compared to the standard SISAK centrifuge degasser (CDG) has the beneficial effect that correspondingly less waste will be produced from an experiment. However the real breakthrough is that the SISAK system can be run with much lower flow rates. Because the gas-liquid transfer always has been the limiting factor [81]. However a drop in the flow rate will increase the travel time correspondingly. This can become a problem for Sg experiment since Sg have a short half-life and therefore a large fraction will decay before it enters the detection cells. However, with the gas-liquid transfer now solved, the rest of the system can be adapted to lower flow-rates with e.g. smaller diameter

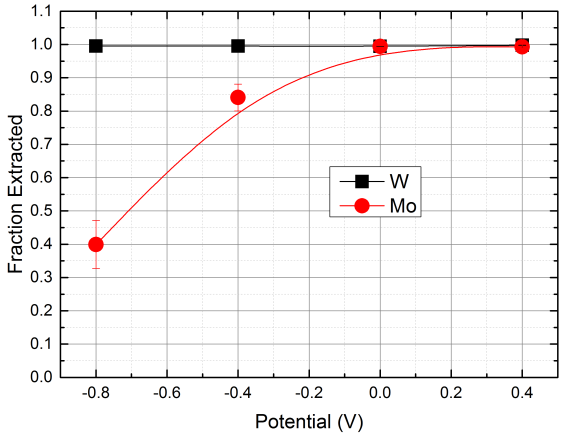

Fig. 7.2: The extraction expressed as fraction extracted instead of D-ratio. The D-ratios drop severely but still 40% of the reduced species is in the organic phase, data from Fig 6.17 .Lines to guide the eye.

tubing and entry/exit channels. Even the inner part of the centrifuge, currently with four separation chambers, can easily be made much faster for lower flow-rates by removing e.g. two chambers. Certainly, a lower flow-rate is much more compatible with the FEC, which originally was designed for much lower flow rates (mL/min range, not mL/sec.).

That it is possible to couple the FEC, the MDG and the SISAK was clearly demonstrated during the work described in this thesis. Furthermore, it was clearly demonstrated that a difference in the D-ratio of Mo as a function of potential can be measured. However, as can be seen in Fig 6.3 the difference is not as large as for the experiments performed in batch mode. That said, it should be remembered that currently the projects efforts is directed at investigating the behaviour of the FEC and this is best done with batch extractions. Running the full SISAK system complicates such explorative experiments without providing any gain. When more effort is put into tuning the conditions for on-line extractions it is most likely that significant improvements will be achieved.

7.2.3 Reduction

When using a 0.2 mL/s flow rate there seemed to be a high uncertainty in the D-ratio when the potential was below -0.6 V, see Fig 6.10. The suggested explanation was that the kinetics was not completely under control. Therefore, the kinetics was tested by sending a solution several times through the FEC at 0.2 mL/s flow rate at -0.8 V. In the graph on the left in Fig 6.11 the change as function of times passed through the FEC can be seen. This clearly shows that there is a clear kinetic effect, since the D-ratio drops (i.e. a higher degree of reduction is achieved) as a function of times run through the FEC.

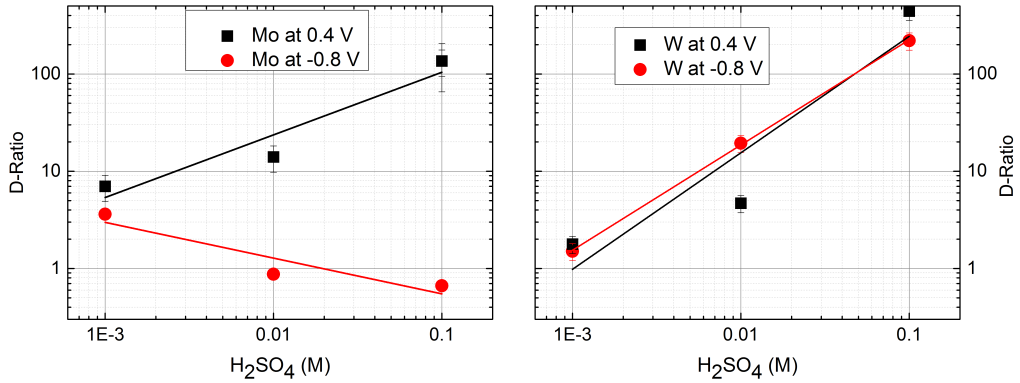

Fig. 7.3: D-ratio of Mo and W plotted as a function of increasing H_2SO_4 concentration in 0.1 M $HClO_4$. Extractant 0.2 M TOA in toluene. The black squares shows the D-ratio of Mo at an oxidizing potential while the red circles show the D-ratio at a reducing potential. The points are gathered from Fig 6.16 and Fig 6.17

Due to a pump malfunction and no more available beam time, this experiment could not repeated and extended until there was no change in the D-ratio. The true rate of reduction could therefore not be calculated.

While the broken cogwheel in the pump was exchanged the remaining solution was left in contact with air. This was done to check if the Mo would oxidise in contact with air. As can be seen on the graph on the right in Fig 6.11 the complex is stable for at a minimum 4 h.

An even stronger indicator for determining reduction is to see the extraction trend as function of e.g. acid concentration changes. In the left graph in Fig 7.3 the only difference between extraction curves obtained as function of H_2SO_4 concentration is that in one case (black squares) a none-reducing potential was used and for the other case (red circles) a reducing potential was applied. Clearly, there is a striking difference. This shows that the potential applied to the FEC has reduced Mo. However, same conditions and the potential has no effect on W, see the right graph in Fig 7.3.

Comparing the data for extraction at 0.2 M TOA concentration with extraction at 0.1 M TOA concentration but otherwise the same concentration the difference is staggering. In Fig 7.4 extraction with 0.1 M TOA has been performed.

The same trend was also tested with HDEHP to see if the reduced species would exhibit a similar behaviour with this extraction agent. Comparing the results with TOA with the results from HDEHP (Fig 7.5) the reduction of Mo and the separation of the oxidation states are clear. However, contrary to the TOA case the difference between reduction/no reduction do not increase as the H_2SO_4 concentration increases. Again, no difference is observed for W.

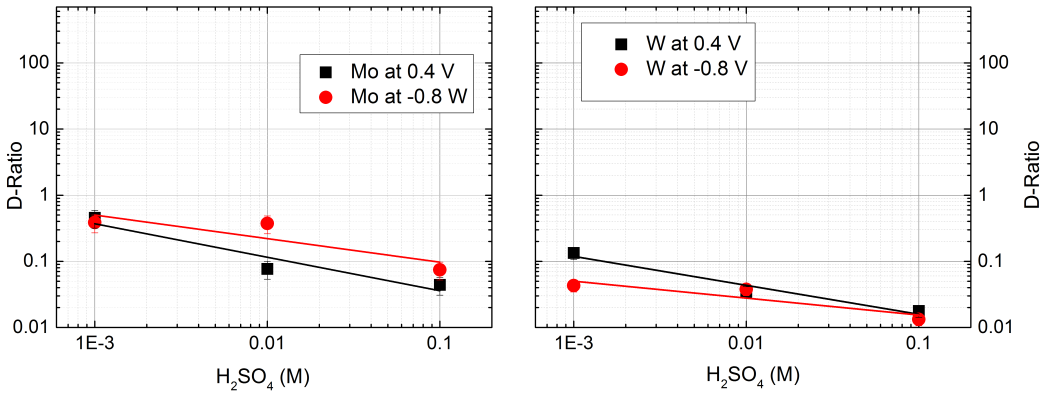

Fig. 7.4: D-ratio of Mo and W plotted as a function of increasing H_2SO_4 concentration in 0.1 M $HClO_4$. Extractant 0.1 M TOA in toluene. The black squares shows the D-ratio of Mo at an oxidizing potential while the red circles show the D-ratio at a reducing potential.

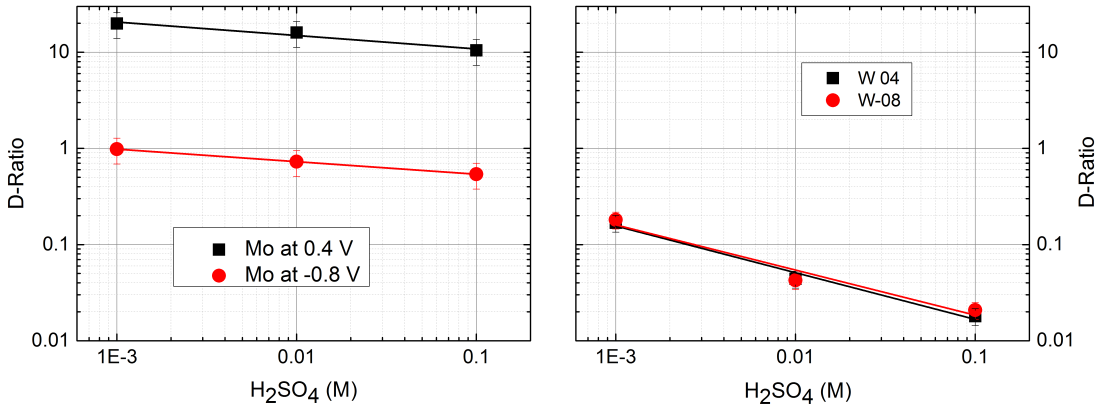

Fig. 7.5: D-ratio of Mo in a and W in b plotted as a function of H_2SO_4 concentration in 0.1 M $HClO_4$. Extractant 0.1 M HDEHP in toluene. The black squares shows the D-ratio of Mo at an oxidizing potential while the red circles show the D-ratio at a reducing potential.

Comparing the 1 mL/min flow rate used in the batch experiments with the 0.2 mL/s when using the SISAK equipment or testing the kinetic in Oslo is interesting. The volume of the vycor glass tube is 500 μL when it is filled with the normal amount of carbon fibre, abut 54 cm, the volume inside the vycor glass tube is estimated to be 250 μL. When using a 1 ml/min flow rate the hold up time was measured to be 15 s. Assuming that there is plug flow and that the hold up time scales linearly with the flow rate the hold up time when using 0.2 mL/s flow rate is 1.3 s. In the kinetic experiments slightly less carbon fibre was used giving a residence time of 1.7 s. In Fig 6.10 the residence time is too low and the distribution of the D-ratio becomes high. Therefore the left graph in Fig 6.11 was performed to see how the residence time affected the reduction. This shows that there is a clear drop in the D ratio by each pass through the FEC.

From recent data measured by A. Toyoshima et al. [82] it became clear that Mo was retained in the working electrode in different amount depending on what kind of aquatic solution was used. In acid concentrations of 10^{-3}-0.1 HF + 0.1 M $HClO_4$ and 0.01-0.1 M H_2SO_4 + 0.1 M $HClO_4$ the yield at -0.8 dropped to 20% compared to the yield at 0.4 V. In 0.1 M $HClO_4$ it dropped to 10%, while in solutions 0.1 M H_2SO_4 and H_2SO_4 + 0.1 M HF it dropped to only 60% of the yield with 0.4 V. Therefore, it is also unclear if the data measured in the present work has similar effects. Of course, if e.g. W when reduced sticks to the electrode, then the measured D-ratio will not change because only none-reduced species are present in the solution, even if a significant amount of reduction has taken place. This clearly needs to be investigated further.

In [77] an experiment was performed were trace amount of W was left in contact with 10^{-4} $Ce(SO_4)_2$ in a solution of 0.01 M H_2SO_4. Left in this solution for around 2 hours the D-ratio of W will change from around 1.8 to around 0.3. This could be because W is oxidized or it could be because it is hydrolysed over the long time period. Also some solutions containing different concentrations of sulphuric acid and different concentrations of H_2O_2. A This was done to see if it was possible to use this to determine the oxidation state of W. However with bot the aspect of time and the fact that H_2O_2 can work as a ligand, it is unclear what is the cause of change in extraction.

7.2.4 Extraction Schemes

Acid concentrations from 0.1 to 0.2 M was used for most experiments. This was done to be able to differentiate between the hexavalent oxidation species and the tetravalent oxidation species as shown in Fig 3.6. In addition if the concentration of $[H^+]$ exceeds much above 1 molar the potential needed will be impossible to discern [83]. One of the possible explanations for the low separation between the species in the HT experiments could be due to the 1 M Cl^- solution used, as chlorine forms negative ions with Mo in a similar way as fluoride. Therefore, an acid which is less prone to form stable ligand bonds to the central atom should be used. A good candidate for this is perchloric acid

should have a great difficulty in complexing with Mo and W. As explained in chapter 3.1 Liquid-liquid Extraction, that the perchlorate ion is the weakest ligand.

7.3 Future Perspectives and Experiments

In addition to the experiments described in the current work, a significant effort was also made (by all project members, included the candidate presenting this thesis) to set up two complete SISAK-FEC systems, one in Oslo and one in Tokai. This was successful and as a result the collaboration can now perform experiments in parallel at both places. This is of great benefit to the collaboration, in particular since proper alignment of experiments are ensured by frequent video conferences. Thus, the collaboration now has a very good basis to work fast and efficiently to advance the search for a suitable chemistry for reduction studies of Sg.

The level of activity produced from a mixed Zr/Mo target at OCL is not high enough to be useful for this kind of experiments. The reason for this is that the Oslo Cyclotron is not set up properly for producing high intensity beams suitable for this kind of experiments, as this would require a different radiation protection regime. Furthermore, a new target station with suitable cooling arrangement for the target and target chamber window would also be required. This means that it is not possible to clarify if group four can be used as a model for reduced species of group six atoms in Oslo, at least not with on-line activity. The amount of Mo activity produced at OCL is also rather low, and the available isotope has a rather long half-life (6.9 h). The Oslo group is currently looking into replacing the OCL with a neutron induced fission source, which would improve the situation significantly [84].

Currently the best extraction scheme seems to be using TOA. However, any TOA system will raise complications in regards to what it extracts. It seems that a rather high TOA concentration is needed in order to extract sufficient amount of Mo and W. Since TOA also extracts the acid this will change the acid concentration significantly. This will radically change which ligands Mo and W will be bound to. Therefore, it should also significantly change the chemistry of Sg.

The HDEHP was initially promising but the great difference in the separation factor between Mo and W makes this system unsuitable. A likely explanation is that W binds more strongly to sulphate thereby creating a more negative adduct, which will not be extracted by a cation extracting agent. However from [77] it seems that adding more sulphuric acid will hinder this formation. Thereby, by adding more acid more positive adducts should be formed.

There are strict demands for purity in electrochemistry. One of the main reasons for this is because it is highly likely that impurities will adsorb to the surface of the electrode. Adsorption like this can actually reach several molecular layers. In a worst case scenario the metal ion is actually not interacting with the carbon surface but with

impurities adsorbed to it [85]. A suggested solution to this is to use a electrode with a high surface area and a negative potential to pre-treat the solution. The fluid interacts with this electrode before it interacts with the gas-jet and is transported to the FEC. In addition, oxygen will slowly start binding to the glassy carbon surface according to [86]. In [85] the suggested way to renew an electrode from these contaminations is to either heat the electrode using a laser or by using a suitable series of potential pulses.

In the future the solute used for reduction should be pre-cleaned/treated in an additional electrolysis cell before entering the SISAK-FEC system. This will reduce the likelihood for impurities to interact with the working electrode.

The ionic strength is also important to consider. Most of the batch experiments were done with a too low concentration to be used in the SISAK system and achieve phase separation. The rule of thumb is that the concentration of the salt at least must be 0.5 M for it to be possible to achieve phase separation [81].

The reductive kinetics have to be more stringently researched. The kinetics of the reaction should be tested with different amount of carbon fibre. This would aid in the optimisation regarding reduction. When there is more certanity about what kind of extraction scheme can be used. How temperature affects the reduction kinetics should be examined closer.

Several different aquatic solutions have been tested. These different solutions should be tested to see how high the acid content is after TOA has been used. This would yield important information about the difference in the speciation from reduction to extraction.

Sulphuric acid form strong bonds with Mo and W. From F. Schulz master thesis [77] The higest D-ratio for extraction of W with TOA was when a aquatic solution of 0.1 M H_2SO_4. How sulphuric acid affects extraction with TOA has been checked in [77]. However, it would be interesting to see how sulphate salt affects the extraction scheme. Checking the extraction of the reduced and oxidized species with 0.1 M H_2SO_4 and several different concentrations of added Na_2SO_4 would yield interesting insight in the adduct formation of both reduced and oxidized species of Mo and W. In addition to achieve better separation between the species, the dependency on small changes in the free fluoride concentration should be investigated.

To discover if underpotential is the cause of the adsorption the the carbon electrode the surface could be covered in Mo. This could be done by letting a solution of Mo flow trough the cell at a high negative potential thereby covering the electrode. Then performing a experiment with active Mo to see if less activity is retained on the electrode this way.

Other ways to control the adsorption could be to cover the electrode by a more inert material, such as diamond or teflon coating. However more study is needed to determine the best material.

Another possibility to control the adsorption is to do test to check if some ligands

have a harder time adsorbing to the carbon. From previous studies it seems that nucleation can be hindered by certain ligands see [87, 88]. This conforms to the fact that less Mo was adsorbed when there was sulphate in the solution.

7.4 Concluding Remarks

It was shown that it is possible to utilize the different complexing behaviour of tetravalent and hexavalent species. Differences were achieved with both Mo and W as a function of potential. However, it is unclear if it is possible to use the Zr and Hf as homologues for the reduced species of Mo and W.

The experiments with HT shows that it does not function sufficiently well as a extracting agent. The kinetics is fast and reasonable D-ratios are obtained, but it fails in treating W and Mo in similar way. Thus, the large difference in the extraction yield does not make it suitable. It did, however, show that it is possible to separate two oxidation states using SISAK. TOA is seems to be the extracting agent that treats Mo and W equal and the highest D-ratios for both elements have been achieved with this. HDEHP has the same problems as HT, but it manages to have the highest separation between the reduced and the oxidized species.

In Fig 6.3 a proof of concept is shown. Here two new components have been successfully incorporated to the SISAK system. The MDG have an aquatic flow of 0.2 mL/s and a gas flow of 1.5 L/min which means the gas flow is 125 times higher than the aquatic flow. The FEC then reduced enough Mo with the aquatic flow rate at 0.2 mL/s. This could be seen from the D-ratios achieved by using the SISAK system. Where there was a measurable difference in the D-ratio as a function of voltage.

At the present the most important challenge for a future reduction Sg experiment is to control the adsorption to the carbon surface. The recent data from Japan shows that both Mo and W will adsorb to the surface of the electrode given sufficient potential.

Spending three months in Japan greatly added to the amount of experiments that were possible to perform. In addition it gave a great introduction to the FEC and how this could be used. It also enhanced the possibility for both groups to work with both SISAK and FEC.

Part of the worke performed here have been presented at international conferences as listed in Appendix E Posters and Presentation Abstracts

BIBLIOGRAPHY

[1] J. Magill, G. Pfenning, and J. Galy. "Karlsruher Nuklidekarte". In: Scientific and Technical Research Series, 2006. ISBN: 92-79-02175-3.

[2] V. Hanemaayer et al. "Solid Targets for ^{99m}Tc Production on Medical Cyclotrons". In: *Journal of Radioanalytical and Nuclear Chemistry* 299 (2014), pp. 1007–1011.

[3] E. May and M. Thoennessen. "Discovery of Cesium, Lanthanum, Praseodymium and Promethium Isotopes". In: *Atomic Data and Nuclear Data Tables* 98 (2012), pp. 960 –982.

[4] K. W. J. Barnham et al. "Production and Destination of British Civil Plutonium". In: *Nature* 317 (1985), pp. 213–217.

[5] J. Aaltonen et al. "Production of Neptunium and Plutonium Tracers in Nuclear Reactions of ^{236}U with 21-to-60-MeV ^{3}He Ions". English. In: *Radiochemistry* 43 (2001), pp. 442–446.

[6] C. Broeders, E Kiefhaber, and H. Wiese. "Burning Transuranium Isotopes in Thermal and Fast Reactors". In: *Nuclear Engineering and Design* 202 (2000), pp. 157 –172.

[7] H. Bokelund, C. Apostolidis, and J.-P. Glatz. "Recovery and Chemical Purification of Actinides at JRC, Karlsruhe". In: *Journal of Nuclear Materials* 166 (1989), pp. 181 –188.

[8] R. C. Martin, J. B. Knauer, and P. A. Balo. *Production, Distribution, and Application of Californium-252 Neutron Sources*. Chemical Technoloy Division Oak Ridge National Laboratory Oak Ridge, TN 37831-6385 U.S.A. 1999, pp. 1–18.

[9] F. A Paneth. "The Making of the Elements 97 and 98". In: *Nature* 165 (1950), pp. 748–749.

[10] J. Peterson and D. Hobart. "The Chemistry of Berkelium". In: ed. by H. Emeleus and A. Sharpe. Vol. 28. Advances in Inorganic Chemistry. Academic Press, 1984, pp. 29 –72.

[11] C. E. Bemis et al. "Production, L x-ray Identification, and Decay of the Nuclide ^{260}105". In: *Phys. Rev. C* 16 (3 1977), pp. 1146–1158.

[12] A. Türler and V. Pershina. “Advances in the Production and Chemistry of the Heaviest Elements”. In: *Chemical Reviews* 113 (2013), pp. 1237–1312.

[13] R. Eichler et al. “Indication for a Volatile Element 114”. In: *Radiochimica Acta* 98 (2010), pp. 133–139.

[14] Y. T. Oganessian et al. “Synthesis of Superheavy Nuclei in the ^{48}Ca+^{244}Pu Reaction: ^{288}114”. In: *Phys. Rev. C* 62 (4 2000), p. 041604.

[15] P. Pyykkö. “Relativistic Effects in Structural Chemistry”. In: *Chemical Reviews* 88 (1988), pp. 563–594.

[16] R. Guillaumont, J. P. Adloff, and A. Peneloux. “Kinetic and Thermodynamic Aspects of Tracer-Scale and Single Atom Chemistry”. In: *Radiochimica Acta* 46 (1989), pp. 169–176.

[17] J. Nilssen. “Investigations into new Degasser Technology for SISAK”. Master. University Of Oslo, 2009.

[18] H. V. Lerum. “Test of Membrane Degasser for the SISAK System”. Bachelor Project. Kjemisk Institutt Universitetet i Oslo, 2012.

[19] K. Ooe et al. “Development of a new Continuous Dissolution Apparatus with a Hydrophobic Membrane for Superheavy Element Chemistry”. In: *Journal of Radioanalytical and Nuclear Chemistry* (To be Published).

[20] J. P. Omtvedt, ed. *SISAK Collaboration Wiki*. 2014. URL: `https://wiki.uio.no/mn/kjemi/sisak/index.php/SISAK_Collaboration_Wiki`.

[21] A. Ghiorso et al. “Element 106”. In: *Phys. Rev. Lett.* 33 (25 1974), pp. 1490–1493.

[22] M. Schädel et al. “First Aqueous Chemistry with Seaborgium (Element 106)”. In: *Radiochimica Acta* 77 (1997), pp. 149–159.

[23] M. Schädel et al. “Aqueous Chemistry of Seaborgium (Z = 106)”. In: *Radiochimica Acta* 83 (1998), pp. 163–165.

[24] J. P. Omtvedt et al. “Review of the SISAK System in Transactinide Research: Recent Developments and Future Prospects”. In: *Journal of Alloys and compounds* 271-273 (1998), pp. 303–306.

[25] B. Wierczinski et al. “Applications of Fast Solvent Extraction Processes to Studies of Exotic Nuclides”. In: *Journal of Radioanalytical and Nuclear Chemistry* 236 (1998), pp. 193–197.

[26] P. O. Aronsson et al. “SISAK–A new Technique for Rapid, Continuous (radio) Chemical Separations”. In: *Journal of Inorganic and Nuclear Chemistry* 36 (1974), pp. 2397–2403.

[27] G. Skarnemark et al. “Studies of Short-Lived Fission Products by means of the Multistage Solvent Extraction System SISAK”. In: *Journal of Radioanalytical and Nuclear Chemistry* 142 (1990), pp. 145–158.

[28] A. Toyoshima et al. “Development of an Electrochemistry Apparatus for the Heaviest Elements”. In: *Radiochimica Acta* 96 (2008), pp. 323–326.

[29] A. Toyoshima et al. “Oxidation of Element 102, Nobelium, with Flow Electrolytic Column Chromatography on an Atom-at-a-Time Scale”. In: *Journal of the American Chemical Society* 131 (2009), pp. 9180–9181.

[30] A. Toyoshima et al. “Measurement of the Md3+/Md2+ Reduction Potential Studied with Flow Electrolytic Chromatography”. In: *Inorganic Chemistry* 52 (2013), pp. 12311–12313.

[31] K. Izitsu et al. “Voltammetry at a Trioctylphosphine oxide-Coated Glassy Carbon Electrode and its use for the Determination of Trace Uranyl Ions after Preconcentration”. In: *Analytical Chimica Acta* 149 (1983), pp. 147 –155.

[32] K. Izitsu, T. Nakamura, and T. Ando. “Voltammetric Determination of Uranium in Sea Water after Preconcentration of the Trioctylphosphine Oxide-coated Glassy Carbon Electrode”. In: *Analytical Chimica Acta* 152 (1983), pp. 285 –288.

[33] J. Inczedy, T. Lengyl, and A. M. Ure. “Compendium of Analytical Nomenclature (definitive Rules 1997) - The Orange Book”. In: Blackwell Science, 1998. ISBN: 0-632-05127-2.

[34] M. Cox and J. Rydberg. “Introduction to Solvent Extraction”. In: *Principles and Practices of Solvent Extraction*. Ed. by J. Rydberg and C. Musikas and G. R. Choppins. 1992, pp. 1–23. ISBN: 0-0247-8668-8.

[35] P. Muller. “Glossary of Terms used in Physical Organic Chemistry”. In: *Pure and Applied Chemistry* 66 (1994), pp. 1077–1184.

[36] L. Stavsetra. “Achievements Using the Continuous SISAK α-liquid Scintillation Technique, and its Application in Detection of ^{257}Rf Atoms”. PhD dissertion. Department of chemistry Faculty of Mathematics and Natural Sciences University of Oslo, 2005.

[37] J. Noro. “Solvent Extraction of Several Trivalent Metal Ions with 4-Isopropyltropolone into Chloroform”. In: *Analytical Sciences* 14 (1998), pp. 1099–1105.

[38] M. C. Barret et al. “Synthesis and Structural Characterization of Tin(II)and Zinc Derivaties of Cyclic α-Hydroxyketones, Including the Structures if Sn(maltol)$_2$, Sn(tropolone)$_2$, Zn(tropolone)$_2$, and Zn(hinokitiol)$_2$”. In: *Inorganic Chemistry* 40 (2001), pp. 4384–4388.

[39] D. Peppard et al. “Acidic Esters of Orthophosphoric Acid as Selective Extractants for Metallic Cations—Tracer Studies”. In: *Journal of Inorganic and Nuclear Chemistry* 7 (1958), pp. 276 –285.

[40] D. Peppard et al. “Fractional Extraction of the Lanthanides as their di-alkyl Orthophosphates”. In: *Journal of Inorganic and Nuclear Chemistry* 4 (1957), pp. 334 –343.

[41] Z. Kolařík, J. Hejná, and H. Pánková. “Acidic Organophosphorus Extractants—VII: The Dissociation, Self-Association and Distribution of di-n-butyl Phosphoric Acid”. In: *Journal of Inorganic and Nuclear Chemistry* 30 (1968), pp. 2795 –2806.

[42] M. Cox and J. Rydberg. “Solvent Extraction Equilibria”. In: *Principles and Practices of Solvent Extraction*. Ed. by J. Rydberg and C. Musikas and G. R. Choppins. 1992, pp. 109–201. ISBN: 0-0247-8668-8.

[43] A. C. Fisher. In: *Electrode Dynamics*. 2009. ISBN: 978-0-19-855690-9.

[44] J. McMurry and R. C. Fay. “Electrochemistry”. In: *Chemistry*. 2001, pp. 759–810. ISBN: 0-13-087205-9.

[45] E. Gileadi. “Single-Step Electrode Reactions”. In: *Physical Electrochemistry*. 2011, pp. 55–75. ISBN: 978-3-527-31970-1.

[46] S. Trasatti. “The Absolute Electrode Potential: an Explanatory Note”. In: *Pure and Applied Chemistry* 58 (1986), pp. 955 –966.

[47] E. Gileadi. “Experimental Techniques (2)”. In: *Physical Electrochemistry*. 2011, pp. 221–236. ISBN: 978-3-527-31970-1.

[48] D. Trubert and C. L. Naour. “Fundamental Aspects of Single Atom Chemistry”. In: *Superheavy Elements*. Ed. by M Schädel. 2003, pp. 95–113. ISBN: 1-4020-1250-0.

[49] C. M. Guldberg and P. Waage. *Ètudes sur les Affinites Chimiques*. University of Oslo, 1867.

[50] Y. Ishii et al. “Fluorido Complex Formation of Element 104, Rutherfordium (Rf)”. In: *Bulletin of the Chemical Society of Japan* 84 (2001), pp. 903–911.

[51] J. P. Omtvedt et al. “SISAK Liquid-Liquid Extraction Experiments with Preseparated ^{257}Rf”. In: *Journal of Nuclear and Radiochemical Sciences* (2002), pp. 121–124.

[52] D. J. Griffiths. “Introduction to Electrodynamics”. In: 3rd ed. Pearson Benjamin Cummings, 2008. Chap. 5, pp. 202–205. ISBN: 0-13-919960-8.

[53] W. Lovland, D. J. Morrissey, and G. T. Seaborg. “Modern Nuclear Chemistry”. In: Wiley-Interscience, 2006. ISBN: 13 987-0-471-11532-8.

[54] W. Lovland, D. J. Morrissey, and G. T. Seaborg. “Reactors and Accelerators”. In: *Modern Nuclear Chemistry*. Wiley-Interscience, 2006, pp. 383–425. ISBN: 13 987-0-471-11532-8.

[55] W. Lovland, D. J. Morrissey, and G. T. Seaborg. “Radiochemical Techniques”. In: *Modern Nuclear Chemistry*. Wiley-Interscience, 2006, pp. 579–611. ISBN: 13 987-0-471-11532-8.

[56] A. Toyoshima et al. “Hexafluoro Complex of Rutherfordium in Mixed HF/HNO_3 Solutions”. In: *Radiochimica Acta* 96 (2008), pp. 125–134.

[57] A. Kronenberg. “Entwicklung einer online-Chromatographie für Element 106 (Seaborgium)”. Disseretation zur Erlangung des Grades ”Doktor der Naturwissenschap”. Johannes Gutenberg-universität Mainz, 2001.

[58] M. Plaisance and R. Guillaumont. “Fluoro- et Chlorofluoro-Complexes de Protactinium Pentavalent”. In: *Radiochimica Acta* 12 (1969), pp. 32–37.

[59] V. Pershina and J. V. Kratz. “Solution Chemistry of Element 106: Theoretical Predictions of Hydrolysis of Group 6 Cations Mo, W, and Sg”. In: *Inorganic Chemistry* 40 (2001), pp. 776–780.

[60] V. Pershina. “Theoretical Treatment of the Complexation of Element 106, Sg, in HF Solutions”. In: *Radiochimica Acta* 92 (1994), pp. 455–462.

[61] M. T. Pope. “Introduction to Polyoxometalate Chemistry”. In: *Polyoxometalate Molecular Science*. Ed. by J. J. Borrás-Almenar et al. 2001, pp. 3 –28. ISBN: 1-4020-1241-1.

[62] P. Kofstad. “VI. Bigruppe - Kromgruppen”. In: *Uorganisk Kjemi*. 1998, pp. 378–388. ISBN: 978-0-19-855690-9.

[63] V. Pershina, E. Johnson, and B. Fricke. “Theoretical Estimates of Redox Potentials for Group 6 Elements, Including Element 106, Seaborgium, in Acid Solutions”. In: *The Journal of Physical Chemistry A* 103 (1999), pp. 8463–8470.

[64] V. Pershina and B. Fricke. “The Electronic Structure of the Group 6 Oxyanions $[MO_4]^{2-}$, where M = Cr, Mo, W and Element 106”. In: *Radiochimica Acta* 65 (1994), pp. 13–17.

[65] P. Kofstad. “VI. Bigruppe - Titangruppen”. In: *Uorganisk Kjemi*. 1998, pp. 359–369. ISBN: 978-0-19-855690-9.

[66] Z. Szeglowski et al. “Fast and Continuous Chemical Isolation of Short-Lived Isotopes of Hf, Ta and W as Homologs of Elements 104, 105 and 106”. In: *Journal of Radioanalytical and Nuclear Chemistry* 212 (1996), pp. 35–42.

[67] D. Schumann et al. “Sorption Behaviour of Rutherfordium and Thorium from HCl/Hf Containing Aqueous Solution”. In: *Journal of Alloys and Compounds* 271-273 (1998), pp. 307 –311.

[68] K. Yakabe and S. Minami. “Liquid-liquid Extraction of Hafnium Complex Ion from Aqueous Oxalic Acid Solution with high Molecular Weight Amine”. In: *Journal of Inorganic and Nuclear Chemistry* 37 (1975), pp. 1973 –1976.

[69] “Critical Evaluation of Equilibrium Constants in Solution Part A. Stability Constants of Metal Complexes”. In: ed. by A. M. Bond and G. T. Hefter. Pergamon Press, 1980. ISBN: 008022377-x.

[70] H. P. Metals. *HAVAR Technical Data Sheet*. Downloaded 2014.

[71] N. Nica. “252Cf”. In: 106 (2005), p. 813.

[72] K. Kinoshita. “Introduction”. In: *Carbon Electrochemical and Physicochemical Properties*. Wiley-Interscience, 1988, pp. 1–17. ISBN: 0-471-84802-6.

[73] K. Kinoshita. “Characteristics and Properties of Carbon Electrodes”. In: *Carbon Electrochemical and Physicochemical Properties*. Wiley-Interscience, 1988, pp. 226–284. ISBN: 0-471-84802-6.

[74] F. Samadani. “Developing a SISAK Extraction System for Chemical Studies of Element 108, Hassium”. Master. Universitetet i Oslo, 2006.

[75] E. Gileadi. “Underpotential Deposition and Single-Crystal Electrochemistry”. In: *Physical Electrochemistry*. 2011, pp. 165–174. ISBN: 978-3-527-31970-1.

[76] D. C. Harris. “Statistics”. In: *Quantitative Chemical Analysis*. 2010, pp. 68–92. ISBN: 978-1-4292-1815-3.

[77] F. Schulz. “Utviklingen av et SISAK Ekstraksjonssystem for Grunnstoff 106, Seaborgium”. Master. Universitetet i Oslo, 2009.

[78] M. W. Ashraf and A. Mian. “Selective Separation and Preconcentration Studies of Chromium(VI) with Alamine 336 Supported Liquid Membrane”. In: *Toxicological & Environmental Chemistry* 88 (2006), pp. 187–196.

[79] M.-L. Wang and K.-H. Hu. “Model of Chemical Reaction Equilibrium of Sulfuric Acid Salts of Trioctylamine”. In: *Chemical Engineering Communications* 126 (1993), pp. 43–57.

[80] K. A. Allen. “The Equilibria Between Tri-n-octylamine and Sulfuric Acid.” In: *The Journal of Physical Chemistry* 60 (1956), pp. 239–245.

[81] J. P. Omtvedt. *Private Communication*. Spring 2012.

[82] A. Toyoshima. *Sg red Meeting 140324 AT*. Presentation. 2014.

[83] A. Toyoshima. *Private Communication*. 2013.

[84] J. P. Omtvedt. *Private Communication*. Spring 2014.

[85] E. Gileadi. “Specific Examples of Multi-Step Electrode Reactions”. In: *Physical Electrochemistry*. 2011, pp. 93–112. ISBN: 978-3-527-31970-1.

[86] R. L. McCreery. “Electrochemical Properties of Carbon Surfaces”. In: *Interfacial Electrochemistry*. Ed. by A. Wieckowski. 1999, pp. 631–647. ISBN: 0-8247-6000-x.

[87] G. Gunawardena et al. “Electrochemical Nucleation Part 1. General Considerations”. In: *Journal of Electroanalytical Chemistry* 138 (1982), pp. 225–239.

[88] G. Gunawardena, G. Hills, and I. Montenegri. “Electrochemical Nucleation Part 2. THe Electrodeposition of Silver on Vitreous Carbon”. In: *Journal of Electroanalytical Chemistry* 138 (1982), pp. 241–254.

[89] Ortec. “Menu Commands”. In: *Maestro-32 MCA Emulator for Microsoft Windows 98, 2000, NT, and XP A65-b32 Software User’s Manual*. Ortec, 2003, pp. 21–94.

[90] L. P. Ekström and R. B. Firestone. *WWW Table of Radioactive Isotopes*. 1999. URL: `http://ie.lbl.gov/toi/index.htm`.

LIST OF FIGURES

LIST OF TABLES

Appendices

Appendix A

CALCULATION OF PEAK PRECISION IN THE PRESENCE OF BACKGROUND

When there is no background in the measurement of a peak the standard deviation σ is given by:

$$\sigma = \sqrt{N} \tag{A.1}$$

Where N is the integrated counts of the peak. Normaly when radioactivty is measured we have some background. This must be taken into account when we calculate the net peak counts P:

$$N_T = P + B \tag{A.2}$$

Here N_T is the total integrated area. B is the background counts. To estimate B two additional regions are integrated a distance d on the right and left side of the peak. The width of these regions are set to $\frac{\eta_B}{2}$ where η_B is the width of both regions. Both regions are integreated and designated N_{B1}, N_{B2}. Then the estiamte of the background becomes:

$$M_B = \frac{\eta_p}{\eta_B} \cdot (N_{B1} + N_{B2}) \approx B \tag{A.3}$$

where η_p is the width of the peak region. which gives the standard deviation

$$\begin{aligned} \sigma_{MB} &\approx \frac{\eta_p}{\eta_B} \cdot (N_{B1} + N_{B2}) \\ &\approx \frac{\eta_p}{\eta_B} \sqrt{\frac{\eta_p}{\cdot} \eta_B B} \end{aligned} \tag{A.4}$$

Then we get:

$$P \approx N_T - M_B \tag{A.5}$$

giving a standard deviation of

$$\sigma_P = \sqrt{\sigma_{N_T}^2 + \sigma_{M_B}} \tag{A.6}$$

can also be written as

$$\sigma_P = \sqrt{P + \left(1 + \frac{\eta_P}{\eta_B}\right) \cdot B} \tag{A.7}$$

This is the technique used by the ORTEC software further description can be read in [89]

Appendix B

CALCULATION OF D-VALUE UNCERTANITY

The general formula for calculation of the standard uncertainty of a calculated value R which is a function of measured values x, y etc is:

$$s_R = \sqrt{\left(\frac{\delta R}{\delta x} \cdot S_x\right)^2 + \left(\frac{\delta R}{\delta y} \cdot S_y\right)^2} \tag{B.1}$$

for the general formula $R = \frac{x}{y}$ which is very important for D-ratios we get the uncertainty as.

$$S_R = R\sqrt{\left(\frac{S_x}{x}\right)^2 + \left(\frac{S_y}{y}\right)^2} \tag{B.2}$$

Then to calculate the uncertainty where the concentration in the phases are defined from several γ peaks. The uncertainty in the different peaks have to be taken into account. The formula from the calculation:

$$D = \frac{\sum_i [A_i^{org}]}{\sum_i [A_i^{aq}]} \tag{B.3}$$

$$S_D = D\sqrt{\sum_o \left(\frac{S_{A_o^{org}}}{\sum_i [A_i^{org}]}\right)^2 + \sum_o \left(\frac{S_{A_o^{aq}}}{\sum_i [A_i^{aq}]}\right)^2} \tag{B.4}$$

For experiments performed in Japan the uncertainty becomes slightly different as we also have to take into account the uncertainty in regards to the efficiency of the detectors. We have formula 5.2, Where the uncertainty S_J becomes;

$$S_J^2 = \left(\frac{\delta J}{\delta A_{org1}} S_{A_{org1}}\right)^2 + \left(\frac{\delta J}{\delta A_{aq2}} S_{A_{aq2}}\right)^2 + \left(\frac{\delta J}{\delta \epsilon} S_\epsilon\right)^2 \tag{B.5}$$

After partially deriving, and remembering that $\epsilon = \frac{C_{sol1}}{C_{sol2}}$ the formula end up as:

$$S_J = D\epsilon\sqrt{\left(\frac{S_{A_{org1}}}{A_{org}}\right)^2 + \left(\frac{S_{A_{Aq2}}}{A_{Aq2}}\right)^2 + \left(\frac{S_{C_{sol1}}}{C_{sol1}}\right)^2 + \left(-\frac{S_{C_{sol2}}}{C_{sol2}}\right)^2} \tag{B.6}$$

And as several γ-peaks were used for the calculations the end result is:

$$S_J = D\epsilon\sqrt{\sum_o \left(\frac{S_o^{A_{org1}}}{\sum_i A_i^{org}}\right)^2 + \sum_o \left(\frac{S_o^{A_{Aq2}}}{\sum_i A_i^{Aq2}}\right)^2 + \sum_o \left(\frac{S_{C_o^{sol1}}}{\sum_i C_i^{sol1}}\right)^2 + \sum_o \left(-\frac{S_{C_o^{sol1}}}{\sum_i C_i^{sol1}}\right)^2} \tag{B.7}$$

Appendix C

OVERLAPPING γ-PEAKS

In some of the experiments there would be produced some unwanted nuclei. occasional some of these would emit γ-rays with equivalent energy to the nuclei used in the experiments. If there was a significant amount of these nuclei they would have to be taken into account. To do this the count rate from a non-overlapping peak from the nuclei was used.

Now knowing the count rate of the offending nuclei in the overlapping are it is possible to calculate the correct count rate for the useful nuclei. The formula can be presented as:

$$C_{tot} = C_{\gamma_1} + C_{\gamma_2} ... C_{\gamma_n} \tag{C.1}$$

Where C_{γ_1} to C_{γ_n} is all the peaks within the region of interest for the peak C_{tot}. The input from the offending peaks can be removed by using the count rate from other peaks of the same nuclide. The count rate of a peak can be expressed as:

$$C_{\gamma_x} = A_x \epsilon_x I_{\gamma_x} \tag{C.2}$$

Where C_{γ_x} is the count rate of peak x A_x is the activity of peak x ϵ_x is the efficiency of the detector for the energy are of peak x and I_{γ_x} is the intensity of the emitted peak. If we then substitute the A_x value in the overlapping are we can express the count rate of the offending peak with:

$$C_{\gamma_1} = \frac{C_{\gamma_x} \epsilon_1 I_{\gamma_1}}{\epsilon_x I_{\gamma_x}} \tag{C.3}$$

Where anything with the suffix x is an emission that does not overlap. While the suffix 1 overlaps. Assuming then that there is only two peaks in the region of interest and only one of them are important the count rate of the important peak can then be calculated using:

$$C_{\gamma_i} = C_{tot} - C_{\gamma_1} \tag{C.4}$$

Where C_{γ_i} is the value of the peak. The intensity of emission was found in the Lund data base ([90]), the energy efficiency was done with several different nuclei.

C.1 Overlap Between the 909 keV γ-ray of ^{89}Zr and ^{61,60}Cu

Due to the large diameter of the beam during the experiments with creating tracer Zr some ^{61,60}Cu was also made. The extra counts from the copper isotopes were removed by using the formula C.4. The efficiency for the 909 keV regions was measured to be 0.0047. The γ-ray 1185 keV from the ^{61}Cu nuclide was the only one that was measurable this γ-ray had an intensity of 0.0375 and the efficiency of the detector in this area was 0.0043. The intensity of the 909 keV γ-ray of the ^{61}Cu nuclide is 0.01102. The 1332 keV γ-ray of ^{60}Cu was the only one that was usable this γ-ray had an intensity of 0.88 and the efficiency in that area was 0.0041. The intensity of 909 keV γ-ray of the the ^{60}Cu nuclide is 0.0202.

Appendix D

CORRECTIONS

D.1 Decay Corrections

As some solutions were measured in series a decay correction had to be performed:

$$A_1 = A_0 e^{-\lambda \Delta t} \tag{D.1}$$

Where $\Delta t = t_E + \frac{t_{RE}}{3} - t_S - \frac{t_{RS}}{3}$ and t_E is the start of the next measurement t_{RE} is the real time of this measurement and t_S is the start time of the first measurement while t_{RS} is the real time of this measurement.

D.2 Calibration of Liquid Flow

The calibration of the liquid flow was done by pumping the fluid for a time interval Δt and collecting the fluid. The fluid was then weighed. This weight was then compared to the readout from the flow meters. All samples where weighed before and after collection to see if their volumes were correct.

Appendix E

POSTERS AND PRESENTATION ABSTRACTS

During the work for this thesis several posters have been presented at different workshops and conferences. Posters that are related to this thesis is presented here.

1. **Radchem 2014: 11-16 may 2014 Marianske Lazne, Chsech Republic**
    - Preliminary investigations towards the separation of hexavalent and tetravalent seaborgium - extraction of homologs
    - Electrolytic reduction studies of Mo and W towards the reduction of seaborgium
    - Preparations for Redox Studies of Seaborgium with SISAK Coupled to the Flow Electrolytic Column FEC
2. **NRC8 EuCheMS International Conference on Nuclear and Radiochemistry: 16-21 sep 2012 Como, Italy**
    - Liquid-phase Studies of Seaborgium using the Automated Liquid-liquid Extraction system SISAK
3. **Eighth Workshop on the Chemistry of the Heaviest Elements, CHE 8: 19-21 sep 2013 Takayama, Gifu, Japan**
    - On-line Extraction and Reduction of Mo and W using SISAK and FEC
    - Development of new degasser with a hydrophobic membrane for SISAK system
4. **5th Asia-Pacific Symposium on Radiochemistry '13, APSORC 13: 22-27 Sep 2013 Kanazawa, Japan**
    - Solvent Extraction of Hexavalent Mo and W using 4-isopropyltropolone (Hinokitiol) for Seaborgium (Sg) Reduction Experiment
    - Development of a new Continuous Dissolution Apparatus with a Hydrophobic Membrane for Superheavy Element Chemistry
    - Chemical Studies of Mo and W in Preparation of a Seaborgium (Sg) Reduction Experiment using MDG, FEC, and SISAK

Preliminary investigations towards the separation of hexavalent and tetravalent seaborgium

- extraction of homologs

M. F. Attallah[1], H. V. Lerum[1], A.Toyoshima[2], K. Ooe[3], S. Miyashita[2,4], M. Asai[2], N. Goto[3], N. S. Gupta[1], H. Haba[5], M. Huang[5], J. Kanaya[5], Y. Kaneya[2], Y. Kasamatsu[6], Y. Kitatsuji[2], Y. Kitayama[7], K. Koga[4], Y. Komori[6], T. Koyama[3], J. V. Kratz[8], , Y. Oshimi[3], V. Pershina[9], D. Sato[3], T. K. Sato[2], Y. Shigekawa[6], A. Shinohara[6], A. Tanaka[3], K. Tsukada[2], S. Tsuto[3], T. Yokokita[6], A. Yokoyama[7], Y. Nagame[2], and M. Schädel[2,9], J. P. Omtvedt[1]

[1]*Department of Chemistry, University of Oslo, P.O Box 1033 – Blindern, NO-0315 Oslo, Norway*
[2]*Advanced Science Research Center, Japan Atomic Energy Agency, Tokai, Ibaraki 319-1195, Japan*
[3]*Institute of Science and Technology, Niigata University, Niigata 950-2181, Japan*
[4]*Department of Chemistry, Graduate School of Science, Hiroshima University, Kagamiyama, Higashi-Hiroshima 739-8526, Japan*
[5]*Nishina Center for Accelerator-Based Science, RIKEN, Wako, Saitama 351-0198, Japan*
[6]*Graduate School of Science, Osaka University, Toyonaka, Osaka 560-0043, Japan*
[7]*College and Institute of Science and Engineering, Kanazawa University, Kanazawa 920-1192, Japan*
[8]*Institut für Kernchemie, Universität Mainz, 55128 Mainz, Germany*
[9]*GSI Helmholtzzentrum für Schwerionenforschung GmbH, D-64291 Darmstadt, Germany*

Introduction

The aim of the present study is to find a suitable chemical liquid-liquid extraction system to be applied in future ***reduction studies of Sg.***

The idea is to separate and identify reduced Sg-species from none-reduced Sg(VI) by their different extraction behavior in a SISAK liquid-liquid extraction stage following the reduction in an electrochemical cell.

Schematic of Future Sg-experiment

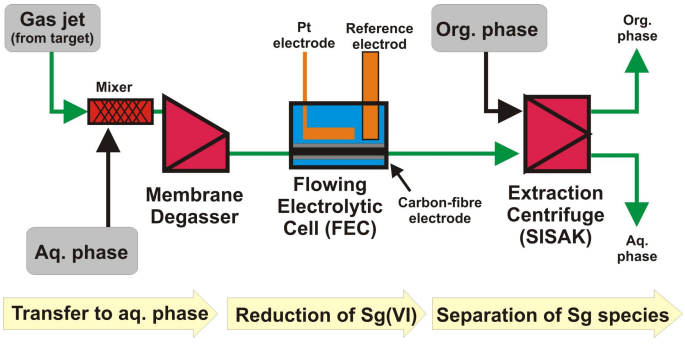

Sg will be produced by intense bombardment by a heavy-ion beam at the RIKEN facility in a suitable nuclear reaction like ^{248}Cm(^{22}Ne,5*n*)^{265}Sg , then pre-separated from unwanted reaction products by a physical, gas-filled separator like e.g. GARIS. Detection will be performed by the on-line SISAK liquid scintillation detection system.

RIKEN and GARIS, see H. Haba et al., Phys. Rev. C **85**, 024611-1-11 (2012).

FEC see Toyoshima *et al.*, Radiochim. Acta **98**, 323-326 (2008). and separate contribution to RadChem'2014.

SISAK see J. P. Omtvedt et al., Eur. Phys. J. D **45**, 91-97 (2007).

Experimental

The Oslo Cyclotron Laboratory's (OCL) MC35 Scanditronix Cyclotron was used for producing the ^{89}Zr and ^{93m}Mo radiotracers with a 30 MeV ^{4}He^{2+} ions beam on targets of ^{nat}Zr and $^{nat}SrO_2$. The nuclear reaction products were transported to the radiochemistry laboratory by a KCl/He gas-jet (1.5 L/min flow). The aerosols were caught on a filter paper and dissolved in the aqueous solution.

The production of $^{176+177}$W radiotracers were performed using the nuclear reactions ^{175}Lu(^{7}Li, xn) at the Tandem accelerator at the Japan Atomic Energy Agency's Advanced Science Research Centre in Tokai. A gas-jet transport similar to the one described for the OCL experiments were used.

All extractions experiments were performed by batch method with equal volumes (4 mL) of organic and aqueous phases in test tubes at room temperature (~ 20 °C).

Summary

- Preparations for performing reduction studies of Sg are underway.
- Reduced Sg(IV) were represented by Zr(IV), none reduced Sg(VI) represented by Mo(VI) and W(VI).
- **It seems likely that none-reduced (VI-state) and reduced (IV-state) Sg can be distinguished by liquid-liquid extraction (followed by on-line liquid scintillation detection).**

Results

Extraction behavior of Mo and W

The extraction of ^{93m}Mo(VI) and $^{176+177}$W(VI) with HDEHP and TOA from 0.1 M H_2SO_4 and 0.1 M $HClO_4$ as well as in these solutions mixed with 0.01 M HF were investigated. Results are shown below:

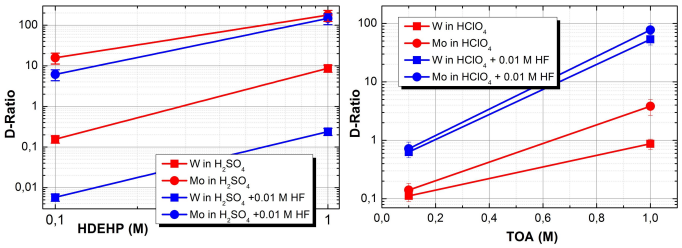

For the Sg reduction experiments we do not want Mo, W, and Sg do behave differently, we only want the (VI) and (IV) states to behave differently. Therefore, the TOA system seems more promising than the HDEHP system.

Extraction behavior of Mo and Zr

The extraction behavior of ^{93m}Mo(VI) and ^{89}Zr(IV) as homologues of Sg(VI) and Sg(IV), respectively, are of special interested for the development of radiochemical separation of Sg. Extraction with TOA and HDEHP in toluene from mixed aqueous solutions of 0.1 M H_2SO_4 + 0.01 M HF were selected to investigate Sg(VI)-like (modeled with Mo(VI)) and Sg(IV)-like (modeled with Zr(IV)) behavior, as illustrated:

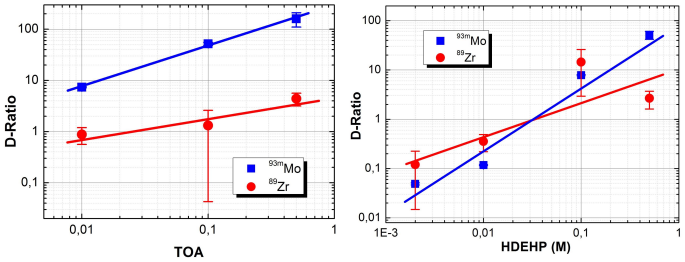

As can be seen, only the TOA system is promising for a clear separation of reduced from none-reduced Sg.

Electrolytic reduction studies of Mo and W towards the reduction of seaborgium

A. Toyoshima,[1] S. Miyashita,[2] K. Ooe,[3] M. Asai,[1] M. F. Attallah,[4] N. Goto,[3] N. S. Gupta,[4] H. Haba,[5] M. Huang,[1,5] M. Kaneko,[2] J. Kanaya,[5] Y. Kaneya,[1,6] Y. Kasamatsu,[7] Y. Kitatsuji,[1] Y. Kitayama,[6] K. Koga,[2] Y. Komori,[5,7] T. Koyama,[3] J. V. Kratz,[9] H. V. Lerum,[4] A. Mitsukai,[1,6] Y. Oshimi,[3] V. Pershina,[10] D. Sato,[3] T. K. Sato,[1] Y. Shigekawa,[7] A. Shinohara,[7] A. Tanaka,[3] K. Tsukada,[1] S. Tsuto,[3] A. Vascon,[1] T. Yokokita,[7] A. Yokoyama,[8] J. P. Omtvedt,[4] Y. Nagame,[1] and M. Schädel[1,10]

[1]Japan Atomic Energy Agency, [2]Hiroshima University, [3]Niigata University, [4]University of Oslo, [5]RIKEN, [6]Ibaraki University, [7]Osaka University, [8]Kanazawa University, [9]University Mainz, [10]GSI Helmholtzzentrum für Schwerionenforschung

1. Introduction

Purpose of the present study

To find a suitable condition to reduce and separate Mo and W between none-reduced (VI-state) and reduced (IV-state) species for our future seaborgium (Sg) reduction study

Future continuous reduction experiment with single Sg ions

1) Production and pre-separation of Sg with GARIS
2) Dissolution of Sg with Membrane degasser (MDG)
3) Reduction of Sg(VI) to Sg(IV) with flow electrolytic column (FEC)
4) Separation between Sg(VI) and Sg(IV) by liquid-liquid extraction with SISAK
5) Liquid scintillation counting

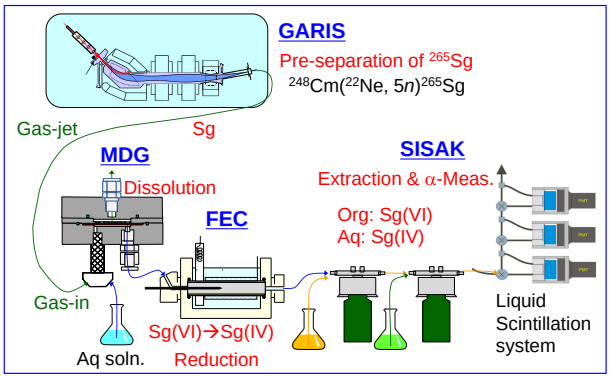

2. Experimental

JAEA tandem accelerator

^{89}Y(^{7}Li, 3n)^{93m}Mo (6.9 h)
^{175}Lu(^{7}Li, 6n)^{176}W (2.5 h)

He/KCl gas-jet

Deposition on a plastic film

dissolution

Aqueous solution (H_2SO_4 etc.)

inject

Number of atoms used in an experiment
^{93m}Mo: 10^8 atoms
^{176}W: 10^6 atoms

FEC, Applied potential: 0.4 to -1.4 V vs. Ag/AgCl reference electrode

Organic solvent (TOA in toluene)

Liquid-liquid extraction with 1 min mixing by a batch method

Centrifuging and sampling

γ-ray spectrometry using a Ge detector

Distribution ratio (D)

$$D = \frac{[M]_{org}}{[M]_{aq}}$$

3. Results

According to our extraction results, – please see No.118 poster –, we used TOA (Trioctylamine) as an extractant. In addition to the mixed 0.1 M H_2SO_4+0.01 M HF solution proposed, H_2SO_4 and 0.1 M H_2SO_4+0.1 M $HClO_4$ were also examined.

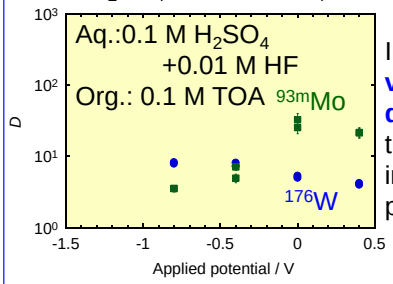

In 0.1 M H_2SO_4+0.01 M HF, ***D* values of ^{93m}Mo show a decrease below -0.4 V**, while those of ^{176}W have a slight increase at almost the same potential.

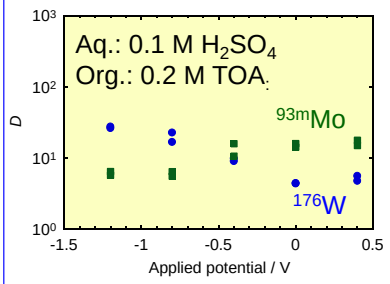

In 0.1 M H_2SO_4, *D* values of ^{93m}Mo slightly decrease at -0.8 V, while **those of ^{176}W have a gradual increase** below 0 V.

Aq.: 0.1 M H_2SO_4+0.1 M $HClO_4$
Org.: 0.2 M TOA

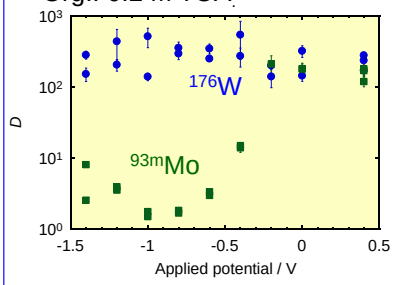

In 0.1 M H_2SO_4+0.1 M $HClO_4$, ***D* values of ^{93m}Mo show a very large decrease** starting at -0.4 V, while those of ^{176}W have no variation.

We have successfully observed the electrolytic reduction of carrier-free ^{93m}Mo and ^{176}W with identification by liquid-liquid extraction, although Mo and W were reduced under different conditions.

4. Summary

- Mo was successfully reduced and separated in 0.1 M H_2SO_4/0.1 M $HClO_4$ and 0.2 M TOA.
- W showed a gradual reduction in 0.1 M H_2SO_4, while not reduced in 0.1 M H_2SO_4/0.1 M $HClO_4$.
- We will further study the reduction of Mo and W under another conditions such as 1 M H_2SO_4 to find much better separation conditions for both Mo and W.

SEP-I17, (Id: 341)

PREPARATIONS FOR REDOX STUDIES OF SEABORGIUM WITH SISAK COUPLED TO THE FLOW ELECTROLYTIC COLUMN FEC

Jon Petter Omtvedt[a], Kazuki Koga[b], Yukiko Komori[c], Takumi Koyama[d], Jens V. Kratz[e], Hans V. Lerum[f], Sunao Miyashita[b], Kazuhiro Ooe[d], Yoshinari Oshimi[d], Valeria Pershina[g], Daisuke Sato[d], Tetsuya K. Sato[h], Yudai Shigekawa[c], Atsushi Shinohara[c], Akira Tanaka[d], Atsushi Toyoshima[h], Kazuaki Tsukada[h], Shohei Tsuto[d], Takuya Yokokita[c], Akihiko Yokoyama[i], Yuichiro Nagame[h], Matthias Schädel[h], Masato Asai[h], Mohamed F. Attallah[f], Naoya Goto[d], Nalinava S. Gupta[f], Hiromitsu Haba[j], Minghui Huang[j], Jumpei Kanaya[j], Yusuke Kaneya[h], Yoshitaka Kasamatsu[c], Yoshihiro Kitatsuji[h], Yuta Kitayama[i]

[a]*University of Oslo, Department of Chemistry*
[b]*Hiroshima University*
[c]*Osaka University*
[d]*Niigata University*
[e]*Universität Mainz*
[f]*University of Oslo*
[g]*GSI Helmholtzzentrum für Schwerionenforschung GmbH*
[h]*Japan Atomic Energy Agency*
[i]*Kanazawa University*
[j]*RIKEN*
j.p.omtvedt@kjemi.uio.no

An important motivation for investigating chemical properties of the transactinide elements is whether the Periodic Table keeps its validity as an ordering scheme in the transactinide region, i.e. for element number 104 and onwards. Strong relativistic effects, which increase approximately as a function of Z_2 and are thus most pronounced in the heaviest elements, are expected to make the properties of transactinide elements different from their lighter homologs. Therefore, the heaviest elements provide the best "laboratory" to study the influence of relativistic effects. A close link between experiment and theory is in-dispensable as relativistic effects can only be "detected" by comparing experimental results with those predicted by modern quantum-chemical calculations. However, due to the short half-lives and extremely low synthetisation rates of transactinide elements, the experimental challenges are huge: Experiments are performed under “one-atom-at-a-time” conditions which of course restrict available chemical methods significantly. Finding suitable experimental methods is challenging, but in addition these methods should shed light on relevant and interesting properties which can be related to theoretical calculations.

A property which can be studied both experimentally [1] and theoretically [2] is redox potentials. A Japanese-German-Norwegian collaboration has undertaken to investigate redox potentials of element 106, seaborgium, using the fast liquid-liquid extraction system SISAK [3] coupled to the newly developed flow electrolytic column (FEC) [1]. SISAK consist of a series of purpose built small centrifuges coupled to a liquid scintillation detection system. The complete system operates in a true continuous manner, i.e. it is true “on-line”, which makes it one of the fastest liquid-phase systems available for chemical investigation of transactinide elements. The system was successfully used for studies of element 104, rutherfordium [3]. The main idea is to differentiate between seaborgium in its hexavalent state and lower oxidation states (after “on-line” reduction in the FEC). By selecting suitable ligands which make e.g. hexavalent species positively charged and lower oxidation states (tetravalent or pentavalent) negatively charged (or vica versa), an anion or cation extracting reagent should in principle clearly distinguish between reduced and none-reduced seaborgium. Work has been performed at the JAEA tandem accelerator laboratory in Tokai and at the Oslo Cyclotron Laboratory, University of Oslo, to test and further develop the combined SISAK-FEC system to achieve necessary performance for redox experiments on seaborgium, and to find chemical conditions satisfying, or at least approaching, the above mentioned principle.

This presentation will give an overview of the status and achievement of the collaborative effort described above. Further details on the FEC and redox chemistry can be found in a contribution to this conference by A. Toyoshima et al. In a second contribution by M. F. Attallah et al., details about the selection and testing of suitable liquid-liquid extraction schemes are provided. [1] A. Toyoshima et al., Radiochim. Acta 96, 323-326 (2008). [2] V. Pershina and J. V. Kratz: Inorg. Chem. 40, 776-780 (2001) [3] J. P. Omtvedt et al., Eur. Phys. J. D 45, 91-97 (2007).

Liquid-phase Studies of Seaborgium using the Automated Liquid-liquid Extraction system SISAK

J. P. Omtvedt[1], K. Ooe[2], H. V. Lerum[1], A. Toyoshima[2], H. Haba[3], K. Tsukada[2], J. V. Kratz[4], Y. Nagame[2], M. Schädel[2]

[1]*Department of Chemistry, University of Oslo, Oslo*
[2]*Japan Atomic Energy Agency, Tokai*
[3]*Nishina Center for Accelerator Based Science, RIKEN, Wako*
[4]*Institut für Kernchemie, Universität Mainz, Mainz*

1. Introduction

Redox studies of transactinides using SISAK

Providing Information on the binding energies of the valence electrons influenced by increasingly strong relativistic effects

Present study

- Toyoshima et al. are developing an electrolytic cell for connection to the automatic Liquid-Liquid Extraction (LLE) system SISAK for studies of redox properties of element 106, seaborgium (Sg).
- SISAK (**S**hort-lived **I**sotopes **S**tudied with the **AK**ufve technique) has been successfully used to study element 104, rutherfordium (Rf).
- The more demanding experiments on Sg require shorter transport time, improved reliability and ease of use.

Toyoshima *et al.*, Radiochim. Acta **96**, 323-326 (2008).
Toyoshima *et al.*, contribution to NRC8 (2012)
J.P. Omtvedt, *et al.*, J. Nucl. Radiochem. Sci. **3** (2002) p. 121.

2. New Membrane Degasser

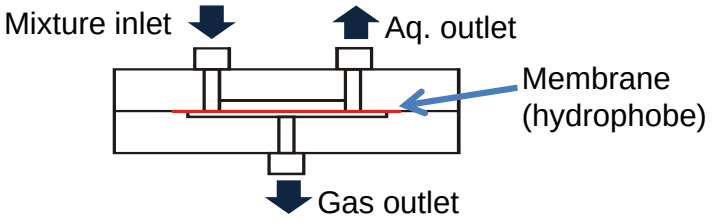

- The new degasser (prototype), based on a hydrophobe membrane, has no moving parts and can be made very small and thus fast. It consist of about eight parts (plus screws), compared to the centrifuge which rotates at 25 000 RPM and consist of about 50 parts machined to very high precision.
- A disadvantage of the new degasser is that it has no pumping capacity, as provided by the old (rotating) degasser.

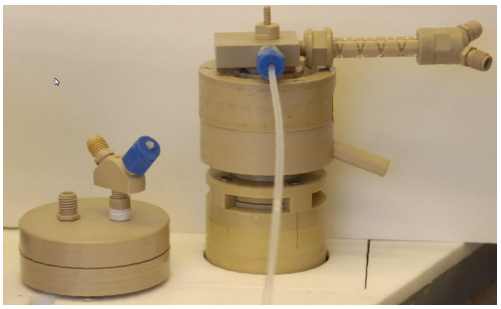

Picture of the new (left) and old (right) degasser. The old degasser is fitted with a premixer, which also can be fitted to the new one. Next version of the membrane degasser will be substantially smaller.

Summary

- The new degasser, based on a hydrophoibic membrane, performs better than the old centrifuge based degasser.
- Yields around 90% was achieved in preliminary tests with a prototype.
- Transport time through the membrane degasser is very fast, even for low flow-rates.
- Tests were performed at the Oslo Cyclotron Laboratory at University of Oslo, Norway.

3. Results

Yield Tests for Transfer from Gas to Liquid

Tests with new and old degasser at very low flow rates (for SISAK) show (graph below) that the membrane degasser fitted with a premixer made of a tube tightly packed with peak wool performs better than the old degasser, providing yields around 90%.

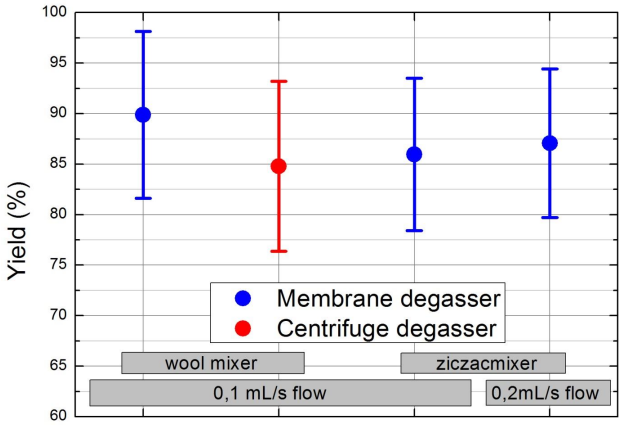

Flow Rates

The electrolytic cell being developed by Toyoshima et al. requires lower flow-rates (0.1 – 0.2 mL/s) than previously used by SISAK ((0.4 – 0.5 mL/s). The new degasser method presented here will enable the overall transport-time through SISAK to be maintained even at the low flow-rates.

Heating

An important advantage with the new degasser is that solutions do not need to be heated to achieve good yield. This is an advantage with respect to complexity and performance of the scintillation detection.

On-line Extraction and Reduction of Mo and W using SISAK and FEC

H. V. Lerum [a,], M. Asai[b], M. F. Attallah[a] , N.S. Gupta[a], Y. Kaneya[b], Y. Kasamatsu[e], Y. Kitatsuji[b], Y. Kitayama[d], Y. Komori[e], S. Miyashita[b], K. Ooe[c], T. K. Sato[b], K. Tsukada[b], T. Yokokita[e], A. Yokoyama[d], A. Shinohara[e], M. Thorèn[a] A. Toyoshima[b], J.V. Kratz[g] , Y. Nagame[b], J. P. Omtvedt[a], V. Pershina[f], M. Schädel[b].*

[a] Department of Chemistry, University of Oslo, P. O. Box 1033 Blindern, NO-0315 Oslo, Norway; [b] Advanced Science Research Center, Japan Atomic Energy Agency, Tokai, Ibaraki 319-1195, Japan; [c] Institute of Science and Technology, Niigata University, Niigata 950-2181, Japan;[d] College and Institue of Scinence and Engineering, Tokyo Metropolitian University, Hachioji, Tokyo 192-0397 , Japan; [e] Graduate school of Science, Osaka University, Toyonaka, Osaka 560-0043, Japan; [f] GSI Helmholtzzentrum für Schwerionenforschung GmbH, D-64291 Darmstad, Germany; [g] Institut für Kernchemie, Universität Mainz, 55128 Mainz, Germany Corresponding author: hansvl@kjemi.uio.no*

SISAK is a liquid-liquid extraction system which quickly and continuously mixes two immiscible phases and subsequently separates them using a centrifuge [1]. We plan to perform a Sg reduction experiment using a newly developed Membrane DeGasser (MDG) [2] to dissolve nuclear reaction products delivered by a gas-jet aerosol system in a liquid. Sg in the liquid phase will then be reduced with a Flow Electrolytic Column (FEC) [3-5] from hexavalent to penta or tetravalent states. This yields important experimental information on the redox behavior of Sg. SISAK is then utilized to separate the ions in the (V) or (IV) states from that in the (VI) state by solvent extraction. In preparation for the future seaborgium (Sg) reduction experiments, we have carried out on-line extraction and reduction experiments of its lighter homologs, Mo and W.

1. Extraction of Mo and W with SISAK

Extraction experiments of Mo and W were performed with the new MDG and the SISAK system. The radioisotopes ^{91m}Mo ($T_{1/2}$ = 60 s), ^{93m}Mo ($T_{1/2}$ = 6,9 h) and ^{176}W ($T_{1/2}$ = 2,5 h) were produced in the ^{89}Y(^{7}Li, 6*n*)^{91m}Mo, ^{89}Y(^{7}Li, 3n)^{93m}Mo and ^{175}Lu(^{7}Li, 6*n*)^{176}W reactions, respectively, at the JAEA tandem accelerator. Reaction products were transported by a He/KCl gas-jet to the chemistry laboratory with a gas flow of 1,5 L/min. The products were dissolved in aqueous solutions using the MDG. Extraction was performed with flow rates from 0,1 mL/s to 0,2 mL/s. The aqueous phase (0,1 M HCl/ 0,9 M LiCl) from the MDG was then mixed with an organic phase of hinokitiol (HT) dissolved in toluene at the flow rate of 0,2 mL/min to extract Mo(VI) and W(VI) ions to the organic solution. These two phases were then separated using a SIAK centrifuge. Both of the phases were separately collected and measured using HPGe detectors.

The experiments represent non-reduced species of group-IV and clearly showed that more Mo and W were extracted with higher concentration of HT.

2. Reduction of Trace amount of Mo

Reduction experiments of ^{91m,93m}Mo were performed using FEC coupled to MDG and the SISAK system. The experimental procedure was the same as the extraction experiments described above, but with the FEC inserted between the MDG and the SISAK extraction stage. A glassy carbon rod covered with carbon fiber was used as working electrode and a silver mesh as the counter electrode in the FEC. The applied potential was between -0,6 and 0,8 V vs. a standard hydrogen electrode (StHE).

The distribution ratio (commonly referred to as the *D value*) defined as the ratio of the extracted element in the organic phase to that in the aqueous phase is shown in Fig. 1 for Mo as a function of the applied potential vs. StHE. The *D* value of Mo decrease for potentials below 0,2 V. In our separate macro amount reduction experiments, (VI)Mo was reduced to (V)Mo around this potential. Thus, our experiments show that Mo(VI) is reduced to Mo(V) in the rapid and continuous on-line experiments, although the difference of the D values of Mo is smaller than those observed in batch reduction-experiments. Work to improve the separation and the extraction of the two states is on-going and progress will be reported at CHE8.

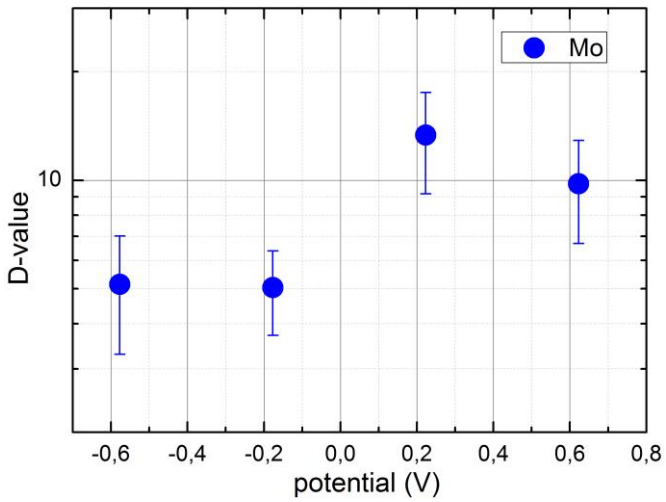

Fig. 1: Extraction of Mo using 10^{-2} HT/toluene and aqueous solution 0,1 M HCl mixed with 0,9 M LiCl.

References

[1] J.P. et al., *J. Nucl. Radiochem. Sci.* **3** 121 (2002).
[2] K. Ooe et al. Presentation CHE8 (2013).
[3] A. Toyoshima et al., *Radiochim. Acta* **96,** 323 (2008).
[4] A. Toyoshima et al., *J. Am. Chem. Soc.* **126,** 9180 (2009)
[5] A. Toyoshima et al., to be submitted.

Development of new degasser with a hydrophobic membrane for SISAK system

K. Ooe[a, b,], K. Tsukada[a], M. Asai[a], T. K. Sato[a], A. Toyoshima[a], S. Miyashita[a], Y. Nagame[a], M. Schädel[a], Y. Kaneya[c], H. V. Lerum[d], J. P. Omtvedt[d], J. V. Kratz[e], H. Haba[f], A. Wada[g], Y. Kitayama[h]*

[a]*Advanced Science Research Center, Japan Atomic Energy Agency, Tokai, Ibaraki 319-1195, Japan;* [b]*Institute of Science and Technology, Niigata University,Niigata, Niigata 950-2181, Japan;* [c]*Department of Chemistry, Graduate School of Science and Engineering, Ibaraki University, Mito, Ibaraki 310-8512, Japan;* [d]*Department of Chemistry, University of Oslo, Oslo N-0315, Norway;* [e] *Institut für Kernchemie, Universität Mainz, D-55128 Mainz, Germany;* [f]*Nishina Center for Accelerator-Based Science, RIKEN, Wako, Saitama 351-0198, Japan;* [g] *Department of Chemistry, Tokyo Metropolitan University, Hachioji, Tokyo 192-0397, Japan;* [h]*Graduate School of Natural Science and Technology, Kanazawa University, Kanazawa, Ishikawa 920-1192, Japan; * Corresponding author: ooe@chem.sc.niigata-u.ac.jp*

1. Introduction

We plan to investigate the redox potentials of element 106, seaborgium (Sg), using a flow electrolytic column (FEC) [1] in combination with the rapid liquid-liquid extraction apparatus SISAK [2].There is a technical problem in connection of these two apparatuses; a typical liquid flow rate for SISAK of ~24 mL/min is quite higher than that for FEC of ~1 mL/min. To successfully work with these two apparatuses, we need to reduce the liquid flow rate of the SISAK system. However, the dissolution efficiency with SISAK centrifuging degasser, which continuously dissolves gas-jet transported nuclear reaction products into aqueous solution, drops with decreasing the liquid flow rate. In the present study, therefore, we fabricated a completely new degasser which successfully works with a lower liquid flow rate.

2. New degasser with a hydrophobic membrane

Our new degasser has a hydrophobic Teflon membrane for separation of aqueous solution from gas (hereafter called membrane degasser (MDG)). It continuously dissolves transported products by a gas-jet as follows. The mixture of gas and aqueous solution enters MDG. Then, only the gas is sucked through the membrane with a vacuum pump. On the other hand, aqueous solution does not pass through the hydrophobic membrane and flows along a channel in MDG. Then, it elutes from an outlet.

3. Performance test

Dissolution efficiencies of gas-jet transported products were measured using MDG. Short-lived isotopes, ^{91m}Mo ($T_{1/2}$ = 65 s), ^{93m}Mo ($T_{1/2}$ = 6.9 h), and ^{176}W ($T_{1/2}$ = 2.5 h), which are lighter homologues of Sg, were produced simultaneously in the ^{89}Y(^{7}Li, 5n)^{91m}Mo, ^{89}Y(^{7}Li, 3n)^{93m}Mo, and ^{175}Lu(^{7}Li, 6n)^{176}W reactions, respectively, at the JAEA tandem accelerator. Reaction products recoiling out of the targets were transported to the chemistry laboratory by a He/KCl gas-jet. The pressure in the target chamber was 130–140 kPa. The transported products were mixed with 1 M HCl/10^{-4} M HF solution before entering MDG. The carrier gas was then sucked thorough the membrane in MDG, while the aqueous solution was eluted from MDG. The aqueous sample was collected in a plastic bottle and was then measured with a Ge detector.

4. Results and discussion

The dissolution efficiencies for Mo and W at a He gas flow rate of 1.5 L/min are shown in Fig. 1 as a function of aqueous flow rate. In this experiment, the dependence of dissolution efficiencies on a half-life was observed; the efficiency for ^{93m}Mo ($T_{1/2}$ = 6.9 h) was higher than that for ^{91m}Mo ($T_{1/2}$ = 65 s) at aqueous flow rate of 0.6–6 mL/min. Nevertheless, a dissolution efficiency of more than 80% was obtained for short-lived ^{91m}Mo at the aqueous flow rate of 6–24 mL/min. A high yield of around 70% was also observed at a flow rate of 1.8–3 mL/min. These results show that MDG works with a lower aqueous flow rate than the previous SISAK degasser. The dependence of dissolution efficiency on a He gas flow rate was also investigated at aqueous flow rate of 0.6–24 mL/min. The efficiencies were almost independent of the studied gas flow rates of 1.0, 1.5, and 2.0 L/min. This shows that MDG works with various gas flow rates.

In the near future, on-line experiments for Mo and W using MDG will be conducted in combination with SISAK and FEC.

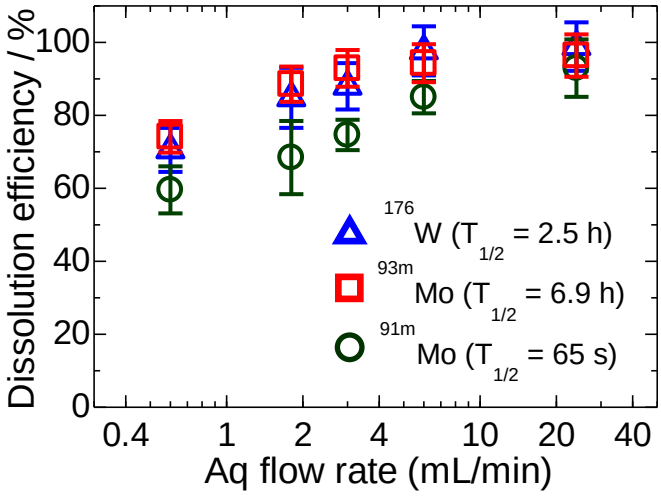

Fig. 1: Dissolution efficiencies of gas-jet transported nuclides with MDG as a function of aqueous flow rate.

[1] A. Toyoshima et al., *Radiochim. Acta* **2008**, **96**, 323-326.
[2] J. P. Omtvedt et al., *Eur. Phys. J. D* **2007**, 45, 91-97.

APSORC'13 - 5th Asia-Pacific Symposium on Radiochemistry
Kanazawa, Japan, 22-27 September 2013

Solvent extraction of hexavalent Mo and W using 4-isopropyltropolone (Hinokitiol) for Seaborgium (Sg) reduction experiment

S. Miyashita[1], A. Toyoshima[1], K. Ooe[2], M. Asai[1], T. K. Sato[1], K. Tsukada[1], Y. Nagame[1], M. Schädel[1], Y. Kaneya[3], H. Haba[4], J. Kanaya[4], M. Huang[4], Y. Kitayama[5], A. Yokoyama[5], A. Wada[6], Y. Oura[6] J. V. Kratz[7], H. V. Lerum[8] and J. P. Omtvedt[8]

[1] Advanced Science Research Center, Japan Atomic Energy Agency, Tokai, Ibaraki 319-1195, Japan
[2] Institute of Science and Technology, Niigata University, Niigata 950-2181, Japan
[3] Graduate School of Science and Engineering, Ibaraki University, Mito, Ibaraki 310-8512, Japan
[4] Nishina Center for Accelerator-Based Science, RIKEN, Wako, Saitama 351-0198, Japan
[5] College and Institute of Science and Engineering, Kanazawa University, Kanazawa 920-1192, Japan
[6] Graduate School of Science and Engineering, Tokyo Metropolitan University, Hachioji, Tokyo 192-0397, Japan
[7] Institut für Kernchemie, Universität Mainz, 55128 Mainz, Germany
[8] Department of Chemistry, University of Oslo, P.O. Box 1033 - Blindern, NO-0315, Oslo, Norway

Abstract – *Solvent extraction of ^{93m}Mo and ^{176}W using 4-isopropyltropolone (Hinokitiol, HT) was investigated. Extraction mechanism of Mo and W with HT was examined by slope analysis. The slopse of the distribution ratio of Mo and W vs. [HT] in logarithmic scale are 1.88 and 1.54, respectively.*

Keywords – *Superheavy elements, Solvent extraction, Hinokitiol, Molybdenum, Tungsten, Seaborgium*

I. INTRODUCTION

For the determination of the reduction potentials of Seaborgium (Sg), we plan to carry out reduction experiments using a rapid and continuous system consisting of a flow electrolytic column (FEC) [1] combined with the liquid-liquid extraction apparatus SISAK [2]. The oxidation states of Sg will be chemically characterized its extraction behavior, and thus, rapid extraction enabling separation of Sg with different oxidation states is required. From our results of extraction-kinetics studies of ^{181}W as lighter homologue of Sg into toluene containing several extractants from 0.1 M HCl, we found that 4-isopropyltropolone (Hinokitiol, HT) has fast kinetics enough to be used together with SISAK. In the work presented here, we examined the extraction with HT of ^{93m}Mo ($T_{1/2}$ = 6.9 h) and ^{176}W ($T_{1/2}$ = 2.5 h) from a mixed solution 1.0 M HCl and 1.0 M LiCl solution.

II. EXPERIMENTAL

^{93m}Mo and ^{176}W were produced in the ^{89}Y(^{7}Li, 3n)^{93m}Mo and ^{175}Lu(^{7}Li, 6n)^{176}W reactions, respectively. ^{89}Y metallic foil and $^{nat}Lu_2O_3$ on Be foil were irradiated by a 62 MeV ^{7}Li beam from a tandem accelerator in JAEA. Reaction products recoiling out of the target foils were transported with a He/KCl gas-jet to the chemistry laboratory. Transported products were collected on a PTFE sheet, and dissolved by a mixed solution of 1.0 M HCl and 1.0 M LiCl. Then, a hydrogen ion concentration of solution was adjusted to desired ones. An organic phase was toluene containing a certain concentration of HT. 700 μL of each aqueous and organic phase was mixed in a vial and shaken for 600 s using a mechanical shaker. After shaking, two phases were separated by centrifugation for 30 s. 500 μL of each aqueous and organic phase was taken into the vials. Radioactivity of both phases, 263 keV γ-rays of ^{93m}Mo and 102 keV γ-rays of ^{176}W, was detected by a Ge-detector. The distribution ratio (D) was calculated by the ratio of radioactivity of ^{93m}Mo and ^{176}W in the two phases.

III. RESULT AND DISCUSSION

Figure 1 show that the variation of the D value of Mo and W with respect to the concentration of HT in the organic phase ([HT]) when the concentration of hydrogen ion in the aqueous phase was 0.1 M. The D value of Mo and W increased by increasing of [HT]. The slopes of the D value of Mo and W vs. [HT] in logarithmic scale are 1.88 and 1.54, respectively. Those results indicated that Mo is formed an extractable complex with two HT molecules and W is one and/or two molecules.

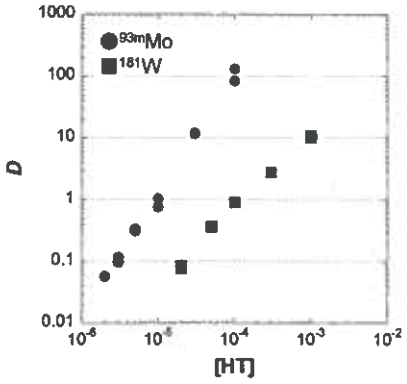

Figure 1. Variation of the distribution ratio of Mo and W vs. the concentration of HT in the organic phase when aqueous phase was 0.1 M HCl / 0.9 M LiCl. Closed cycles and squares represent Mo and W, respectively.

[1] A. Toyoshima et al., *Radiochim. Acta*, **2008**, *96*, 323
[2] J. P. Omtvedt et al., *Eur. Phys. J. D*, **2007**, *45*, 91

APSORC'13 - 5th Asia-Pacific Symposium on Radiochemistry
Kanazawa, Japan, 22-27 September 2013

25-NCP-03

Development of a new continuous dissolution apparatus with a hydrophobic membrane for superheavy element chemistry

K. Ooe[1,2], K. Tsukada[2], M. Asai[2], T. K. Sato[2], A. Toyoshima[2], S. Miyashita[2], Y. Nagame[2], M. Schädel[2], Y. Kaneya[3], H. V. Lerum[4], J. P. Omtvedt[4], J. V. Kratz[5], H. Haba[6], A. Wada[7], Y. Kitayama[8]

[1]Institute of Science and Technology, Niigata University
[2]Japan Atomic Energy Agency
[3]Graduate School of Science and Engineering, Ibaraki University
[4]Department of Chemistry, University of Oslo
[5]Institut für Kernchemie, Universität Mainz
[6]Nishina Center for Accelerator-Based Science, RIKEN
[7]Department of Chemistry, Tokyo Metropolitan University
[8]Graduate School of Natural Science and Technology, Kanazawa University

Abstract –A new continuous dissolution apparatus of gas-jet transported products was developed for superheavy element chemistry. The new apparatus has a hydrophobic membrane for separation of aqueous solution from the gas. We investigated the dissolution efficiencies with the apparatus for short-lived nuclides. In the conference, the dependence of the efficiencies on the aqueous- and gas-flow rates will be reported.

Keywords – Molybdenum, Tungsten, Continuous dissolution, Hydrophobic membrane

I. INTRODUCTION

For investigation of the redox potentials of element 106, seaborgium (Sg), we plan to combine a flow electrolytic column (FEC) [1] with the rapid liquid-liquid extraction apparatus SISAK [2]. There is a technical problem in connection with these two apparatuses; a typical liquid flow rate for SISAK of ~24 mL/min is quite higher than that for FEC of ~1 mL/min. To successfully work with these two apparatuses, it is required to reduce the liquid flow rate of the SISAK system. However, the dissolution efficiency with the SISAK centrifuging degasser, which continuously dissolves gas-jet transported nuclear reaction products into an aqueous solution, drops with decreasing liquid flow rate. In the present study, therefore, we fabricated a completely new continuous dissolution apparatus which successfully works with a lower liquid flow rate.

II. NEW CONTINUOUS DISSOLUTION APPARATUS WITH A HYDROPHOBIC MEMBRANE

Our new degasser utilizes a hydrophobic Teflon membrane to separate aqueous solution from gas (hereafter called membrane degasser, MDG). It continuously dissolves transported products by a gas-jet as follows. The mixture of gas and aqueous solution enters the MDG. Then, only the gas is sucked through the membrane with a vacuum pump. On the other hand, the aqueous solution does not pass through the hydrophobic membrane and elutes from an outlet.

III. PERFORMANCE TEST

Dissolution efficiencies of gas-jet transported products were measured using the MDG. Short-lived isotopes, ^{91m}Mo ($T_{1/2}$ = 65 s), ^{93m}Mo ($T_{1/2}$ = 6.9 h), and ^{176}W ($T_{1/2}$ = 2.5 h), which are lighter homologues of Sg, were produced simultaneously in the ^{89}Y(^{7}Li, 5n)^{91m}Mo, ^{89}Y(^{7}Li, 3n)^{93m}Mo, and ^{175}Lu(^{7}Li, 6n)^{176}W reactions, respectively, at the JAEA tandem accelerator. Reaction products recoiling out of the targets were transported to the chemistry laboratory by a He/KCl gas-jet. The pressure in the target chamber was 130–140 kPa. The transported products were mixed with 1 M HCl/10^{-4} M HF solution before entering the MDG. The carrier gas was then sucked through the membrane in the MDG, while the aqueous solution was eluted from the MDG. The aqueous sample was collected in a plastic bottle and was then measured with a Ge detector.

IV. RESULTS AND DISCUSSION

The dissolution efficiencies for Mo and W at a He gas flow rate of 1.5 L/min were investigated as a function of aqueous flow rate. In the result, a dependence of the dissolution efficiencies on the half-life was observed; the efficiency for ^{93m}Mo ($T_{1/2}$ = 6.9 h) was higher than that for ^{91m}Mo ($T_{1/2}$ = 65 s) at aqueous flow rate of 0.6–6 mL/min. The dissolution efficiency for ^{176}W ($T_{1/2}$ = 2.5 h) was almost the same as that for ^{93m}Mo. Nevertheless, a dissolution efficiency of more than 80% was obtained for short-lived ^{91m}Mo at aqueous flow rates of 6–24 mL/min. A high yield of around 70% was also observed at flow rates of 1.8–3 mL/min. These results show that the MDG works with a lower aqueous flow rate than the previous SISAK degasser.

In the conference, the dependence of dissolution efficiency on the He gas flow rate will be also reported.

[1] A. Toyoshima et al., *Radiochim. Acta* **96**, 323-326 (2008).
[2] J. P. Omtvedt et al., *Eur. Phys. J. D* **45**, 91-97 (2007).

Chemical studies of Mo and W in preparation of a seabogrium (Sg) reduction experiment using MDG, FEC, and SISAK

A. Toyoshima[1], S. Miyashita[1], M. Asai[1], T. K. Sato[1], Y. Kaneya[1], K. Tsukada[1], Y. Kitatsuji[1], Y. Nagame[1], M. Schädel[1], H. V. Lerum[2], J. P. Omtvedt[2], Y. Oshimi,[3] K. Ooe[3], Y. Kitayama[4], A. Yokoyama[4], A. Wada[5], Y. Oura[5], H. Haba[6], J. Kanaya[6], M. Huang[6], Y. Komori[7], T. Yokokita[7], Y. Kasamatsu[7], A. Shinohara[7], V. Pershina[8], J. V. Kratz[9]

[1]Advanced Science Research Center, Japan Atomic Energy Agency, Tokai, Ibaraki 319-1195, Japan
[2]Department of Chemistry, University of Oslo, Oslo 0371, Norway
[3]Institute of Science and Technology, Niigata University, Niigata 950-2181, Japan
[4]College and Institute of Science and Engineering, Kanazawa University, Kanazawa 920-1192, Japan
[5]Graduate School of Science and Engineering, Tokyo Metropolitan University, Hachioji, Tokyo 192-0397, Japan
[6]Nishina Center for Accelerator-Based Science, RIKEN, Wako, Saitama 351-0198, Japan
[7]Graduate School of Science, Osaka University, Toyonaka, Osaka 560-0043, Japan
[8]GSI Helmholtzzentrum für Schwerionenforschung GmbH, D-64291 Darmstadt, Germany
[9]Institut für Kernchemie, Universität Mainz, 55128 Mainz, Germany

Abstract –We are developing a new chemistry assembly to perform continuous reduction experiments of seaborgium (element 106, Sg). In preparation for the Sg experiment, we have begun studies on the dissolution, reduction, and extraction of Mo and W isotopes. Our present status of the preparation with Mo and W will be presented.

Keywords – Superheavy elements, Seaborgium (Sg), Electrochemistry, Solvent extraction, Flow electrolytic column, SISAK, Membrane degasser

Seaborgium (Sg) is expected to be redox-active similarly to its lighter group-6 homologs, Mo and W. Theoretical calculation show that Sg can be reduced from the most stable hexavalent state Sg(VI) to, e.g., the tetravalent one [1]. They also predict that the Sg(VI)/Sg(IV) couple will have a more negative redox potential than those of the corresponding W ions in acidic solution [1]. In such reduction reactions, electrons occupy the vacant valence 6d orbital of the Sg(VI) ion. The redox potential of the Sg(IV)/Sg(VI) couple, therefore, provides information on the stability of the 6d orbital which is anticipated to be influenced by increasingly strong relativistic effects.

Because of low production rates of ^{265a,b}Sg (a and b stand for two different states) in the ^{248}Cm(^{22}Ne, 5*n*) reaction and their short half-lives of 8.5 and 1.4 s [2], only single atoms of Sg are present. This means that standard electrochemical techniques are not applicable to its reduction study. In our previous works, we have developed a novel electrochemical method of electrolytic column chromatography available for single ions [3]. Carbon fibers modified with Nafion perfluorinated cation-exchange resin were employed as a working electrode as well as a cation-exchanger. This technique was successfully applied to the oxidation of nobelium (No) [4] and the reduction of mendelevium (Md) [5]. It is, however, technically difficult to apply this batch-wise chromatographic method to the reduction study of Sg because of its very short half-lives. We are, therefore, developing a new chemistry assembly consisting of a membrane degasser (MDG), a flow electrolytic column (FEC), the continuous liquid-liquid extraction apparatus, and the liquid scintillation counting system (SISAK) [6] to continuously perform the dissolution, reduction, separation, and detection of Sg, respectively.

In preparation for our future experiment with Sg, we have begun studies on the dissolution, reduction, and extraction of Mo and W isotopes. On-line experiments using the newly developed MDG were carried out to examine the dissolution efficiency of nuclear reaction products transported by a gas-jet. The aqueous solution dissolving the reaction products was successfully separated from the carrier gas using the MDG after continuous mixing of the carrier gas with the aqueous solution. Electrolytic reduction of Mo and W was examined using a FEC. Redox couples of Mo(VI)/Mo(V) and W(VI)/W(V) in HCl have been so far characterized for macro amounts of Mo and W with cyclic voltammetry and UV/Vis. absorption spectrometry. Batch extractions of hexavalent ^{93m}Mo and ^{181}W were performed to search for suitable conditions in the separation between Sg(IV) and Sg(VI). Variations of extraction ratios of Mo(VI) and W(VI) between toluene containing hinokitiol (HT) and HCl were successfully observed as a function of HT and HCl concentrations. On-line extractions of short-lived ^{91m}Mo and ^{176}W were also carried out using SISAK and MDG. Extraction ratios of these elements were increased with increasing HT concentration, reflecting results of the batch experiments. In the symposium, our present status of the preparation with Mo and W will be presented.

[1] V. Pershina *et al.*, J. Phys. Chem. A**103**, 8463 (1999).
[2] H. Haba et al., Phys. Rev. C**85**, 024611 (2012).
[3] A. Toyoshima et al., Radiochim. Acta **96**, 323 (2008).
[4] A. Toyoshima et al., J. Am. Chem. Soc. **126**, 9180 (2009).
[5] A. Toyoshima et al., to be submitted.
[6] For example, J. P. Omtvedt et al., Eur. Phys. J. D**45**, 91 (2007).